

KONINKLIJKE NEDERLANDSCHE AKADEMIE VAN
WETENSCHAPPEN

PROCEEDINGS

VOLUME XLII

No. 5

President: J. VAN DER HOEVE

Secretary: M. W. WOERDEMAN

CONTENTS

- BURGERS, J. M.: "Some considerations on the fields of stress connected with dislocations in a regular crystal lattice". II. (Solutions of the equations of elasticity for a non-isotropic substance of regular crystalline symmetry), p. 378.
- CORPUT, J. G. VAN DER, et CH. PISOT: "Sur un problème de WARING généralisé". II, p. 400.
- SITTER, L. U. DE: "The principle of concentric folding and the dependence of tectonical structure on original sedimentary structure". (Communicated by Prof. F. A. VENING MEINESZ), (With one plate), p. 412.
- HEYN, A. N. J.: "Some remarks on the mechanism of spiral growth of the sporangiophore of *Phycomyces* and a suggestion for its further explanation". (Communicated by Prof. G. VAN ITERSON), p. 431.
- HARTSEMA, ANNIE M., en IDA LUYTEN: "Proeven over het uitloopen van de knollen en het vervroegen van den bloei bij *Freesia* hybriden" (with summary). (Aangeboden door Prof. A. H. BLAAUW). (With two plates), p. 438.
- BRUMMELKAMP, R.: "Rindenoberfläche, resp. Rindengewicht und Gehirngewicht". (Communicated by Prof. C. U. ARIËNS KAPPERS), p. 446.
-

Physics. — *Some considerations on the fields of stress connected with dislocations in a regular crystal lattice. II. (Solutions of the equations of elasticity for a non-isotropic substance of regular crystalline symmetry.)* By J. M. BURGERS. (Mededeeling N^o. 34 uit het Laboratorium voor Aero- en Hydrodynamica der Technische Hoogeschool te Delft.)

(Communicated at the meeting of April 29, 1939.)

1. In Part I of this communication it has been attempted to make some contributions towards the investigation of the geometrical relations characteristic of dislocations in a simple regular crystal lattice, and of the fields of stress connected with them¹⁾. As stated in section 6 of Part I the calculations referring to the fields of stress provisionally had been built upon the equations valid for isotropic elastic substances. However, as is known, the relations between stress and strain in a crystalline body are different from those valid for an isotropic substance, even when the crystalline body belongs to the regular class. When coordinate axes are introduced parallel to the axes of the regular crystal, then, u, v, w denoting the components of the displacement, the stress components are given by²⁾:

$$\left. \begin{aligned} \sigma_{xx} &= c_{11} \frac{\partial u}{\partial x} + c_{12} \left(\frac{\partial v}{\partial y} + \frac{\partial w}{\partial z} \right) \\ \sigma_{xy} &= \sigma_{yx} = c_{44} \left(\frac{\partial v}{\partial x} + \frac{\partial u}{\partial y} \right) \end{aligned} \right\} \dots \dots \dots (1)$$

etc.

where c_{11}, c_{12}, c_{44} , according to the notation introduced by VOIGT, represent the three elastic constants which are characteristic for such a crystal. For convenience in the following lines we shall write:

$$c_{11} = \lambda + 2\mu + \mu' \quad ; \quad c_{12} = \lambda \quad ; \quad c_{44} = \mu. \quad \dots \dots (2)$$

The equations for isotropic substances are obtained by taking μ' equal to zero; μ and λ then are the ordinary coefficients as used by LOVE and other writers on problems of elasticity.

When external forces are acting upon the substance, having the

¹⁾ See these Proceedings 42, p. 293, 1939.

²⁾ Compare e.g. A. E. H. LOVE, *Treatise on the Mathematical Theory of Elasticity* (Cambridge 1920), Ch. VI, p. 147 seq., where the expression for the strain-energy function has been given.

components X, Y, Z per unit volume, the stresses must satisfy the equations:

$$\left. \begin{aligned} \frac{\partial \sigma_{xx}}{\partial x} + \frac{\partial \sigma_{yx}}{\partial y} + \frac{\partial \sigma_{zx}}{\partial z} &= -X \\ \text{etc.} \end{aligned} \right\} \dots \dots \dots (3)$$

Substituting the expressions (1) we obtain the equations:

$$\left. \begin{aligned} \mu \Delta u + \mu' \frac{\partial^2 u}{\partial x^2} + (\lambda + \mu) \frac{\partial \theta}{\partial x} &= -X \\ \text{etc.} \end{aligned} \right\} \dots \dots \dots (4)$$

where:

$$\theta = \frac{\partial u}{\partial x} + \frac{\partial v}{\partial y} + \frac{\partial w}{\partial z}.$$

The corresponding equations for an isotropic substance are obtained from (4) by omitting the terms with μ' .

In the theoretical treatment of the fields of stress in an isotropic substance an important part is played by a particular solution of the equations, referring to the case where the forces X, Y, Z are zero everywhere except at the origin of the system of coordinates, at which point a concentrated force of unit magnitude is assumed to act, *e.g.* in the direction of the x -axis. This particular solution is given by the following formulae³⁾:

$$\left. \begin{aligned} u &= \frac{1}{4\pi\mu r} + \frac{\partial \psi}{\partial x} \\ v &= \frac{\partial \psi}{\partial y} \\ w &= \frac{\partial \psi}{\partial z} \end{aligned} \right\} \dots \dots \dots (5)$$

with:

$$\psi = -\frac{(\lambda + \mu)}{8\pi\mu(\lambda + 2\mu)} \frac{\partial r}{\partial x}$$

It is the object of the first part of the present communication (sections 2–8) to construct a solution of similar type for the case of the regular crystalline substance. The formulae obtained then are applied to the investigation of the fields of stress connected with dislocations (sections 9–11). By means of the results derived it becomes possible to find out

³⁾ See A. E. H. LOVE, *l.c.* p. 183. — In Part I this solution is given by eqs. (1), p. 300.

in how far the provisional equations of the previous communication will need correction.

2. We begin by constructing a solution of eqs. (4) for the case:

$$X = e^{i(\alpha x + \beta y + \gamma z)}, \quad Y = 0, \quad Z = 0 \quad (6)$$

α, β, γ denoting real parameters. For shortness it is convenient to denote the exponential function occurring here by E . A solution is found by assuming:

$$u = aE, \quad v = bE, \quad w = cE \quad (7)$$

in which a, b, c are three unknown constants. Substituting these expressions into eqs. (4) we obtain three linear equations for a, b, c :

$$\left. \begin{aligned} (M\varrho^2 + Na^2)a + La\beta b + La\gamma c &= 1 \\ La\beta a + (M\varrho^2 + N\beta^2)b + L\beta\gamma c &= 0 \\ La\gamma a + L\beta\gamma b + (M\varrho^2 + N\gamma^2)c &= 0 \end{aligned} \right\} (8)$$

where: $M = \mu, \quad L = \lambda + \mu, \quad N = \lambda + \mu + \mu'$; and:

$$\varrho^2 = \alpha^2 + \beta^2 + \gamma^2. \quad (9)$$

The determinant of the system (8) can be given in the form AD , where:

$$D = \varrho^6 + \frac{B}{A} \varrho^2 (\alpha^2 \beta^2 + \alpha^2 \gamma^2 + \beta^2 \gamma^2) + \frac{C}{A} \alpha^2 \beta^2 \gamma^2 \quad . . . (10)$$

and:

$$\left. \begin{aligned} A &= M^2(M + N) = \mu^2(\lambda + 2\mu + \mu') \\ B &= M(N^2 - L^2) = \mu\mu'(2\lambda + 2\mu + \mu') \\ C &= N^3 - 3L^2N + 2L^3 = (\mu')^2(3\lambda + 3\mu + \mu') \end{aligned} \right\} . . . (11)$$

The solution of the system (8) then can be written:

$$\left. \begin{aligned} a &= \{M^2\varrho^4 + MN\varrho^2(\beta^2 + \gamma^2) + (N^2 - L^2)\beta^2\gamma^2\} / AD \\ b &= - \{ML\varrho^2\alpha\beta + (NL - L^2)\alpha\beta\gamma^2\} / AD \\ c &= - \{ML\varrho^2\alpha\gamma + (NL - L^2)\alpha\beta^2\gamma\} / AD \end{aligned} \right\} . . . (12)$$

3. A more general solution is obtained by assuming:

$$\left. \begin{aligned} X &= \int \int \int da \, d\beta \, d\gamma \, f(\alpha, \beta, \gamma) \cdot E \\ Y &= 0, \quad Z = 0 \end{aligned} \right\} (13)$$

where $f(\alpha, \beta, \gamma)$ is an arbitrary function of α, β, γ , subjected to the

condition that the integral in (13) must have a definite sense. The corresponding solution of eqs. (4) then will be:

$$u = \iiint da \, d\beta \, d\gamma \, f(a, \beta, \gamma) \cdot a \cdot E, \text{ etc.} \quad (14)$$

with a, b, c given by (12).

As the parameters a, β, γ occurring in eqs. (8) and in eqs. (12) owe their origin to differentiations with respect to x, y, z resp., it is not difficult to see that the quantities u, v, w defined by (14) can be represented as follows:

$$\left. \begin{aligned} u &= \frac{1}{A} \left\{ M^2 \Delta^2 + MN \left(\frac{\partial^2}{\partial y^2} + \frac{\partial^2}{\partial z^2} \right) \Delta + (N^2 - L^2) \frac{\partial^4}{\partial y^2 \partial z^2} \right\} \Phi \\ v &= -\frac{1}{A} \left\{ ML \frac{\partial^2}{\partial x \partial y} \Delta + (NL - L^2) \frac{\partial^4}{\partial x \partial y \partial z^2} \right\} \Phi \\ w &= -\frac{1}{A} \left\{ ML \frac{\partial^2}{\partial x \partial z} \Delta + (NL - L^2) \frac{\partial^4}{\partial x \partial y^2 \partial z} \right\} \Phi \end{aligned} \right\} \quad (15)$$

where Φ stands for a function which is defined by the integral:

$$\Phi = \iiint da \, d\beta \, d\gamma \frac{f(a, \beta, \gamma)}{\mathbf{D}} E \quad (16)$$

This function satisfies the differential equation:

$$D_{\text{oper.}} \Phi = -X \quad (17)$$

$D_{\text{oper.}}$ having been written for the differential operator corresponding to \mathbf{D} :

$$D_{\text{oper.}} \equiv \Delta^3 + \frac{B}{A} \left(\frac{\partial^4}{\partial x^2 \partial y^2} + \frac{\partial^4}{\partial x^2 \partial z^2} + \frac{\partial^4}{\partial y^2 \partial z^2} \right) \Delta + \frac{C}{A} \frac{\partial^6}{\partial x^2 \partial y^2 \partial z^2} \quad (18)$$

When now we choose the function $f(a, \beta, \gamma)$ in such a way that X will be zero everywhere except at the origin, where it must become infinite in a certain specified way, the required solution of eqs. (4) will be obtained.

For this purpose we take ⁴⁾:

$$f(a, \beta, \gamma) = \frac{1}{8\pi^3} \cdot \quad (19)$$

the integration with respect to a, β, γ being extended over the domain of the a, β, γ -space comprised between a sphere with a very large radius ϱ_{II} and another sphere with a very small radius ϱ_I ; in the results obtained we afterwards assume $\varrho_{II} \rightarrow \infty$ and $\varrho_I \rightarrow 0$.

⁴⁾ Integrals of this type have been considered e.g. by N. ZEILON, Das Fundamentalintegral der allgem. lin. part. Differentialgleichung mit konst. Koeffizienten. Arkiv f. Matem., Astron. och Fysik, **6**, No. 23, 1911. ZEILON uses these integrals for purposes of a different nature, and does not introduce the limits ϱ_I, ϱ_{II} .

Introducing a system of polar coordinates $\varrho, \delta, \varepsilon$ into the α, β, γ -space, with the polar axis along the direction determined by $\alpha:\beta:\gamma :: x:y:z$, we have:

$$\alpha x + \beta y + \gamma z = \varrho r \cos \delta. \quad (20)$$

Hence (13) will become:

$$X = \frac{1}{8\pi^3} \int_{\varrho_I}^{\varrho_{II}} d\varrho \int_0^\pi d\delta \int_0^{2\pi} d\varepsilon \varrho^2 \sin \delta e^{i\varrho r \cos \delta} \quad (21)$$

Performing the integrations with respect to ε and to δ , we obtain:

$$X = \frac{1}{2\pi^2 r} \int_{\varrho_I}^{\varrho_{II}} d\varrho \varrho \sin(\varrho r) = -\frac{1}{2\pi^2 r} \frac{d^2}{dr^2} \int_{\varrho_I}^{\varrho_{II}} d\varrho \frac{\sin(\varrho r)}{\varrho} \quad (21a)$$

The integral occurring in the latter expression has the value zero for $r=0$, while for all positive values of r it approaches to $\pi/2$. Consequently X will be practically equal to zero for all finite values of r , whereas it will assume very high values for $r \rightarrow 0$. Moreover, we have:

$$\left. \begin{aligned} \int_0^r dr 4\pi r^2 X &= -\frac{2}{\pi} \int_0^r dr r \frac{d^2}{dr^2} \int_{\varrho_I}^{\varrho_{II}} d\varrho \frac{\sin(\varrho r)}{\varrho} = \\ &= -\frac{2}{\pi} r \frac{d}{dr} \int_{\varrho_I}^{\varrho_{II}} d\varrho \frac{\sin(\varrho r)}{\varrho} + \frac{2}{\pi} \int_{\varrho_I}^{\varrho_{II}} d\varrho \frac{\sin(\varrho r)}{\varrho} \end{aligned} \right\} \quad (21b)$$

from which equation it is evident that the integral of X over a sphere of radius r assumes the value unity already for very small values of r .

4. We now will investigate the integral (16) which defines the function Φ .

It is convenient to introduce the following notations:

$$\left. \begin{aligned} \alpha &= \varrho \cos \vartheta & x &= r \cos \vartheta_1 \\ \beta &= \varrho \sin \vartheta \cos \chi & y &= r \sin \vartheta_1 \cos \chi_1 \\ \gamma &= \varrho \sin \vartheta \sin \chi & z &= r \sin \vartheta_1 \sin \chi_1 \\ \tau &= \alpha^2 \beta^2 + \alpha^2 \gamma^2 + \beta^2 \gamma^2, & t &= x^2 y^2 + x^2 z^2 + y^2 z^2 \\ \sigma &= \alpha^2 \beta^2 \gamma^2 & s &= x^2 y^2 z^2 \end{aligned} \right\} \quad (22)$$

and:

$$F = \frac{\varrho^6}{\mathbf{D}} = \left(1 + \frac{B}{A} \frac{\tau}{\varrho^4} + \frac{C}{A} \frac{\sigma}{\varrho^6} \right)^{-1} \quad (23)$$

Along with the polar coordinates ϱ, ϑ, χ , the system $\varrho, \delta, \varepsilon$, already defined

in 3 and having its polar axis in the direction determined by $\alpha:\beta:\gamma::x:y:z$, will be used in the α, β, γ -space. — As is known we have the relation:

$$\cos \delta = \cos \vartheta \cos \vartheta_1 + \sin \vartheta \sin \vartheta_1 \cos (\chi - \chi_1).$$

The function Φ now is determined by the integral:

$$\Phi = \frac{1}{8\pi^3} \int \int \int d\alpha d\beta d\gamma \frac{e^{i\varrho r \cos \delta}}{\varrho^6} F \quad . \quad . \quad . \quad . \quad . \quad (24)$$

The quantity F in this expression is a function of the angles ϑ and χ , which function can vary only between definite limits, in consequence of the relations:

$$0 \leq \tau/\varrho^4 \leq 1/3; \quad 0 \leq \sigma/\varrho^6 \leq 1/27.$$

Data concerning the values of the coefficients A, B, C for tungsten (Wo) and sylvine (KCl) are given in section 12; it is found that in the case of tungsten $B = C = 0$, so that in this case we fall back upon the equations for the isotropic substance; whereas in the case of sylvine we have (omitting a factor 10^{33}): $A = 2,3$; $B = 4,7$; $C = 10,5$, so that F will vary from 1 to 0,54.

In view of the bounded character of F it is possible to develop this function into a series of surface harmonics. As F is symmetrical with respect to α, β, γ and is not affected by a change of sign of these variables, the surface harmonics occurring in the development must correspond to spherical harmonic functions of integral order which are homogeneous symmetric functions of $\alpha^2, \beta^2, \gamma^2$. These functions consequently must be rational integral functions of the three invariants ϱ^2, τ and σ .

Some of the spherical harmonic functions of integral order which can play a part in these considerations are:

order (or degree)	function
0	1
2	(no function existing of this order)
4	$\varrho^4 - 5\tau$
6	$2\varrho^6 - 21\varrho^2\tau + 231\sigma$
8	$\varrho^8 - 18\varrho^4\tau - 52\varrho^2\sigma + 65\tau^2$

The corresponding surface harmonics are given by the formulae:

$$\left. \begin{aligned} S_0 &= 1 \\ S_4 &= \sqrt{\frac{21}{4}} (1 - 5\tau/\varrho^4) \\ S_6 &= \sqrt{\frac{13}{32}} (2 - 21\tau/\varrho^4 + 231\sigma/\varrho^6) \\ S_8 &= \sqrt{\frac{561}{64}} (1 - 18\tau/\varrho^4 - 52\sigma/\varrho^6 + 65\tau^2/\varrho^8) \end{aligned} \right\} \quad . \quad . \quad . \quad (25)$$

where the numerical factors have been chosen in such a way that the integral of the square of an S -function over the surface of a sphere of unit radius is equal to 4π , so that the mean value of the square of every S -function is equal to unity.

We now assume that the development of F according to these functions is given by the expression:

$$F = c_0 + c_4 S_4 + c_6 S_6 + c_8 S_8 + \dots \quad (26)$$

According to known theorems the coefficients c_n occurring here are given by the integrals ⁵⁾:

$$c_n = \frac{1}{4\pi} \int_0^\pi d\vartheta \int_0^{2\pi} d\chi \sin \vartheta S_n F \quad (27)$$

5. When the variables δ, ε are used instead of ϑ, χ , it is possible to express the S -function of order n as a linear combination of the surface harmonics of the same order n , defined in the usual way with respect to the coordinates δ, ε . Hence we may write:

$$S_n = A_n P_n(\cos \delta) + \sum_1^n \{ A_n^{(m)} \cos m\varepsilon + B_n^{(m)} \sin m\varepsilon \} P_n^{(m)}(\cos \delta). \quad (28)$$

Here $A_n, A_n^{(m)}, B_n^{(m)}$ are coefficients, the values of which will depend upon the angles ϑ_1 and χ_1 defining the direction of the axis for the system δ, ε . The values of these coefficients can be obtained from integrals of similar type as (27); in particular we have ⁶⁾:

$$A_n = \frac{2n+1}{4\pi} \int_0^\pi d\delta \int_0^{2\pi} d\varepsilon \sin \delta P_n(\cos \delta) S_n \quad (28a)$$

We now write (24) in the form:

$$\Phi = \frac{1}{8\pi^3} \int_{\varrho_I}^{\varrho_{II}} d\varrho \int_0^\pi d\delta \int_0^{2\pi} d\varepsilon \sin \delta \frac{e^{i\varrho r \cos \delta}}{\varrho^4} \sum c_n S_n \quad (29)$$

When the expression (28) is substituted for S_n , the integration with respect to $d\varepsilon$ can be carried out very simply. When at the same time we write $\cos \delta = \zeta$, we obtain:

$$\Phi = \frac{1}{4\pi^2} \int_{\varrho_I}^{\varrho_{II}} d\varrho \int_{-1}^{+1} d\zeta \frac{e^{i\varrho r \zeta}}{\varrho^4} \sum c_n A_n P_n(\zeta) \quad (29a)$$

⁵⁾ Compare e.g. E. T. WHITTAKER and G. N. WATSON, *Modern Analysis* (Cambridge 1920), p. 393; and W. THOMSON and P. G. TAIT, *Treatise on Natural Philosophy* (Cambridge 1888), Part I, p. 206.

⁶⁾ E. T. WHITTAKER and G. N. WATSON, *l.c.* p. 394.

As the P -functions are polynomials in ζ , the integration with respect to $d\zeta$ can be performed without difficulty and gives:

$$\int_{-1}^{+1} d\zeta e^{i\varrho r \zeta} P_n(\zeta) = 2 \left\{ \frac{\sin(\varrho r)}{\varrho r} + \frac{(n+1)!}{2 \cdot (n-1)!} \frac{\cos(\varrho r)}{(\varrho r)^2} - \frac{(n+2)!}{2^2 \cdot 2! (n-2)!} \frac{\sin(\varrho r)}{(\varrho r)^3} - \frac{(n+3)!}{2^3 \cdot 3! (n-3)!} \frac{\cos(\varrho r)}{(\varrho r)^4} + \dots \right\} \quad (30)$$

There remains to perform the integration with respect to $d\varrho$, which leads to integrals of the types:

$$I_{2m+1} = \int_{\varrho_I}^{\varrho_{II}} d\varrho \frac{\sin(\varrho r)}{\varrho^{2m+1}}; \quad I_{2m} = \int_{\varrho_I}^{\varrho_{II}} d\varrho \frac{\cos(\varrho r)}{\varrho^{2m}}.$$

It will be seen that, e. g.:

$$\frac{d^{2m}}{dr^{2m}} I_{2m+1} = (-1)^m \int_{\varrho_I}^{\varrho_{II}} d\varrho \frac{\sin(\varrho r)}{\varrho}.$$

The value of the latter integral with sufficient approximation can be represented by the expression:

$$I_1 = \frac{\pi}{2} - \varrho_I r - \frac{\varepsilon^*}{\varrho_{II}},$$

where ε^* stands for a numerical quantity, the absolute value of which does not surpass unity. So long as we are content with a finite number of terms in the development of F , only a finite number of integrations with respect to dr will have to be performed upon I_1 in order to obtain the values of the other integrals; hence by taking ϱ_I small enough and ϱ_{II} large enough, the error which arises when we assume:

$$I_1 = \pi/2,$$

for all finite values of r , can be made as small as desired, the more so as the integrals afterwards are divided by r^{2m-3} or by r^{2m-4} . In this way we finally obtain:

$$\int_{\varrho_I}^{\varrho_{II}} d\varrho \int_{-1}^{+1} d\zeta e^{i\varrho r \zeta} P_n(\zeta) = \pi r^3 \left\{ \frac{1}{4!} - \frac{(n+1)!}{2 \cdot (n-1)! 5!} + \frac{(n+2)!}{2^2 \cdot 2! (n-2)! 6!} - \dots \right\} \quad (31)$$

and in particular for:

$$\begin{array}{llll} n=0 & . & . & . & \pi r^3/24 \\ n=4 & . & . & . & \pi r^3/384 \\ n=6 & . & . & . & -\pi r^3/3840 \\ n=8 & . & . & . & +\pi r^3/15360. \end{array}$$

Substituting these results into (29a) we arrive at the following expression for Φ :

$$\Phi = \frac{r^3}{4\pi} \left\{ \frac{c_0 A_0}{24} + \frac{c_4 A_4}{384} - \frac{c_6 A_6}{3840} + \frac{c_8 A_8}{15360} \dots \right\} \dots \quad (32)$$

6. We now return to equation (28a) for the determination of the coefficients A_n . Instead of performing the integration with respect to δ, ε , we avail ourselves of the variables ϑ, χ . It is possible to express both $P_n(\cos \delta)$ and S_n as linear combinations of surface harmonics of order n defined with respect to the system ϑ, χ . According to a known theorem we have ⁷⁾:

$$\begin{aligned} P_n(\cos \delta) &= \\ &= P_n(\cos \vartheta) P_n(\cos \vartheta_1) + 2 \sum \frac{(n-m)!}{(n+m)!} P_n^{(m)}(\cos \vartheta) P_n^{(m)}(\cos \vartheta_1) \cos m(\chi - \chi_1). \end{aligned}$$

Let us assume that the expression for S_n has the form:

$$S_n = \bar{A}_n P_n(\cos \vartheta) + \sum \{ \bar{A}_n^{(m)} \cos m\chi + \bar{B}_n^{(m)} \sin m\chi \} P_n^{(m)}(\cos \vartheta). \quad (33)$$

Substituting into (28a), which now takes the form:

$$A_n = \frac{2n+1}{4\pi} \int_0^\pi d\vartheta \int_0^{2\pi} d\chi \sin \vartheta P_n(\cos \vartheta) S_n \dots \quad (28b)$$

we obtain the result ⁸⁾:

$$A_n = \bar{A}_n P_n(\cos \vartheta_1) + \sum \{ \bar{A}_n^{(m)} \cos m\chi_1 + \bar{B}_n^{(m)} \sin m\chi_1 \} P_n^{(m)}(\cos \vartheta_1). \quad (34)$$

From this formula it follows that A_n is the same function of ϑ_1, χ_1 as S_n is of ϑ, χ . Hence, having regard to (25) we can immediately write down:

$$\left. \begin{aligned} A_0 &= 1 \\ A_4 &= \sqrt{\frac{21}{4}} (1 - 5 t/r^4) \\ A_6 &= \sqrt{\frac{13}{32}} (2 - 21 t/r^4 + 231 s/r^6) \\ A_8 &= \sqrt{\frac{561}{64}} (1 - 18 t/r^4 - 52 s/r^6 + 65 t^2/r^8) \end{aligned} \right\} \dots \quad (35)$$

⁷⁾ E. T. WHITTAKER and G. N. WATSON, *l.c.* p. 395.

⁸⁾ See E. T. WHITTAKER and G. N. WATSON, *l.c.* p. 325.

Consequently the function Φ is fully determined by (32) as soon as the values of the numerical coefficients c_n have been obtained from eqs. (27).

It will be observed that Φ is a homogeneous function of degree +3 of the coordinates x, y, z , symmetrical with respect to x^2, y^2, z^2 .

It is useful to note a relation between the coefficients c_n which is obtained as follows: when $\beta = \gamma = 0$, $\alpha = \varrho$, we have: $\tau = 0$, $\sigma = 0$, and, consequently, $F = 1$. Hence, from (26) in connection with (25):

$$1 = c_0 + c_4 \sqrt{\frac{21}{4}} + c_6 \sqrt{\frac{13}{8}} + c_8 \sqrt{\frac{561}{64}} + \dots \quad (36)$$

assuming that the development has been continued so far that the approximation obtained is satisfactory also for $\alpha = \varrho$, $\beta = \gamma = 0$.

7. *Expressions for the displacement components u, v, w .* Having obtained an expression for Φ we pass on to the displacement components u, v, w , which are to be derived from Φ by means of eqs. (15). When we introduce the function Ψ defined by:

$$\Psi = \Delta \Phi \quad (37)$$

the values of u, v, w can be given in the following form:

$$\left. \begin{aligned} u &= \frac{1}{\lambda + 2\mu + \mu'} \frac{\partial^2 \Psi}{\partial x^2} + \frac{1}{\mu} \left(\frac{\partial^2 \Psi}{\partial y^2} + \frac{\partial^2 \Psi}{\partial z^2} \right) + u' \\ v &= -\frac{\lambda + \mu}{\mu(\lambda + 2\mu + \mu')} \frac{\partial^2 \Psi}{\partial x \partial y} + v' \\ w &= -\frac{\lambda + \mu}{\mu(\lambda + 2\mu + \mu')} \frac{\partial^2 \Psi}{\partial x \partial z} + w' \end{aligned} \right\} \quad (38)$$

where u', v', w' are quantities which contain μ' as a factor. — In the case of an isotropic substance, for which μ' is zero, these quantities disappear. As in this case $c_0 = 1$, $c_4 = c_6 = \dots = 0$, we have: $\Phi = r^3/96\pi$; $\Psi = r/8\pi$, and the expressions (38) become identical with (5), as will be seen by a slight rearrangement of the terms occurring in u . —

The expressions for u', v', w' have the form:

$$\left. \begin{aligned} u' &= \frac{\mu' (2\lambda + 2\mu + \mu')}{\mu^2 (\lambda + 2\mu + \mu')} \frac{\partial^4 \Phi}{\partial y^2 \partial z^2} \\ v' &= -\frac{\mu' (\lambda + \mu)}{\mu^2 (\lambda + 2\mu + \mu')} \frac{\partial^4 \Phi}{\partial x \partial y \partial z^2} \\ w' &= -\frac{\mu' (\lambda + \mu)}{\mu^2 (\lambda + 2\mu + \mu')} \frac{\partial^4 \Phi}{\partial x \partial y^2 \partial z} \end{aligned} \right\} \quad (39)$$

In certain cases it may be useful to restrict to the first two terms of (35). When we write:

$$c_4 \sqrt{21/4} = c',$$

we have:

$$\Phi \cong \frac{c_0 r^3}{96\pi} + \frac{c' r^3}{1536\pi} (1 - 5t/r^4) \dots \dots \dots (40a)$$

$$\Psi = \Delta \Phi = \frac{c_0 r}{8\pi} - \frac{c' r}{192\pi} (1 - 5t/r^4) \dots \dots \dots (40b)$$

$$\Delta \Psi = \Delta^2 \Phi = \frac{c_0}{4\pi r} + \frac{3c'}{32\pi r} (1 - 5t/r^4) \dots \dots \dots (40c)$$

Equation (40) then induces us to assume:

$$c_0 + c' = 1 \dots \dots \dots (41)$$

8. *Expression for the stress component σ_{xx} .* — With the notation defined by eqs. (2) we have:

$$\sigma_{xx} = (\lambda + 2\mu + \mu') \frac{\partial u}{\partial x} + \lambda \left(\frac{\partial v}{\partial y} + \frac{\partial w}{\partial z} \right) \dots \dots \dots (42)$$

Hence, with the aid of eqs. (15), we obtain:

$$\sigma_{xx} = \frac{\partial^3 \Psi}{\partial x^3} + \frac{(\lambda + 2\mu + \mu')^2 - \lambda(\lambda + \mu)}{\mu(\lambda + 2\mu + \mu')} \left(\frac{\partial^3 \Psi}{\partial x \partial y^2} + \frac{\partial^3 \Psi}{\partial x \partial z^2} \right) + \left. \begin{aligned} &+ \frac{\mu'(\lambda + 2\mu + \mu')(2\lambda + 2\mu + \mu') - 2\mu'\lambda(\lambda + \mu)}{\mu^2(\lambda + 2\mu + \mu')} \frac{\partial^5 \Phi}{\partial x \partial y^2 \partial z^2} \end{aligned} \right\} \dots (43)$$

It is of interest to calculate the value of the integral:

$$S = \iint \sigma_{xx} dy dz \dots \dots \dots (44)$$

over a plane perpendicular to the x -axis. The work is greatly simplified when we observe that the first term of σ_{xx} is the only one giving a contribution different from zero. This is proved as follows:

A. For an arbitrary domain of finite extent of a plane perpendicular to the x -axis we have:

$$\iint dy dz \left(\frac{\partial^3 \Psi}{\partial x \partial y^2} + \frac{\partial^3 \Psi}{\partial x \partial z^2} \right) = \int ds \frac{\partial^2 \Psi}{\partial x \partial n},$$

ds being an element of the contour of the domain considered, n the normal to ds , drawn in the outward direction. For s we will take a circumference $y = \omega_1 \cos \chi_1$; $z = \omega_1 \sin \chi_1$. Then it can be shown that $\partial^2 \Psi / \partial x \partial n$ consists of a series of terms of the general form: $x^{p+1} \omega_1^q f(\chi_1)/r^{p+q+2}$. Integration with respect to $ds = \omega_1 d\chi_1$ consequently gives terms of the general type: $x^{p+1} \omega_1^{q+1}/r^{p+q+2}$, which vanish for $\omega_1 \rightarrow \infty$, as in that case $\lim. x/r = 0$ (x being constant).

B. In order to obtain the integral of the last term of (43), it is convenient first to integrate over a rectangular domain of a plane perpendicular to the x -axis, with sides respectively parallel to the y - and

z -axes. When the corners of the rectangle are denoted by a (1st quadrant), b (2nd), c (3rd), d (4th), we find:

$$\iint dy dz \frac{\partial^5 \Phi}{\partial x \partial y^2 \partial z^2} = \left(\frac{\partial^3 \Phi}{\partial x \partial y \partial z} \right)_{a-b+c-d}.$$

By calculating $\partial^3 \Phi / \partial x \partial y \partial z$ it is found that this expression contains terms of the two forms: xyz/r^3 , and $xyzt/r^7$, both of which vanish when the size of the square is increased without limit, x being kept constant.

It thus remains to consider the integral of the first term of (43). By direct calculation we have, assuming that $x \geq 0$:

$$\begin{aligned} \iint dy dz \frac{\partial^3 r}{\partial x^3} &= -4\pi, \\ \iint dy dz \frac{\partial^3}{\partial x^3} \left(\frac{t}{r^3} \right) &= -20\pi. \end{aligned}$$

When $x < 0$, these results change sign.

Hence, if we restrict to the terms of Ψ given in (40b), we find:

$$\iint dy dz \frac{\partial^3 \Psi}{\partial x^3} = -\frac{c_0}{2} - \frac{c'}{2} \dots \dots \dots (45)$$

so that:

$$S = -\frac{1}{2} (c_0 + c' + \dots) \quad (\text{for } x > 0),$$

or, assuming the validity of (41)⁹:

$$\begin{aligned} S &= -\frac{1}{2} \quad (\text{for } x > 0) \\ S &= +\frac{1}{2} \quad (\text{for } x < 0) \end{aligned} \left. \vphantom{\begin{aligned} S &= -\frac{1}{2} \quad (\text{for } x > 0) \\ S &= +\frac{1}{2} \quad (\text{for } x < 0) \end{aligned}} \right\} \dots \dots \dots (46)$$

⁹ When a further term is taken in the development of Φ , we have:

$$\Phi \cong r^3 \left(\frac{c_0 A_0}{96\pi} + \frac{c_4 A_4}{1536\pi} - \frac{c_6 A_6}{15360\pi} \right)$$

and:

$$\Psi \cong r \left(\frac{c_0 A_0}{8\pi} - \frac{c_4 A_4}{192\pi} + \frac{c_6 A_6}{512\pi} \right).$$

Now it is found that, for $x > 0$,

$$\iint dy dz \frac{\partial^3}{\partial x^3} \left(\frac{s}{r^5} \right) = -4\pi.$$

Hence we find:

$$\iint dy dz \frac{\partial^3}{\partial x^3} \left(2r - 21 \frac{t}{r^3} + 231 \frac{s}{r^5} \right) = -512\pi.$$

When we write: $c_6 \sqrt{13/8} = c''$, then with the aid of this result we obtain:

$$\iint dy dz \frac{\partial^3}{\partial x^3} \Psi \cong -\frac{c_0}{2} - \frac{c'}{2} - \frac{c''}{2}$$

for $x > 0$; while eq. (36) takes the form:

$$1 \cong c_0 + c' + c'' \dots$$

This result is in accordance with the condition of equilibrium, as the field is produced by a unit force in the direction of the positive x -axis, acting at the origin.

9. *Application of the solution of eqs. (4) to the investigation of the field connected with a dislocation.* — We now must turn to the problem whether the solution obtained can be applied to find the field of deformations, connected with a dislocation. It will be sufficient to take the case in which only the displacement component u has a cyclic constant differing from zero for every closed line embracing the singular line σ characteristic of the dislocation, while the components v and w are single-valued. The problem can be solved by making use of a method of reasoning similar to that applied by VOLTERRA in his memoir on dislocations in isotropic elastic substances¹⁰).

We consider the displacement u_I, v_I, w_I , produced at the point ξ, η, ζ , by a unit force acting at the point x, y, z in the direction of the x -axis. The values of u_I, v_I, w_I are given by the formulae (15), in which now all differentiations refer to ξ, η, ζ . From the expressions for u_I, v_I, w_I we can deduce the stress components $\sigma_{I\xi\xi}$, etc. by means of eqs. (1). Introducing a surface element $d\Sigma$ at ξ, η, ζ with the normal in a direction ν , we calculate:

$$\sigma_I = \sigma_{I\xi\xi} \cdot (\nu\xi) + \sigma_{I\eta\xi} \cdot (\nu\eta) + \sigma_{I\zeta\xi} \cdot (\nu\zeta) \cdot \cdot \cdot \cdot \quad (47)$$

$(\nu\xi), (\nu\eta), (\nu\zeta)$ representing the cosines of the angles which the normal ν makes with the coordinate axes. It will be seen that σ_I is the x -component of the stress acting on the element $d\Sigma$, and it follows that for a closed surface Σ :

$$\left. \begin{aligned} \iint d\Sigma \sigma_I &= -1, \text{ when the point } x, y, z \text{ is inside } \Sigma \\ \iint d\Sigma \sigma_I &= 0, \text{ when } x, y, z \text{ is outside } \Sigma \end{aligned} \right\} \cdot \cdot \cdot \quad (48)$$

We next introduce two further fields: u_{II}, v_{II}, w_{II} , produced by a unit force at x, y, z in the direction of the y -axis; and $u_{III}, v_{III}, w_{III}$, produced by a unit force at x, y, z in the direction of the z -axis. The expressions for $u_{II}, v_{II}, \dots, w_{III}$ can be derived from the formulae (15) by means of suitable interchanges of the coordinates, and it is to be noted that we have:

$$u_{II} = v_I, \quad u_{III} = w_I, \quad v_{III} = w_{II} \cdot \cdot \cdot \cdot \cdot \quad (49)$$

¹⁰ V. VOLTERRA, Sur l'équilibre des corps élastiques multiplement connexes, Ann. Ecole Norm. Supér. (3) 24, p. 400, 1907, in particular pp. 421—425.

For these fields we calculate:

$$\sigma_{II} = \sigma_{II\xi\xi} \cdot (\nu \xi) + \sigma_{II\eta\xi} \cdot (\nu \eta) + \sigma_{II\zeta\xi} \cdot (\nu \zeta) \quad . \quad . \quad . \quad (47a)$$

$$\sigma_{III} = \sigma_{III\xi\xi} \cdot (\nu \xi) + \sigma_{III\eta\xi} \cdot (\nu \eta) + \sigma_{III\zeta\xi} \cdot (\nu \zeta) \quad . \quad . \quad . \quad (47b)$$

in every case thus taking the stress component parallel to the x -axis. Then for every closed surface Σ we shall have:

$$\iint d\Sigma \sigma_{II} = 0 \quad . \quad . \quad . \quad . \quad . \quad . \quad . \quad (48a)$$

$$\iint d\Sigma \sigma_{III} = 0 \quad . \quad . \quad . \quad . \quad . \quad . \quad . \quad (48b)$$

independently of the position of the point x, y, z .

It can be proved that $\sigma_I, \sigma_{II}, \sigma_{III}$, considered *qua* functions of x, y, z , satisfy the differential equations:

$$\mu \Delta \sigma_I + \mu' \frac{\partial^2 \sigma_I}{\partial x^2} + (\lambda + \mu) \frac{\partial}{\partial x} \left(\frac{\partial \sigma_I}{\partial x} + \frac{\partial \sigma_{II}}{\partial y} + \frac{\partial \sigma_{III}}{\partial z} \right) = 0 \quad \left. \vphantom{\frac{\partial}{\partial x}} \right\} \quad . \quad (50)$$

etc.

This result is a consequence of the fact that each of the three systems u_I, v_I, w_I ; u_{II}, v_{II}, w_{II} ; $u_{III}, v_{III}, w_{III}$ separately satisfies the same equations; and further of the relations expressed by (49), which make it possible, e.g., to write σ_I in terms of u_I, u_{II}, u_{III} instead of in terms of u_I, v_I, w_I , and similarly for σ_{II} and σ_{III} .

After these preliminaries we now return to the consideration of the field connected with a dislocation for which the u -component should have the cyclic constant $\lambda_0 = 1$. When the dislocation is characterized by the singular line σ , we introduce a (not closed) surface Σ bounded by this line, and, following VOLTERRA's example, put:

$$\left. \begin{aligned} u &= \iint d\Sigma \sigma_I \\ v &= \iint d\Sigma \sigma_{II} \\ w &= \iint d\Sigma \sigma_{III} \end{aligned} \right\} \quad . \quad . \quad . \quad . \quad . \quad . \quad . \quad (51)$$

Then the quantities u, v, w given by these formulae are the components of the displacement of the field connected with the dislocation. This is proved as follows: In the first place, in consequence of eqs. (50), u, v, w satisfy the equations of elasticity for crystalline substances of regular structure. In the second place, when the surface Σ is replaced by another surface, Σ' , also bounded by the singular line σ , and situated, e.g., on the positive side of Σ , then by introducing a closed surface Σ'' ,

composed of Σ' and of Σ taken with the normal in the negative direction, we can write:

$$\begin{aligned}\iint d\Sigma' \sigma_I &= \iint d\Sigma \sigma_I + \iint d\Sigma'' \sigma_I \\ \iint d\Sigma' \sigma_{II} &= \iint d\Sigma \sigma_{II} + \iint d\Sigma'' \sigma_{II} \\ \iint d\Sigma' \sigma_{III} &= \iint d\Sigma \sigma_{III} + \iint d\Sigma'' \sigma_{III}.\end{aligned}$$

Hence, making use of (48), (48a), (48b), we see that the values of v and w are independent of the position of the surface Σ , and even do not change when this surface is moved across the point x, y, z ; whereas the value of u suffers a discontinuous change of amount -1 , when the surface Σ is displaced in such a way that the point x, y, z from lying on the positive side of Σ will be situated on the negative side. — As the derivatives of the integrals (48), (48a), (48b) (referring to a closed surface) with respect to x, y, z are zero, it follows at the same time that the derivatives of u, v, w are wholly independent of the position of Σ . — Finally the values of u, v, w decrease to zero, when the point x, y, z is moved to an infinite distance from the surface Σ , assuming that this surface is of finite extent.

10. The next problem to be considered is the expression of the quantities $\sigma_I, \sigma_{II}, \sigma_{III}$ by means of the function Φ , and the transformation of the integrals (51) into formulae which are more suitable for calculations.

The expressions for $\sigma_I, \sigma_{II}, \sigma_{III}$ can be deduced by means of straightforward calculations, starting from eqs. (15) and making use of eqs. (1), (47), (47a), (47b). The terms obtained then are re-arranged in such a way that an important part of the surface integrals can be transformed into contour integrals along the line σ . Omitting the details of the calculations, we restrict to stating the following results:

$$u = \iint d\Sigma \left\{ \frac{\partial}{\partial v} \Delta^2 + \frac{B}{A} \frac{\partial}{\partial v} \left(\frac{\partial^4}{\partial \xi^2 \partial \eta^2} + \dots + \dots \right) + \frac{C}{A} (v\xi) \frac{\partial^5}{\partial \xi \partial \eta^2 \partial \zeta^2} \right\} \Phi + \left(\begin{aligned} &+ \int d\sigma \left(G_2 \frac{d\eta}{d\sigma} + G_3 \frac{d\zeta}{d\sigma} \right) \end{aligned} \right) \quad (52a)$$

$$v = \int d\sigma \left(H_2 \frac{d\eta}{d\sigma} + H_3 \frac{d\zeta}{d\sigma} \right) \cdot \cdot \cdot \cdot \cdot \quad (52b)$$

$$w = \int d\sigma \left(K_2 \frac{d\eta}{d\sigma} + K_3 \frac{d\zeta}{d\sigma} \right) \cdot \cdot \cdot \cdot \cdot \quad (52c)$$

Here the operator Δ refers to the variables ξ, η, ζ , the same as the

differentiations which have been written out and as the differentiation with respect to ν (the normal to the surface element $d\Sigma$ at ξ, η, ζ). The quantities $G_2, G_3, H_2, H_3, K_2, K_3$ are given by the expressions:

$$G_2 = -\frac{A'}{A} \frac{\partial^2}{\partial \xi \partial \zeta} \Delta \Phi - \frac{B}{A} \frac{\partial^4 \Phi}{\partial \xi \partial \zeta^3} - \frac{B+B'}{A} \frac{\partial^4 \Phi}{\partial \xi \partial \eta^2 \partial \zeta} \quad (53a)$$

$$G_3 = +\frac{A'}{A} \frac{\partial^2}{\partial \xi \partial \eta} \Delta \Phi + \frac{B}{A} \frac{\partial^4 \Phi}{\partial \xi \partial \eta^3} + \frac{B+B'}{A} \frac{\partial^4 \Phi}{\partial \xi \partial \eta \partial \zeta^2} \quad (53b)$$

$$H_2 = -\frac{2M^2L}{A} \frac{\partial^2}{\partial \eta \partial \zeta} \Delta \Phi - \frac{B'}{A} \left(\frac{\partial^4 \Phi}{\partial \xi^2 \partial \eta \partial \zeta} + \frac{\partial^4 \Phi}{\partial \eta \partial \zeta^3} \right) \quad (53c)$$

$$H_3 = -\Delta^2 \Phi + \frac{A'}{A} \frac{\partial^2}{\partial \eta^2} \Delta \Phi - \frac{B}{A} \frac{\partial^4 \Phi}{\partial \xi^2 \partial \zeta^2} + \frac{B'}{A} \frac{\partial^4 \Phi}{\partial \eta^2 \partial \zeta^2} \quad (53d)$$

$$K_2 = +\Delta^2 \Phi - \frac{A'}{A} \frac{\partial^2}{\partial \zeta^2} \Delta \Phi + \frac{B}{A} \frac{\partial^4 \Phi}{\partial \xi^2 \partial \eta^2} - \frac{B'}{A} \frac{\partial^4 \Phi}{\partial \eta^2 \partial \zeta^2} \quad (53e)$$

$$K_3 = +\frac{2M^2L}{A} \frac{\partial^2}{\partial \eta \partial \zeta} \Delta \Phi + \frac{B'}{A} \left(\frac{\partial^4 \Phi}{\partial \xi^2 \partial \eta \partial \zeta} + \frac{\partial^4 \Phi}{\partial \eta^3 \partial \zeta} \right) \quad (53f)$$

with the abbreviations:

$$\left. \begin{aligned} A' &= M^2(L+N) = \mu^2(2\lambda+2\mu+\mu') \\ B' &= ML(N-L) = \mu\mu'(\lambda+\mu) \end{aligned} \right\} \quad (54)$$

For A, B, C , see (11).

In the case of the isotropic substance, for which $\mu' = 0, N = L$, we have:

$$B = B' = C = 0;$$

$$A'/A = 2M^2L/A = 2(\lambda+\mu)/(\lambda+2\mu);$$

$$\Phi = r^3/96\pi; \quad \Delta \Phi = r/8\pi; \quad \Delta^2 \Phi = 1/4\pi r,$$

and the expressions become identical with those given in Part I, eqs. (21).

It is possible to transform the surface integral occurring in the expression for u still further. For this purpose we introduce two functions P, Q , defined by the following integrals:

$$Q = \frac{1}{8\pi^3} \iiint da \, d\beta \, d\gamma \frac{E}{\varrho^2} \quad (55)$$

$$P = \frac{1}{8\pi^3} \iiint da \, d\beta \, d\gamma \frac{C\beta^2\gamma^2}{A\varrho^2} E \quad (56)$$

where E now stands for the exponential function:

$$E = e^{i[\alpha(\xi-x) + \beta(\eta-y) + \gamma(\zeta-z)]}$$

The integral for Q can be worked out quite easily and gives:

$$Q = \frac{1}{2\pi^2 r} \int_{\varrho_I}^{\varrho_{II}} d\varrho \frac{\sin(\varrho r)}{\varrho} = \frac{1}{4\pi r} \cdot \cdot \cdot \cdot \cdot \quad (55a)$$

We then have the following relations:

$$\Delta^2 \Phi + \frac{B}{A} \left(\frac{\partial^4}{\partial \xi^2 \partial \eta^2} + \dots + \dots \right) \Phi = \frac{\partial^2 P}{\partial \xi^2} + Q \quad \cdot \cdot \cdot \quad (57a)$$

$$\frac{C}{A} \frac{\partial^4 \Phi}{\partial \eta^2 \partial \xi^2} = -\Delta P \quad \cdot \cdot \cdot \cdot \cdot \quad (57b)$$

The surface integral occurring in (52a) consequently can be written:

$$\iint d\Sigma \left\{ \frac{\partial Q}{\partial \nu} + \frac{\partial}{\partial \nu} \left(\frac{\partial^2 P}{\partial \xi^2} \right) - (\nu_\xi^\xi) \frac{\partial}{\partial \xi} \Delta P \right\}$$

and this expression can be transformed into:

$$\frac{1}{4\pi} \iint d\Sigma \frac{\partial}{\partial \nu} \left(\frac{1}{r} \right) + \int d\sigma \left(\frac{\partial^2 P}{\partial \xi d\zeta} \frac{d\eta}{d\sigma} - \frac{\partial^2 P}{\partial \xi \partial \eta} \frac{d\zeta}{d\sigma} \right).$$

When we introduce the hydrodynamic potential φ , defined by eq. (5) of Part I, we finally obtain:

$$u = \varphi + \int d\sigma \left\{ \left(G_2 + \frac{\partial^2 P}{\partial \xi \partial \zeta} \right) \frac{d\eta}{d\sigma} + \left(G_3 - \frac{\partial^2 P}{\partial \xi \partial \eta} \right) \frac{d\zeta}{d\sigma} \right\} \quad \cdot \quad (58)$$

The presence of the potential φ in this expression introduces the desired multi-valued character of the function u , while the fact that all other terms of u are expressed by means of integrals along the line σ proves that u is independent of the position given to the surface Σ , and that its derivatives are continuous at Σ . — As according to (52b) and (52c) ν and w can be wholly expressed by integrals along σ , the latter result applies also to them.

For purposes of calculation it is convenient to introduce a function R defined by:

$$R = -\frac{1}{8\pi^3} \iiint da d\beta d\gamma \frac{E}{\varrho^2 \mathbf{D}} \quad \cdot \cdot \cdot \cdot \cdot \quad (59)$$

so that:

$$P = -\frac{C}{A} \frac{\partial^4 R}{\partial \eta^2 \partial \xi^2} \quad \cdot \cdot \cdot \cdot \cdot \quad (60)$$

The function R is connected with Φ by the relation:

$$\Phi = \Delta R.$$

Applying the method of calculation explained in section 5, we find:

$$R = \frac{r^5}{4\pi} \left\{ \frac{c_0 A_0}{720} + \frac{c_4 A_4}{3840} - \frac{c_6 A_6}{46080} \dots \right\} \quad (61)$$

where $c_0, c_4, \dots A_0, A_4, \dots$ are the quantities occurring in (32); A_0, A_4, \dots being explicitly given by eqs. (35). — Equation (58) then takes the form:

$$u = \varphi + \int d\sigma \left\{ \left(G_2 - \frac{C}{A} \frac{\partial^6 R}{\partial \xi \partial \eta^2 \partial \zeta^3} \right) \frac{d\eta}{d\sigma} + \left(G_3 + \frac{C}{A} \frac{\partial^6 R}{\partial \xi \partial \eta^3 \partial \zeta^2} \right) \right\}. \quad (58a)$$

11. Application of the results obtained to the determination of the fields connected with some simple types of dislocations. — The formulae developed in the preceding sections refer to the case in which the displacement component u possesses a cyclic constant equal to unity for every closed line embracing the singular line σ characteristic of the dislocation, whereas the components v, w are single-valued. Although it is not difficult to generalize the equations, in the following examples we will restrict to dislocations of this kind.

A. For a segment of a singular line which is parallel to the x -axis all integrals with respect to $d\sigma$ vanish, as will be evident from (58a), (52b), (52c).

In the particular case of an infinite straight line parallel to the x -axis the expressions for u, v, w reduce to:

$$\left. \begin{aligned} u &= \varphi \\ v &= 0 \\ w &= 0 \end{aligned} \right\} \quad \dots \dots \dots (62)$$

with:

$$\varphi = -\frac{1}{2\pi} \operatorname{arctg} \frac{z}{y} + \text{const.} \quad (62a)$$

The elastic constants have disappeared from this result, which is identical with that for the isotropic substance in the same case, as given in Part I, eqs. (26) and (27). As for this solution:

$$\partial u / \partial x = 0, \quad \theta = 0,$$

it will be evident that it satisfies eqs. (4) above with $X=Y=Z=0$, independently of the values of λ, μ, μ' .

B. For a segment of a singular line parallel to the z -axis, extending from ζ_I to ζ_{II} ($\zeta_I < \zeta_{II}$), the integrals with respect to $d\sigma$ become¹¹⁾

¹¹⁾ The same as in Part I, section 11 A, we must take the factor $d\xi/d\sigma$ to be equal to -1 . When this value has been substituted, the integration with respect to $d\sigma$ further

$$\text{in } u : - \int_{\xi_I}^{\xi_{II}} d\xi \left[\frac{A'}{A} \frac{\partial^2}{\partial \xi \partial \eta} \Delta \Phi + \frac{B}{A} \frac{\partial^4 \Phi}{\partial \xi \partial \eta^3} \right] - \left. \frac{B+B'}{A} \frac{\partial^3 \Phi}{\partial \xi \partial \eta \partial \zeta} \right|_I^{II} - \left. \frac{C}{A} \frac{\partial^5 R}{\partial \xi \partial \eta^3 \partial \zeta} \right|_I^{II} \quad (63a)$$

$$\text{in } v : + \int_{\xi_I}^{\xi_{II}} d\xi \left[\Delta^2 \Phi - \frac{A'}{A} \frac{\partial^2}{\partial \eta^2} \Delta \Phi \right] + \left. \frac{B}{A} \frac{\partial^3 \Phi}{\partial \xi^2 \partial \zeta} \right|_I^{II} - \left. \frac{B'}{A} \frac{\partial^3 \Phi}{\partial \eta^2 \partial \zeta} \right|_I^{II} \quad (63b)$$

$$\text{in } w : - \frac{2M^2 L}{A} \frac{\partial}{\partial \eta} \Delta \Phi \Big|_I^{II} - \frac{B'}{A} \left(\frac{\partial^3 \Phi}{\partial \xi^2 \partial \eta} + \frac{\partial^3 \Phi}{\partial \eta^3} \right) \Big|_I^{II} \quad (63c)$$

When the line is of infinite extent, all integrated terms in (63a), (63b), (63c) will vanish; all these terms indeed are of degree zero, while each one of them at least contains either a factor $(\hat{x}-\xi)/r$ or a factor $(y-\eta)/r$, which vanishes for $r \rightarrow \infty$. This case corresponds to that in which an extra layer of atoms is introduced along the half plane $x=0$, $y > 0$ (see Part I, fig. 1, and section 11, A). The expressions for u , v , w become ¹²⁾:

$$u = \varphi - \int_{-\infty}^{+\infty} d\xi \left[\frac{A'}{A} \frac{\partial^2}{\partial \xi \partial \eta} \Delta \Phi + \frac{B}{A} \frac{\partial^4 \Phi}{\partial \xi \partial \eta^3} \right] \quad (64a)$$

$$v = + \int_{-\infty}^{+\infty} d\xi \left[\Delta^2 \Phi - \frac{A'}{A} \frac{\partial^2}{\partial \eta^2} \Delta \Phi \right] \quad (64b)$$

$$w = 0 \quad (64c)$$

can be replaced by one with respect to $d\xi$ with the limits inverted, so that we integrate from $\xi = \xi_I$ to $\xi = \xi_{II}$.

¹²⁾ In order to prove that the expressions (64a) — (64c) satisfy the equations (4) (with $X=Y=Z=0$) we observe that differentiations with respect to x and y can be replaced by differentiations with respect to $-\xi$ and $-\eta$, performed under the integral sign; and further that terms containing derivatives with respect to ξ can be discarded, as they vanish in consequence of the integration with respect to $d\xi$.

Now from (64a) — (64c) we obtain:

$$\begin{aligned} \Delta u &= - \int d\xi \left[\frac{A'}{A} \frac{\partial^2}{\partial \xi \partial \eta} \Delta^2 \Phi + \frac{B}{A} \frac{\partial^4}{\partial \xi \partial \eta^3} \Delta \Phi \right] \\ \frac{\partial^2 u}{\partial x^2} &= \frac{xy}{\pi(x^2+y^2)^2} - \int d\xi \left[\frac{A'}{A} \frac{\partial^4}{\partial \xi^3 \partial \eta} \Delta \Phi + \frac{B}{A} \frac{\partial^6 \Phi}{\partial \xi^3 \partial \eta^3} \right] \\ \theta &= - \frac{y}{2\pi(x^2+y^2)} + \int d\xi \left[\frac{A'}{A} \left(\frac{\partial^3}{\partial \xi^2 \partial \eta} + \frac{\partial^3}{\partial \eta^3} \right) \Delta \Phi + \frac{B}{A} \frac{\partial^5 \Phi}{\partial \xi^2 \partial \eta^3} - \frac{\partial}{\partial \eta} \Delta^2 \Phi \right] \end{aligned}$$

with:

$$\varphi = \frac{1}{2\pi} \operatorname{arctg} \frac{y}{x} + \text{const.} \quad . \quad . \quad . \quad . \quad . \quad (64d)$$

In the case of the isotropic substance these expressions reduce to eqs. (25) of Part I.

C. The value of stress component σ_{xz} ($=\sigma_{13}$) for a dislocation as considered in Part I, sections 17–19 (compare figs. 9, 10 of Part I) is given by the expression:

$$\sigma_{xz} = \mu \left(\frac{\partial w}{\partial x} + \frac{\partial u}{\partial z} \right).$$

When the expressions (58a) and (52c) are substituted for u and w , the differentiations with respect to x and z can be replaced by such with respect to $-\xi$ and $-\zeta$, performed before carrying out the integration. In this way it is possible to obtain a formula of the following type:

$$\sigma_{xz} = \mu \frac{\partial \varphi}{\partial z} + \mu \int d\sigma \left[G' \frac{d\eta}{d\sigma} + G'' \frac{d\zeta}{d\sigma} \right] \quad . \quad . \quad . \quad . \quad (65)$$

where the quantities G', G'' are built up from terms each of which contains an uneven number of differentiations with respect to ξ . As the only segments which contribute to the line-integral are CB, BA, AF

Substituting these results into the first one of eqs. (4), and again having regard to the above observations, we obtain:

$$\begin{aligned} & (\lambda + \mu + \mu') \pi \frac{xy}{(x^2 + y^2)^2} - \\ & - \frac{\partial^2}{\partial x \partial y} \int d\zeta \left[+ \frac{\mu A'}{A} \Delta^2 \Phi + \left(\frac{\mu B}{A} \frac{\partial^2}{\partial \eta^2} + \frac{\mu' A'}{A} \frac{\partial^2}{\partial \xi^2} \right) \Delta \Phi + \frac{\mu' B}{A} \frac{\partial^4 \Phi}{\partial \xi^2 \partial \eta^2} + \right. \\ & \quad \left. + \frac{(\lambda + \mu) A'}{A} \left(\frac{\partial^2}{\partial \xi^2} + \frac{\partial^2}{\partial \eta^2} \right) \Delta \Phi + \frac{(\lambda + \mu) B}{A} \frac{\partial^4 \Phi}{\partial \xi^2 \partial \eta^2} - (\lambda + \mu) \Delta^2 \Phi \right]. \end{aligned}$$

As $\frac{\partial^2}{\partial \xi^2} + \frac{\partial^2}{\partial \eta^2}$ may be replaced by Δ under the integral sign, this expression can be reduced to:

$$N \frac{xy}{\pi(x^2 + y^2)^2} - \frac{\partial^2}{\partial x \partial y} \int d\zeta \left[N \Delta^2 \Phi + \frac{NB}{A} \frac{\partial^4 \Phi}{\partial \xi^2 \partial \eta^2} \right].$$

On the other hand from (57a), having regard to (60), we deduce:

$$\int d\zeta \left[\Delta^2 \Phi + \frac{B}{A} \frac{\partial^4 \Phi}{\partial \xi^2 \partial \eta^2} \right] = \int Q d\zeta = -\frac{1}{2\pi} \ln \sqrt{x^2 + y^2} + \text{const.},$$

provided the same method of approximation is applied as was used in eq. (24b) of Part I.

By means of this result it is not difficult to prove that the first one of eqs. (4) is satisfied.

and $F'E'$, $E'D'$, $D'C'$, it will be seen that the contribution of each of these sets of segments is zero at points situated in the plane of the set considered, while outside this plane it vanishes at least inversely proportional to the square of the distance, as all terms are of degree -2 . Hence, when the length $FF' = L$ is sufficiently great in comparison with $F'C' = l$, we may write, just as for the isotropic body:

in points of the plane of the rectangle $F'E'D'C'$:

$$\sigma_{xz} = \frac{\mu l}{4\pi} \frac{y^2 - z^2 - l^2/4}{(y^2 + z^2 + l^2/4)^2 - y^2 l^2} \quad \cdot \quad \cdot \quad \cdot \quad \cdot \quad \cdot \quad (66a)$$

and in points situated in the neighbourhood of the central part of $FF'C'C$:

$$\sigma_{xz} = \frac{\mu l}{4\pi} \frac{y^2 - z^2 - l^2/4}{(y^2 + z^2 + l^2/4)^2 - y^2 l^2} (\cos \beta_1 + \cos \beta_2) \quad \cdot \quad \cdot \quad (66b)$$

The examples considered will have shown that the expressions derived for the stresses in the preceding sections give sufficient means for investigating the fields connected with simple dislocations, while it has been found, moreover, that in a number of cases the difference between the formulae for the isotropic substance and those for the regular crystalline substance even wholly vanishes.

12. *Appendix.* — Values of the (reciprocal) elastic constants for regular and other crystals have been given e. g. by P. W. BRIDGMAN, Proc. Amer. Acad. of Arts and Sciences (Boston) **60**, p. 332, 1925; **64**, p. 35, 1929. For other data the reader may be referred to LANDOLT-BÖRNSTEIN, Physik.-Chem. Tabellen, 3. Erg. Band (Berlin 1935), p. 74.

As instances of regular crystals *tungsten* (Wo) and *sylvine* (KCl) may be mentioned.

For *tungsten* BRIDGMAN gives (in c. g. s.-units):

$$s_{11} = +2,534.10^{-13}; \quad s_{12} = -0,726.10^{-13}; \quad s_{44} = +6,55.10^{-13}.$$

From these data we find:

$$\lambda + 2\mu + \mu' = c_{11} = 5,12.10^{12} \text{ c. g. s.}$$

$$\lambda = c_{12} = 2,06.10^{12}$$

$$\mu = c_{44} = 1,53.10^{12}$$

and:

$$\mu' = c_{11} - c_{12} - 2c_{44} = 0.$$

Hence in the case of *tungsten* the equations for isotropic elastic substances are valid. We further have:

$$M = 1,53.10^{12}; \quad L = N = 3,59.10^{12}$$

$$A = 12,0 \cdot 10^{36}; \quad B = C = 0.$$

For *sylvine* BRIDGMAN gives (in c. g. s.-units):

$$s_{11} = +0,294.10^{-11}; s_{12} = -0,053.10^{-11}; s_{44} = +1,27.10^{-11}.$$

From these data we find:

$$\lambda + 2\mu + \mu' = c_{11} = 3,70.10^{11} \text{ c. g. s.}$$

$$\lambda = c_{12} = 0,81.10^{11}$$

$$\mu = c_{44} = 0,79.10^{11}$$

and:

$$\mu' = c_{11} - c_{12} - 2c_{44} = 1,31.10^{11}.$$

The practical equality of c_{12} and c_{44} proves that *sylvine* satisfies the Cauchy relation. The elastic constant μ' , however, is very large, so that there is no approximation to isotropy. We obtain:

$$M = 0,79.10^{11}; L = 1,60.10^{11}; N = 2,91.10^{11}$$

$$A = 2,3 \cdot 10^{33}; B = 4,7 \cdot 10^{33}; C = 10,5 \cdot 10^{33}.$$

Mathematics. — *Sur un problème de WARING généralisé. II.* Par
J. G. VAN DER CORPUT et CH. PISOT.

(Communicated at the meeting of April 29, 1939.)

Dans la deuxième partie du paragraphe 2, nous démontrerons que la condition citée (p. 349) est suffisante pour que l'inégalité (3) soit vérifiée. Nous allons d'abord démontrer un lemme.

Lemme 2: Soit $\theta(y)$ une fonction arbitraire, nous désignerons par $\triangle_h \theta(y)$ l'expression $\theta(y + u_h) - \theta(y)$ où u_h est un entier auxiliaire. Si ⁴⁾ alors $f_\delta(y)$ est un polynôme en y de degré effectif $k \equiv h$, à coefficients entiers,

$$\triangle_1 \triangle_2 \dots \triangle_h f_\delta(y) = u_1 u_2 \dots u_h F_\delta(y, u_1, \dots, u_h),$$

où $F_\delta(y, u_1, \dots, u_h)$ est un polynôme en y, u_1, \dots, u_h de degré $k-h$ exactement en y , à coefficients entiers.

Soient h et r deux entiers tels que $2 \equiv h \equiv r \equiv k$. Posons $g = 2^{h-3}$ et $d = 2^{r-2}$. Soient b'_μ et $b'_{\mu\lambda}$ ($\mu = 1, 2, \dots, m; \lambda = d+1, \dots, l$) des entiers donnés.

Désignons par N'_δ le nombre de solutions $(y_1, z_1, \dots, y_l, z_l)$ du système :

$$\left. \begin{aligned} b'_\mu \sum_{\lambda=1}^d (f_\delta(y_\lambda) - f_\delta(z_\lambda)) + \sum_{\lambda=d+1}^l b'_{\mu\lambda} (f_\lambda(y_\lambda) - f_\lambda(z_\lambda)) &= 0 \quad (\mu = 1, 2, \dots, m) \\ |f_\delta(y_\lambda)| &\leq X, \quad |f_\delta(z_\lambda)| \leq X \quad (\lambda = 1, 2, \dots, d) \\ |f_\lambda(y_\lambda)| &\leq X, \quad |f_\lambda(z_\lambda)| \leq X \quad (\lambda = d+1, \dots, l) \end{aligned} \right\} \quad (19)$$

Enfin soit $T(h, r)$ le nombre de solutions

$$(y, u_1, \dots, u_{h-1}, y_{2g+1}, z_{2g+1}, \dots, y_l, z_l)$$

du système

$$\left. \begin{aligned} b'_\mu \triangle_1 \triangle_2 \dots \triangle_{h-1} f_\delta(y) &= b'_\mu \sum_{\lambda=2g+1}^d (f_\delta(y_\lambda) - f_\delta(z_\lambda)) + \sum_{\lambda=d+1}^l b'_{\mu\lambda} (f_\lambda(y_\lambda) - f_\lambda(z_\lambda)) \\ &\quad (\mu = 1, \dots, m) \\ |f_\delta(y)| &\leq X, \quad |\triangle_1 \triangle_2 \dots \triangle_{\eta} f_\delta(y)| \leq 2^\eta X \quad (\eta = 1, 2, \dots, h-1) \\ |f_\delta(y_\lambda)| &\leq X, \quad |f_\delta(z_\lambda)| \leq X \quad (\lambda = 2g+1, \dots, d) \\ |f_\lambda(y_\lambda)| &\leq X, \quad |f_\lambda(z_\lambda)| \leq X \quad (\lambda = d+1, \dots, l). \end{aligned} \right\} \quad (20)$$

⁴⁾ Il va sans dire que nous pourrions supprimer l'indice δ dans ce lemme, mais cet indice nous sera utile plus loin.

Alors on a l'inégalité

$$N'_\delta \leq c_5 X^{\frac{4g-h}{k}} T(h, r) \text{ pour } 2 \leq h \leq r \leq k. \quad (21)$$

où c_5 est constant, c. à d. indépendant de X .

L'artifice de la démonstration consiste à trouver, grâce à l'inégalité de CAUCHY, une borne supérieure pour N'^2_δ contenant en facteur N'_δ . Nous ferons la démonstration par récurrence sur h .

L'inégalité (21) est évidente pour $h=2$. En effet en posant $z_1=y+u_1$, $y_1=y$, tout système vérifiant (19) satisfait à (20) avec $h=2$. Donc $N'_\delta \leq T(2, r)$.

Supposons alors le lemme 2 démontré pour $h-1$ au lieu de h . $T(h-1, r)$ est le nombre de solutions $(y, u_1, \dots, u_{h-2}, y_{g+1}, z_{g+1}, \dots, y_l, z_l)$ vérifiant le système (20) avec $h-1$ au lieu de h , ce que nous pouvons écrire

$$\begin{aligned} b'_\mu \triangle_1 \triangle_2 \dots \triangle_{h-2} f_\delta(y) + b'_\mu \sum_{\lambda=2g+1}^d f_\delta(z_\lambda) + \sum_{\lambda=d+1}^l b'_{\mu\lambda} f_\lambda(z_\lambda) = \\ b'_\mu \sum_{\lambda=g+1}^{2g} (f_\delta(y_\lambda) - f_\delta(z_\lambda)) + b'_\mu \sum_{\lambda=2g+1}^d f_\delta(y_\lambda) + \sum_{\lambda=d+1}^l b'_{\mu\lambda} f_\lambda(y_\lambda) \quad (\mu=1, \dots, m) \\ |f_\delta(y)| \leq X, \quad |\triangle_1 \triangle_2 \dots \triangle_\eta f_\delta(y)| \leq 2^\eta X \quad (\eta=1, 2, \dots, h-2) \\ |f_\delta(y_\lambda)| \leq X, \quad |f_\delta(z_\lambda)| \leq X \quad (\lambda=g+1, \dots, d) \\ |f_\lambda(y_\lambda)| \leq X, \quad |f_\lambda(z_\lambda)| \leq X \quad (\lambda=d+1, \dots, l). \end{aligned}$$

Soit u le système $(u_1, u_2, \dots, u_{h-2})$, considérons encore le système $v=(v_1, \dots, v_m)$ de m entiers auxiliaires donnés. Désignons par $R(u, v)$ le nombre de systèmes $(y, z_{2g+1}, \dots, z_l)$ tels que

$$\begin{aligned} b'_\mu \triangle_1 \triangle_2 \dots \triangle_{h-2} f_\delta(y) + b'_\mu \sum_{\lambda=2g+1}^d f_\delta(z_\lambda) + \sum_{\lambda=d+1}^l b'_{\mu\lambda} f_\lambda(z_\lambda) = v_\mu \quad (\mu=1, \dots, m) \\ |f_\delta(y)| \leq X, \quad |\triangle_1 \triangle_2 \dots \triangle_\eta f_\delta(y)| \leq 2^\eta X \quad (\eta=1, 2, \dots, h-2) \\ |f_\delta(z_\lambda)| \leq X \quad (\lambda=2g+1, \dots, d), \quad |f_\lambda(z_\lambda)| \leq X \quad (\lambda=d+1, \dots, l) \end{aligned}$$

et désignons par $R(v)$ le nombre de systèmes $(y_{g+1}, \dots, y_l, z_{g+1}, \dots, z_{2g})$ tels que

$$\begin{aligned} b'_\mu \sum_{\lambda=g+1}^{2g} (f_\delta(y_\lambda) - f_\delta(z_\lambda)) + b'_\mu \sum_{\lambda=2g+1}^d f_\delta(y_\lambda) + \sum_{\lambda=d+1}^l b'_{\mu\lambda} f_\lambda(y_\lambda) = v_\mu \quad (\mu=1, \dots, m) \\ |f_\delta(y_\lambda)| \leq X \quad (\lambda=g+1, \dots, d) \quad |f_\lambda(y_\lambda)| \leq X \quad (\lambda=d+1, \dots, l) \\ |f_\delta(z_\lambda)| \leq X \quad (\lambda=g+1, \dots, 2g). \end{aligned}$$

On a

$$T(h-1, r) = \sum_{u, v} R(u, v) R(v)$$

où $\sum_{u,v}$ est étendu aux systèmes u et v possibles. L'inégalité de CAUCHY donne

$$(T(h-1, r))^2 \leq \sum_{u,v} R^2(u, v) \sum_{u,v} R^2(v) \dots \dots \dots (22)$$

Or $\sum_{u,v} R^2(u, v)$ est le nombre de systèmes

$$(y, y', u_1, \dots, u_{h-2}, z_{2g+1}, z'_{2g+1}, \dots, z_l, z'_l)$$

tels que

$$b'_\mu \Delta_1 \dots \Delta_{h-2} f_\partial(y) + b'_\mu \sum_{\lambda=2g+1}^d f_\partial(z_\lambda) + \sum_{\lambda=d+1}^l b'_{\mu\lambda} f_\lambda(z_\lambda) =$$

$$b'_\mu \Delta_1 \dots \Delta_{h-2} f_\partial(y') + b'_\mu \sum_{\lambda=2g+1}^d f_\partial(z'_\lambda) + \sum_{\lambda=d+1}^l b'_{\mu\lambda} f_\lambda(z'_\lambda) \quad (\mu=1, \dots, m)$$

$$|f_\partial(y)| \leq X, |f_\partial(y')| \leq X, |\Delta_1 \dots \Delta_\eta f_\partial(y)| \leq 2^\eta X, |\Delta_1 \dots \Delta_\eta f_\partial(y')| \leq 2^\eta X$$

$$(\eta = 1, \dots, h-2)$$

$$|f_\partial(z_\lambda)| \leq X, |f_\partial(z'_\lambda)| \leq X \quad (\lambda = 2g+1, \dots, d)$$

$$|f_\lambda(z_\lambda)| \leq X, |f_\lambda(z'_\lambda)| \leq X \quad (\lambda = d+1, \dots, l).$$

Posons $y = y' + u_{h-1}$, alors on a

$$b'_\mu \Delta_1 \dots \Delta_{h-2} f_\partial(y) - b'_\mu \Delta_1 \dots \Delta_{h-2} f_\partial(y') = b'_{\mu l} \Delta_1 \dots \Delta_{h-1} f_\partial(y')$$

et on voit que $\sum_{u,v} R^2(u, v) \leq T(h, r)$.

De même $\sum_v R^2(v)$ est le nombre de solutions

$$(y_{g+1}, y'_{g+1}, \dots, y_l, y'_l, z_{g+1}, z'_{g+1}, \dots, z_{2g}, z'_{2g})$$

du système

$$b'_\mu \sum_{\lambda=g+1}^{2g} (f_\partial(y_\lambda) - f_\partial(z_\lambda)) + b'_\mu \sum_{\lambda=2g+1}^d f_\partial(y_\lambda) + \sum_{\lambda=d+1}^l b'_{\mu\lambda} f_\lambda(y_\lambda) =$$

$$b'_\mu \sum_{\lambda=g+1}^{2g} (f_\partial(y'_\lambda) - f_\partial(z'_\lambda)) + b'_\mu \sum_{\lambda=2g+1}^d f_\partial(y'_\lambda) + \sum_{\lambda=d+1}^l b'_{\mu\lambda} f_\lambda(y'_\lambda) \quad (\mu=1, \dots, m)$$

$$|f_\partial(y_\lambda)| \leq X, |f_\partial(y'_\lambda)| \leq X \quad (\lambda = g+1, \dots, d)$$

$$|f_\lambda(y_\lambda)| \leq X, |f_\lambda(y'_\lambda)| \leq X \quad (\lambda = d+1, \dots, l)$$

$$|f_\partial(z_\lambda)| \leq X, |f_\partial(z'_\lambda)| \leq X \quad (\lambda = g+1, \dots, 2g).$$

Nous retrouvons donc le système (19) et $\sum_v R^2(v) = N'_\partial$. C'est d'ici que provient le facteur N'_∂ qui figure, comme nous l'avons annoncé, dans la borne supérieure pour N_∂^2 .

Il suit de (20) qu'il existe une constante c_6 telle que

$$|u_\eta| \leq c_6 X^{\frac{1}{k}} (\eta = 1, 2, \dots, h-2).$$

Le système $u = (u_1, \dots, u_{h-2})$ prend donc au plus $c_7 X^{\frac{h-2}{k}}$ valeurs et l'on a

$$\sum_{u,v} R^2(v) \leq c_7 X^{\frac{h-2}{k}} N'_o.$$

L'inégalité (22) devient donc

$$(T(h-1, r))^2 \leq c_7 X^{\frac{h-2}{k}} T(h, r) N'_o.$$

En portant cette valeur dans l'inégalité (21) avec $h-1$ au lieu de h , il vient

$$N_o'^2 \leq c_8 X^{2\frac{2g-h+1}{k}} c_7 X^{\frac{h-2}{k}} T(h, r) N'_o$$

c'est à dire

$$N'_o \leq c_5 X^{\frac{4g-h}{k}} T(h, r)$$

et le lemme 2 est démontré.

Pour démontrer que la condition citée (p. 349) est suffisante pour que l'inégalité (3) soit vérifiée, nous sommes obligés de démontrer un résultat plus général, à savoir le suivant⁵⁾:

Lemme 3: Soit r un entier arbitraire avec $1 \leq r \leq k$ et soit

$$l \geq (2^{k-1} - 1)(m-1) + 2^{r-1} \text{ si } k \geq 3$$

et

$$l \geq 2(m-1) + 2^{r-1} \text{ si } k = 2.$$

Il existe alors au moins un ensemble $E_m(r)$ tel que tous les entiers figurant dans $E_m(r)$ soient au plus égaux à l . Pour chaque matrice B telle que les déterminants $D(v_1, \dots, v_m)$ définis par (8) soient $\neq 0$ pour tous les systèmes (v_1, \dots, v_m) de l'ensemble $E_m(r)$, on a l'inégalité

$$N \leq C_8 X^{\frac{2l}{k} - m + 1 - \frac{r}{k} + \varepsilon} \dots \dots \dots (23)$$

L'inégalité (3) est le cas particulier $r = k$ de l'inégalité (23).

⁵⁾ Remarque ajoutée à la correction de l'épreuve: Le cas particulier $m = 1$ a déjà été traité par M. LOO-KENG HUA, Quarterly Journal of Mathematics, Oxford Series, 9, p. 199-202 (1938).

Démontrons d'abord l'existence d'un ensemble $E_m(r)$ avec la propriété considérée. Soit $a_m(r)$ le plus petit nombre d'entiers qui permettent de former un ensemble $E_m(r)$. D'après la définition de $E_m(r)$, on a

$$a_m(r) = 2^{r-2} + \max \{a_{m-1}(k), a_m(r-1)\}$$

quand $m \geq 2$ et $2 \leq r \leq k$. Cette égalité entraîne de proche en proche

$$\begin{aligned} a_m(r) &= 2^{r-2} + 2^{r-3} + \dots + 2^0 + \max \{a_{m-1}(k), a_m(1)\} \\ &= 2^{r-1} - 1 + \max \{a_{m-1}(k), a_m(1)\}. \end{aligned}$$

Or d'après la définition de $E_m(1)$ on voit que $a_m(1) = 2 + a_{m-1}(k-1)$, donc

$$a_m(r) = 2^{r-1} - 1 + \max \{a_{m-1}(k), a_{m-1}(k-1) + 2\}.$$

Cette formule montre pour $m \geq 2$ la relation

$$a_m(k) = a_m(k-1) + 2^{k-1} - 2^{k-2}$$

qui est aussi vérifiée pour $m = 1$.

Or on a $2^{k-1} - 2^{k-2} \geq 2$ ou < 2 selon que $k \geq 3$ ou $k = 2$. Nous trouvons ainsi

$$\begin{aligned} a_m(r) &= 2^{r-1} - 1 + a_{m-1}(k) \text{ si } k \geq 3 \text{ et} \\ a_m(r) &= 2^{r-1} - 1 + a_{m-1}(k-1) + 2 \text{ si } k = 2. \end{aligned}$$

Si $k \geq 3$ et $m \geq 3$, on a donc

$$a_{m-1}(k) - a_{m-2}(k) = 2^{k-1} - 1 \text{ et } a_1(k) = 2^{k-1},$$

d'où

$$\begin{aligned} a_{m-1}(k) &= (2^{k-1} - 1)(m-1) + 1 \text{ et par conséquent} \\ a_m(r) &= (2^{k-1} - 1)(m-1) + 2^{r-1}. \end{aligned}$$

Cette dernière égalité est aussi valable pour $m = 1$ et 2 .

Si $k = 2$ et $m \geq 3$, on a

$$a_{m-1}(k-1) - a_{m-2}(k-1) = 2^{k-2} + 1 \text{ et } a_1(k-1) = 2^{k-2}$$

d'où

$$\begin{aligned} a_{m-1}(k-1) &= (2^{k-2} + 1)(m-1) - 1 \text{ et par conséquent} \\ a_m(r) &= (2^{k-2} + 1)(m-1) + 2^{r-1}, \text{ c'est à dire comme } k = 2 \\ a_m(r) &= 2(m-1) + 2^{r-1}. \end{aligned}$$

Cette dernière égalité est aussi valable pour $m = 1$ et 2 .

où

$$N_{\hat{c}} = \int_0^1 \int_0^1 \dots \int_0^1 |S_{\hat{c}}|^{2d} |S_{d+1} \dots S_l|^2 da$$

$N_{\hat{c}}$ est donc le nombre de solutions d'un système déduit de (2) en remplaçant la matrice B définie p. 348 par la matrice

$$B_{\hat{c}} = \begin{pmatrix} b_{1\hat{c}} & \dots & b_{l\hat{c}} & b_{1,d+1} & \dots & b_{l,d+1} \\ \cdot & \cdot & \cdot & \cdot & \cdot & \cdot \\ \cdot & \cdot & \cdot & \cdot & \cdot & \cdot \\ \underbrace{b_{m\hat{c}} \dots b_{m\hat{c}}}_d & \dots & b_{m\hat{c}} & b_{m,d+1} & \dots & b_{m,d+1} \end{pmatrix}$$

et les fonctions f_1, f_2, \dots, f_d par $f_{\hat{c}}$.

Or chaque solution de ce système est aussi solution du système (19) figurant dans le lemme 2 où les entiers b'_{μ} et $b'_{\mu\lambda}$ ont les valeurs définies par (26). Nous avons donc $N_{\hat{c}} \leq N'_{\hat{c}}$, d'où $N \leq \sum_{\hat{c}=1}^d N'_{\hat{c}}$. Or le lemme 2 appliqué avec $h=r$ nous donne pour $2 \leq r \leq k$

$$N'_{\hat{c}} \leq c_9 X^{\frac{2d-r}{k}} T(r, r).$$

Au lieu de (23) il suffit donc de démontrer que

$$N'_{\hat{c}} \leq C_9 X^{\frac{2l}{k} - m + 1 - \frac{1}{k} + \varepsilon} \text{ si } r=1 \quad . \quad . \quad . \quad . \quad . \quad (27)$$

et

$$T(r, r) \leq C_{10} X^{\frac{2l-2d}{k} - m + 1 + \varepsilon} \text{ si } 2 \leq r \leq k. \quad . \quad . \quad . \quad . \quad . \quad (28)$$

L'inégalité (23) est vérifiée pour $m=1$, $r=1$, $l=1$. En effet l'ensemble $E_1(1)$ se compose du seul entier $v_1=1$. D'après l'hypothèse on a $b_{11} \neq 0$; considérons les relations (2) qui prennent dans ce cas la forme:

$$b_{11}(f_1(y_1) - f_1(z_1)) = 0, \quad |f_1(y_1)| \leq X, \quad |f_1(z_1)| \leq X.$$

D'après la dernière inégalité z_1 prend au plus $c_{10} X^{\frac{1}{k}}$ valeurs, et pour une valeur donnée de z_1 , la première relation montre que y_1 prend au plus k valeurs, donc le système (y_1, z_1) prend au plus $k c_{10} X^{\frac{1}{k}} = c_{11} X^{\frac{1}{k}}$ valeurs. En vertu du lemme 1, on a donc pour $m=1$, $r=1$ et $l \leq 1$ l'inégalité

$$N \leq c_{12} X^{\frac{2l-1}{k}}.$$

Le lemme 3 est démontré dans ce cas.

Pour démontrer le lemme 3 dans le cas général, nous le supposons démontré pour tous les systèmes de m' équations et avec un nombre r' au lieu de r tels que l'on ait ou bien $m' \equiv m-1$, $1 \equiv r' \equiv k$ ou bien $m' = m$, $1 \equiv r' \equiv r-1$.

1. $m \equiv 2$, $r = 1$. Nous devons démontrer l'inégalité (27). Pour cela écrivons le système (19) sous la forme suivante

$$b'_1(f_{\bar{v}}(z_1) - f_{\bar{v}}(y_1) + f_{\bar{v}}(z_2) - f_{\bar{v}}(y_2)) = \sum_{\lambda=3}^l b'_{1\lambda}(f_{\lambda}(y_{\lambda}) - f_{\lambda}(z_{\lambda})) \left(\begin{array}{c} |f_{\bar{v}}(z_1)| \leq X, |f_{\bar{v}}(y_1)| \leq X, |f_{\bar{v}}(z_2)| \leq X, |f_{\bar{v}}(y_2)| \leq X \end{array} \right) \quad (29)$$

$$0 = \sum_{\lambda=3}^l b'_{\mu\lambda}(f_{\lambda}(y_{\lambda}) - f_{\lambda}(z_{\lambda})) \quad (\mu = 2, 3, \dots, m) \left(\begin{array}{c} |f_{\lambda}(y_{\lambda})| \leq X, |f_{\lambda}(z_{\lambda})| \leq X \quad (\lambda = 3, \dots, l) \end{array} \right) \quad (30)$$

Comme v_1 peut prendre ici les valeurs 1 et 2 qui forment l'ensemble $E_1(2)$ intervenant dans la définition de $E_m(1)$, le déterminant

$$D' = \begin{vmatrix} b'_1 & b'_{1v_2} \dots b'_{1v_m} \\ 0 & b'_{2v_2} \dots b'_{2v_m} \\ \dots & \dots \\ 0 & b'_{mv_2} \dots b'_{mv_m} \end{vmatrix} = b'_1 \begin{vmatrix} b'_{2v_2} \dots b'_{2v_m} \\ \dots \\ b'_{mv_2} \dots b'_{mv_m} \end{vmatrix} = b'_1 D'' \quad (31)$$

n'est pas nul quand le système (v_2, \dots, v_m) appartient à l'ensemble $E_{m-1}(k-1)$; dans cet ensemble v_2, \dots, v_m sont tous $\equiv 3$. Donc $D'' \neq 0$ pour tout système (v_2, \dots, v_m) de $E_{m-1}(k-1)$ et on peut appliquer le lemme 3 au système (30) avec $m' = m-1$ et $r' = k-1$. Le nombre des systèmes $(y_3, z_3, \dots, y_l, z_l)$ vérifiant (30) est donc au plus

$$C_{13} X^{\frac{2(l-2)}{k} - (m-1) + 1 - \frac{k-1}{k} + \frac{\varepsilon}{2}} = C_{13} X^{\frac{2l-3}{k} - m + 1 + \frac{\varepsilon}{2}}.$$

Soit

$$w = \sum_{\lambda=3}^l b'_{1\lambda}(f_{\lambda}(y_{\lambda}) - f_{\lambda}(z_{\lambda}))$$

la valeur obtenue en remplaçant $y_{\lambda}, z_{\lambda} (\lambda = 3, \dots, l)$ par une solution particulière de (30), et posons

$$w_1 = b'_1(f_{\bar{v}}(z_1) - f_{\bar{v}}(y_1)), \quad w_2 = b'_1(f_{\bar{v}}(z_2) - f_{\bar{v}}(y_2)).$$

Le système (29) nous montre alors que $w = w_1 + w_2$. Si nous donnons à y_2 et à z_2 des valeurs arbitraires compatibles avec (29), on obtient au plus $c_{13} X^{\frac{2}{k}}$ systèmes (y_2, z_2) . Un tel système étant choisi, w_2 et par suite $w_1 = w - w_2$ sont déterminés. Mais

$$f_{\bar{v}}(z_1) - f_{\bar{v}}(y_1) = (z_1 - y_1) P(z_1, y_1),$$

où $P(z_1, y_1)$ est un polynôme en z_1, y_1 à coefficients entiers. $b'_1(z_1 - y_1)$ et $P(z_1, y_1)$ sont donc des diviseurs de w_1 et il y a au plus $C_{14} X^{\frac{\varepsilon}{2}}$ systèmes (y_1, z_1) possibles. En résumé, à chaque solution $(y_3, z_3, \dots, y_l, z_l)$ de (30) correspondent au plus $C_{14} c_{13} X^{\frac{2}{k} + \frac{\varepsilon}{2}}$ systèmes (y_1, z_1, y_2, z_2) vérifiant (29); on a donc (27).

2. $m \geq 1$, $2 \leq r \leq k$. Dans ce cas nous cherchons une limite supérieure pour le nombre $T(r, r)$ de systèmes $(y, u_1, \dots, u_{r-1}, y_{d+1}, z_{d+1}, \dots, y_l, z_l)$ vérifiant les relations suivantes:

$$b'_1 \Delta_1 \Delta_2 \dots \Delta_{r-1} f_\partial(y) = \sum_{\lambda=d+1}^l b'_{1\lambda} (f_\lambda(y_\lambda) - f_\lambda(z_\lambda)) \left\{ \begin{array}{l} f_\partial(y) \mid \equiv X, \mid \Delta_1 \dots \Delta_r f_\partial(y) \mid \equiv 2^o X \quad (r = 1, 2, \dots, r-1) \end{array} \right\} \quad (32)$$

$$\left\{ \begin{array}{l} 0 = \sum_{\lambda=d+1}^l b'_{\mu\lambda} (f_\lambda(y_\lambda) - f_\lambda(z_\lambda)) \quad (\mu = 2, \dots, m) \\ \mid f_\lambda(y_\lambda) \mid \equiv X, \mid f_\lambda(z_\lambda) \mid \equiv X \quad (\lambda = d+1, \dots, l) \end{array} \right\} \quad (33)$$

Prenons d'abord les solutions pour lesquelles le nombre

$$\Delta_1 \Delta_2 \dots \Delta_{r-1} f_\partial(y) = u_1 u_2 \dots u_{r-1} F_\partial(y, u_1, \dots, u_{r-1}) \neq 0.$$

a. $m = 1$. Chaque y_λ ou z_λ pour $\lambda = d+1, \dots, l$ prend au plus $c_{14} X^{\frac{1}{k}}$ valeurs. Il y a donc au plus $c_{15} X^{\frac{2(l-d)}{k}}$ systèmes $(y_{d+1}, z_{d+1}, \dots, y_l, z_l)$. Un tel système étant choisi, u_1, \dots, u_{r-1} et y prennent au plus $C_{15} X^{\frac{\varepsilon}{r}}$ valeurs. En effet $F_\partial(y, u_1, \dots, u_{r-1})$ dépend effectivement de y , car F_∂ est de degré $k-r+1 \geq 1$ en y . Il y a donc au plus $C_{16} X^{\frac{\varepsilon}{r}}$ systèmes (y, u_1, \dots, u_{r-1}) et par conséquent au plus $C_{17} X^{\frac{2(l-d)}{k} + \frac{\varepsilon}{r}}$ solutions de (32) avec $u_1 u_2 \dots u_{r-1} F_\partial(y, u_1, \dots, u_{r-1}) \neq 0$.

b. $m \geq 2$. Comme v_1 peut prendre les valeurs $1, 2, \dots, d$ qui forment l'ensemble $E_1(r-1)$ figurant dans la définition (25) de $E_m(r)$, le déterminant D' défini par (31) n'est pas nul quand le système (v_2, \dots, v_m) appartient à l'ensemble $E_{m-1}(k)$. Dans cet ensemble v_2, \dots, v_m sont tous $\geq d+1$, donc D'' figurant dans (31) est $\neq 0$ pour tout système (v_2, \dots, v_m) de l'ensemble $E_{m-1}(k)$. On peut donc appliquer le lemme 3 au système (33) avec $m' = m-1$ et $r' = k$. Le nombre de solutions $(y_{d+1}, z_{d+1}, \dots, y_l, z_l)$ de (33) est par conséquent au plus $C_{18} X^{\frac{2(l-d)}{k} - (m-1) + 1 - 1 + \frac{\varepsilon}{2}}$. Une telle solution étant donnée on voit comme pour $m = 1$ que le système (32) donne au plus $C_{19} X^{\frac{\varepsilon}{2}}$ systèmes (y, u_1, \dots, u_{r-1}) .

En résumé, pour $m \geq 1$, il y a au plus

$$C_{20} X^{\frac{2l-2d}{k} - m + 1 + \frac{\varepsilon}{2}} \text{ systèmes } (y, u_1, \dots, u_{r-1}, y_{d+1}, z_{d+1}, \dots, y_l, z_l)$$

avec $u_1 u_2 \dots u_{r-1} F_\partial(y, u_1, \dots, u_{r-1}) \neq 0$.

Passons maintenant aux solutions avec $u_1 u_2 \dots u_{r-1} F_0(y, u_1, \dots, u_{r-1}) = 0$. Dans la définition (25) de l'ensemble $E_m(r)$ figure un ensemble $E_m(r-1)$ ne contenant aucun nombre de $E_1(r-1)$, c'est à dire dont tous les nombres sont $\geq d+1$. Les déterminants $D(v_1, \dots, v_m)$ définis par (8) étant $\neq 0$ pour tous les systèmes (v_1, \dots, v_m) de $E_m(r-1)$, on voit que le système

$$\left. \begin{aligned} 0 &= \sum_{\lambda=d+1}^l b'_{\mu\lambda} (f_\lambda(y_\lambda) - f_\lambda(z_\lambda)) \quad (\mu = 1, \dots, m) \\ |f_\lambda(y_\lambda)| &\leq X, \quad |f_\lambda(z_\lambda)| \leq X \quad (\lambda = d+1, \dots, l) \end{aligned} \right\} \quad (34)$$

vérifie les conditions du lemme 3 avec $m' = m$ et $r' = r-1$.

Il y a donc au plus $C_{21} X^{\frac{2(l-d)}{k} - m + 1 - \frac{r-1}{k} + \varepsilon}$ systèmes $(y_{d+1}, z_{d+1}, \dots, y_l, z_l)$ vérifiant (34). D'autre part, il y a au plus $c_{16} X^{\frac{r-1}{k}}$ systèmes (y, u_1, \dots, u_{r-1}) vérifiant les inégalités de (32) tels que $u_1 u_2 \dots u_{r-1} F_0(y, u_1, \dots, u_{r-1}) = 0$.

Il y a donc au plus $C_{22} X^{\frac{2l-2d}{k} - m + 1 + \varepsilon}$ systèmes $(y, u_1, \dots, u_{r-1}, y_{d+1}, z_{d+1}, \dots, y_l, z_l)$ avec $u_1 u_2 \dots u_{r-1} F_0(y, u_1, \dots, u_{r-1}) = 0$.

En réunissant les deux résultats précédents on trouve (28) et le lemme 3 est démontré.

§ 3. Démonstration du théorème II.

Dans ce paragraphe nous aurons besoin du lemme suivant:

Lemme 4: Soient $\zeta \geq 0$, $\beta \geq 1$, $b_{\mu\nu}$ et t_μ entiers, p un nombre premier et $f_\nu(y)$ un polynôme à coefficients entiers. Désignons par $p^{(n-m), 3} Q'_3$ le nombre de solutions du système

$$\sum_{\nu=1}^n b_{\mu\nu} f_\nu(y_\nu) \equiv t_\mu \pmod{p^\beta} \quad (\mu = 1, \dots, m), \quad (35)$$

à chacune desquelles correspondent m nombres naturels différents v_1, \dots, v_m , tous $\leq n$, tels que le déterminant (8) soit différent de zéro et que chacune des m dérivées $f'_\nu(y_\nu)$ ($\nu = v_1, \dots, v_m$) possède au plus ζ facteurs p .

Dans ces conditions il existe un nombre β'_0 dépendant uniquement de ζ et de la matrice

$$B' = \begin{pmatrix} b_{11} & \dots & b_{1n} \\ \vdots & & \vdots \\ b_{m1} & \dots & b_{mn} \end{pmatrix},$$

tel que Q'_β possède pour chaque $\beta \geq \beta'_0$ la même valeur.

Démonstration: Nous pouvons trouver un nombre β_1 dépendant uniquement de la matrice B' tel que chaque déterminant $\neq 0$ d'ordre m ,

figurant dans B' , possède au plus β_1 facteurs p . Démontrons que $\beta_0 = 2\beta_1 + 2m\zeta + 1$ possède la propriété désirée.

A chaque solution $y = (y_1, \dots, y_n)$ de (35) correspond la matrice

$$M(y) = \begin{pmatrix} b_{11} f'_1(y_1) & \dots & b_{1n} f'_n(y_n) \\ \dots & \dots & \dots \\ b_{m1} f'_1(y_1) & \dots & b_{mn} f'_n(y_n) \end{pmatrix}.$$

Si $p^{\alpha_1 + \dots + \alpha_\mu}$ désigne pour $\mu = 1, \dots, m$ la puissance la plus élevée de p qui divise chaque déterminant d'ordre μ de cette matrice, $p^{\alpha_1}, \dots, p^{\alpha_m}$ s'appellent les diviseurs élémentaires ⁶⁾ modulo p de la matrice. Comme $M(y)$ contient le déterminant

$$D(v_1, \dots, v_m) = \prod_{v=v_1, \dots, v_m} f'_v(y_v),$$

chaque solution y de (35) qui entre en considération possède la propriété que le dernier diviseur élémentaire modulo p de la matrice $M(y)$ est $\equiv p^{\beta_1 + m\zeta}$.

Considérons maintenant m entiers non négatifs $\alpha_1 \leq \dots \leq \alpha_m \leq \beta_1 + m\zeta$ et un système w formé par n entiers w_1, \dots, w_n ; posons $\alpha_m = v$. Soit H l'ensemble des solutions de

$$\sum_{v=1}^n b_{\mu v} f'_v(y_v) \equiv t_\mu \pmod{p^\beta}; \quad y_v \equiv w_v \pmod{p^{\beta-v}}. \quad (36)$$

($\mu = 1, \dots, m$; $v = 1, \dots, n$) telles que $p^{\alpha_1}, \dots, p^{\alpha_m}$ soient les diviseurs élémentaires modulo p de $M(y)$. En vertu de

$$\beta \equiv \beta_0 = 2\beta_1 + 2m\zeta + 1$$

on a

$$\beta - v \equiv \beta_1 + m\zeta + 1 \equiv \zeta + 1$$

et il suit de (36) que $f'_v(y_v) - f'_v(w_v)$ est divisible par $p^{\beta-v}$, donc par $p^{\zeta+1}$. Si à w correspondent m nombres naturels différents v_1, \dots, v_m , tous $\leq n$, avec $D(v_1, \dots, v_m) \neq 0$ tels que chacune des m dérivées $f'_v(w_v)$ ($v = v_1, \dots, v_m$) possède au plus ζ facteurs p , le nombre des facteurs p de chacune des m dérivées $f'_v(y_v)$ ($v = v_1, \dots, v_m$) est $\leq \zeta$ pour chaque système y appartenant à H ; dans ce cas chacun de ces systèmes y fournit la contribution 1 au nombre $p^{(n-m)\beta} Q'_\beta$. Si par contre à w ne correspondent pas m nombres v_1, \dots, v_m avec les propriétés citées, aucun des systèmes y appartenant à H ne fournit de contribution à $p^{(n-m)\beta} Q'_\beta$. En vertu de $\beta \equiv 2v + 1$ la proposition 2 de l'article cité dans le renvoi ⁶⁾ nous apprend que le

⁶⁾ Comparer J. G. VAN DER CORPUT, Sur quelques systèmes de congruences. These Proceedings, 42, 329 (1939).

nombre N_1 des systèmes y appartenant à H est égal à p^{m-n} multiplié par le nombre N_2 des solutions y du système

$$\sum_{v=1}^n b_{\mu v} f_v(y_v) \equiv t_{\mu} \pmod{p^{\beta+1}}; y_v \equiv w_v \pmod{p^{\beta-\gamma}};$$

($\mu = 1, \dots, m; v = 1, \dots, n$). On trouve ainsi

$$p^{(m-n)\beta} N_1 = p^{(m-n)(\beta+1)} N_2$$

et en sommant pour $\alpha_1, \dots, \alpha_m$ et pour les systèmes w qui entrent en considération, on trouve $Q'_{\beta} = Q'_{\beta+1}$, d'où suit l'assertion.

Donnons enfin la démonstration du thécrème II. Il suit de l'article, cité dans le renvoi ¹⁾, qu'il suffit de démontrer que le facteur arithmétique $\prod_p Q(p, t)$ est supérieur à un nombre positif indépendant de $t = (t_1, \dots, t_m)$ dans les conditions du théorème II. Le même article nous apprend que le produit $\prod_p Q(p, t)$, étendu à tous les nombres premiers p , converge absolument et uniformément par rapport à t , de sorte qu'il existe un nombre c_{17} , indépendant de t , tel qu'on ait

$$\prod_{p \geq c_{17}} Q(p, t) > \frac{1}{2}.$$

Il suffit donc de considérer les nombres premiers $p < c_{17}$. D'après l'article cité dans le renvoi ¹⁾ on a

$$Q(p, t) = \lim_{\beta \rightarrow \infty} \frac{N_{\beta}(p, t)}{p^{(n-m)\beta}},$$

où $N_{\beta}(p, t)$ désigne le nombre des solutions de (35). Nous savons que

$$\frac{N_{\beta}(p, t)}{p^{(n-m)\beta}} \geq Q'_{\beta},$$

où Q'_{β} est le nombre défini dans le lemme précédent et d'après ce lemme Q'_{β} possède la même valeur pour $\beta \geq \beta_0$, où β_0 est un entier convenable, indépendant de t .

De cette manière nous trouvons

$$Q(p, t) \geq Q'_{\beta_0},$$

Il résulte des conditions du théorème II que $p^{(n-m)\beta_0} Q'_{\beta_0}$ est ≥ 1 , d'où il suit que

$$Q(p, t) \geq p^{-(n-m)\beta_0}$$

et que le facteur arithmétique est supérieur à

$$\frac{1}{2} \prod_{p < c_{17}} p^{-(n-m)\beta_0}.$$

Ce nombre étant positif et indépendant de t , nous avons démontré le théorème II.

Geophysica. — *The principle of concentric folding and the dependence of tectonical structure on original sedimentary structure.* By L. U. DE SITTER. (Communicated by Prof. F. A. VENING MEINESZ).

(Communicated at the meeting of April 29, 1939.)

I. 1. The detailed study of simple folds in oil fields and elsewhere led to the conviction that natural laws govern the mechanics of folding, laws, which to a high degree are independent of the nature of the folded rocks and their stratification (DE SITTER 1937).

This general principle I call the concentric folding principle. It is the result of two fundamental laws: 1. the law of retention of volume, 2. the formation of spontaneous shearing planes parallel to the surface.

I. 2. The law of retention of volume signifies that the folding pressure

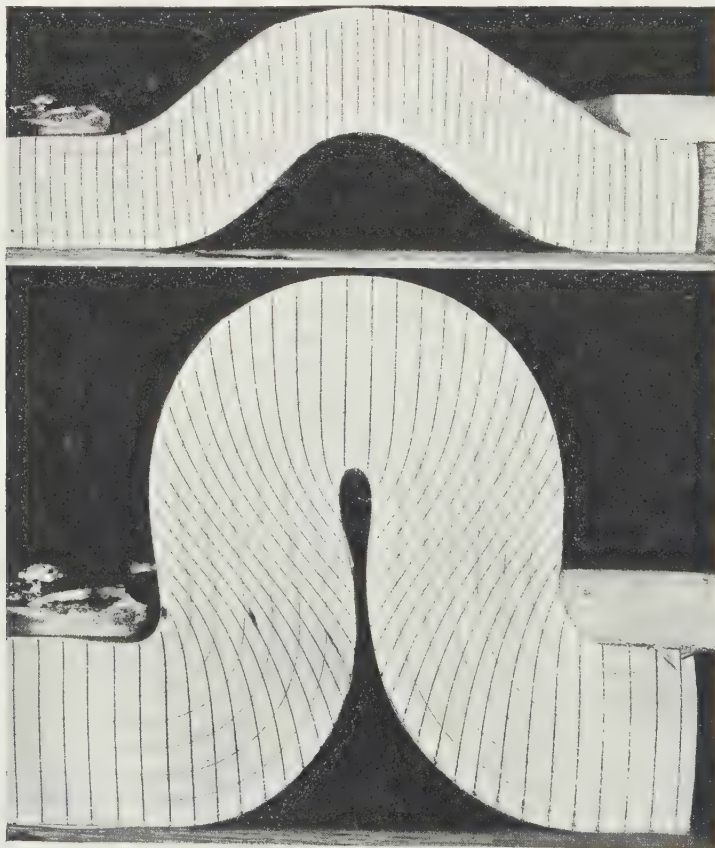


Fig. 1. Concentric folding of a block of paper.

does not compress the material of the folded rock to a denser material, or at any rate, that the compression is a finite phenomenon with very little influence on the folding mechanism.

I. 3. The spontaneous parallel shearing planes explain why an unstratified, thick formation, or a badly stratified complex, shows the same folding mechanism and ultimate shape of fold, as a well stratified complex of sediments. Wherever stratification planes, as planes of minimum cohesion, exist, it can be easily understood that most of the internal shearing during the deformation process will follow these planes of minimum cohesion and that the mechanism of folding will closely resemble the folding of a block of paper. (Fig. 1) (KUENEN and DE SITTER, 1938).

When no stratification planes exist, as in thick limestones, sands, or even clays and shales we still find the same final shape of fold. In order to investigate this apparent general validity of the "paper folding principle", KUENEN executed in close collaboration with myself a series of experiments (KUENEN and DE SITTER, 1938), which finally resulted in a few experiments where unstratified clay was folded as if it were stratified, spontaneous shearing planes having the function of stratification planes (fig. 2).

These shearing planes were formed already in a very early stage of folding and are certainly not due to shearing stresses, as they are parallel to the stress direction. They must be due to tensional stresses perpendicular to the general deformative stress. It is a kind of foliation of the homogeneous mass, taken advantage of by the deformation mechanism in using these foliation planes as shearing planes, in the same way as stratification planes are used as shearing planes. Thus it can be understood why a thick unstratified member of a sedimentary series does not disturb the general folding mechanism.

I. 4. The most general conception of the mechanism of folding of sedimentary rocks is therefore, that the internal differential movements of particles are always parallel to the bedding e.g. neither thickness nor length of a layer changes during the folding process. The contrary conception of a fold is either a fold slowly dying out downwards or a so-called true to shape or similar folding. A fold dying out downwards would infer decreasing dips, increase of thickness on top of the fold as sketched in fig. 3. Such shapes have never, or very seldom been observed in folds where the subsurface structure is really known either by mining operations or by deep erosion.

In the left part of fig. 15, Plate 1, representing the Graiterly fold of the Jura Mts for instance, the fact that the tunnel encountered in the centre of the fold the Hauptrogenstein and the underlying Blagdeni-Murchesoni schists proves that there is no trace of slowly flattening of the anticline comparable to the structure of fig. 3.

In fig. 4, a layer, folded concentrically, is put next to the same layer folded true the shape. The latter folding mechanism is similar to faulting,

the single straight fault plane being replaced by a multitude of small planes, all parallel and straight. When we find such folds we may be certain that

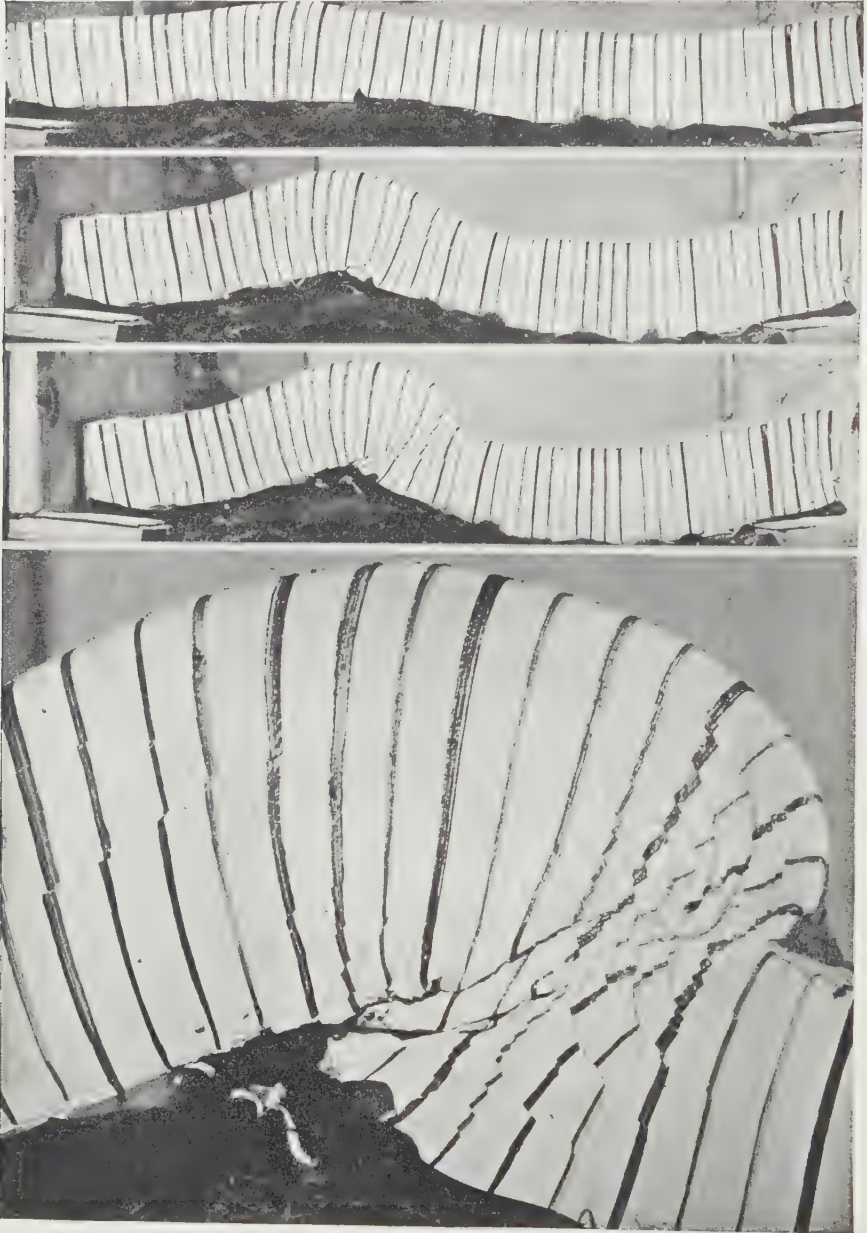


Fig. 2. Concentric folding of a homogeneous unstratified cake of clay.

they actually do replace faults as in flexures or attenuated steep limbs of an anticline.

In general it is a fact that in all folds the flank dips converge towards the centre. This fact and the resulting tectonic complications of the centre,

indicate that concentric folding is the leading principle. Every fold described and reproduced in this article illustrates these facts.

Without entering further into the theoretical merits of the concentric folding principle we will apply the law to well known structures, from the analysis of which it was originally derived. If it gives us a better understanding of the peculiarities and explains general features of folds, it has at least a value as a working hypothesis.

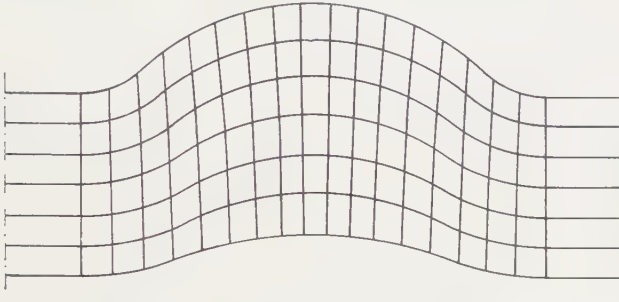


Fig. 3. Compression fold, dying out downwards.

II. 1. A necessary consequence of concentric folding is the fact that the downward extension of a fold is limited, because the disturbance, as noticed at the surface, is concentrated radially downwards and towards the centre of the fold. Therefore we can regard a system of folds as a folded block pushed over a substratum. What really happens to the substratum is a problem on itself, which we will not elaborate in this discussion,



Fig. 4. A. parallel folding. B. folded true to shape.

but we may state our belief that the substratum will be folded mostly downwards and always in folds having a much larger wave length due to its much larger thickness. Also, it may be folded elsewhere as in the case of the Jura folds, where the shortening of the upper sedimentary strata is probably compensated by a shortening of the substratum in the central Alps.

A fold in its most simple form as represented in fig. 5, shows three important boundary planes: 1. The line $AA'FA''$: the upper boundary of concentric folding, 2. the line $BB'OB''$: the lower boundary of concentric folding, 3. the line $CC'EC''$: the basal shearing plane. The upper boundary need not necessarily be the surface of the earth's crust, nor need the basal shearing plane be the boundary between granitic substratum and sedimentary rock. For the sake of simplicity we will provisionally assume however that the above mentioned theoretical boundaries coincide with these natural planes.

II. 2. In fig. 5, the shortening of the sedimentary block of thickness t , has been effected by the displacement of the vertical line ABC to the position $A'B'C'$, regarding only the left half of the figure.

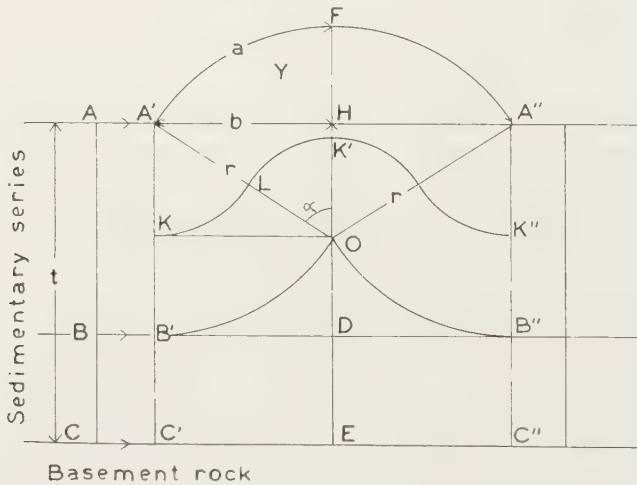


Fig. 5. Simplest shape of a concentric fold.

The pure concentric folding is necessarily confined to the upper part of the sedimentary series of the thickness AB , in the lower half some other way of adjustment to the desired shape has taken place. In the upper half, all the internal movement has been effected along planes parallel to the surface as for instance the line KLK' . Therefore the line KLK' has retained its original length and the same statement is true for all other lines as for instance $A'F$ and $B'O$. As $A'F$ and $B'O$ are sections of circles with the radius r and angle α , with the centres O and A' , both $A'F$ and $B'O$ are equal to ar . The line KLK' has the length:

$$aLO + aA'L = a(LO + A'L) = ar.$$

Therefore every line in a section, representing an originally horizontal plane can retain its original length throughout the folding process, even when the shape of the fold is not a simple circular arc because every curve can be described by a number of successive circular arcs. In the latter case, however, only that part of the fold can be folded purely concentrically

inside which no centres of curves are situated. In fig. 1, the ideal concentric fold with perfect stratification, the fold is actually a circular arc with one centre O and two auxilliary centres at the surface, A' and A'' . Any other shape will necessitate more centres and therefore a restriction of the concentric part of the fold, reducing the thickness $A'B'$.

II. 3. Thus, the assumption that the simplest and fundamental shape of a fold is a set of three circular arcs, seems to have a foundation. As can be easily seen in fig. 6, the length of the fold, a , and its radius, r , must be dependent of the thickness t of the sedimentary series.

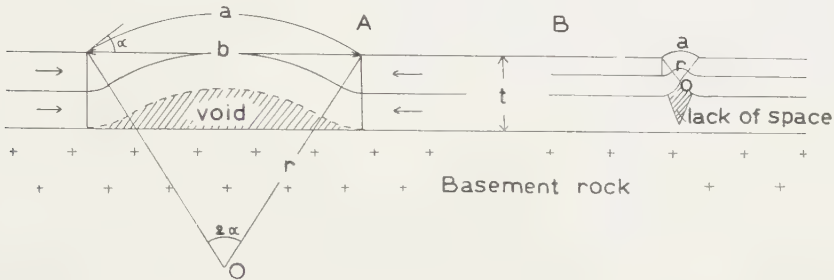


Fig. 6. A, too large radius. B, too small radius.

When the radius r is too large as in fig 6A there must be a void between the basement rock and the sediment and when too small (fig. 6B) the lower part of sedimentary series will not find enough place to fill up when compressed to the same degree as the overlying strata.

Thus, if there is a primary reason why the sediment should be folded, and the basement behave in some other way, then the size of a fold will be determined by the thickness t .

The relation between r , and t can be easily calculated, in the case of a circular arc.

In fig. 5, the upper part, having a thickness $A'B'$, of a sedimentary series is folded concentrically, the lower part necessarily in some other way, the whole gliding on its substratum.

As the original volume has been retained the superficies of triangle $B'DO$ must equal the rectangle $BB'C'C$.

$$BB'C'C = r(t-r)(a - \sin a)$$

$$B'DO = B'DOK - B'OK$$

$$= r^2(\sin a - \frac{1}{2} \sin 2a) - \frac{1}{2} r^2(a - \frac{1}{2} \sin 2a)$$

$$\text{thus } (t-r)(a - \sin a) = r(\sin a - \frac{1}{4} \sin 2a - \frac{1}{2} a)$$

$$t(a - \sin a) = r(\frac{1}{2} a - \frac{1}{4} \sin 2a)$$

and

$$r = 2t \frac{a - \sin a}{a - \frac{1}{2} \sin 2a} \quad \dots \dots \dots (1)$$

further the length $a = ar$ (2)

the width $b = r \sin \alpha$ (3)

the shortening $a - b = r(a - \sin \alpha)$ (4)

and the uplift $y = tr(a - \sin \alpha)$ (5)

Introducing different values of α in (1) we find that for values of $\alpha < 45^\circ$ r will be $\frac{1}{2} t$, larger values of α will be followed by an increase of r until $r = \frac{3}{4} t$ when $\alpha = 90^\circ$.

Thus, in the case of the simplest shape of a fold the radius of a fold and its width is directly dependent on the thickness of the sedimentary series. As we have seen in II. 2, there is some reason to believe that the simplest shape really is the fundamental shape, but even other shapes will possess in some more complicated way a direct connection between their size and thickness.

II. 4. The relation between the size of a fold and the thickness of the sedimentary series participating in the fold is beautifully demonstrated by a comparison between folds in the Jura Mountains. In fig. 7 the Reculet fold of the Western Jura is put next to the Lägern fold of the Eastern Jura, drawn on the same scale (HEIM, 1922).

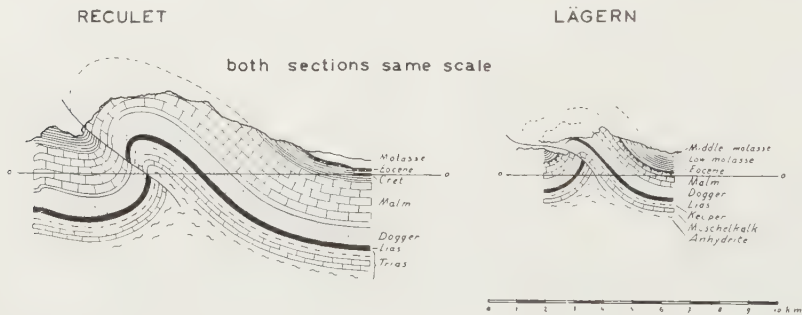


Fig. 7. Comparison between the Reculet and Lägern folds of the Jura Mts.

The sediments participating in the two folds are identical, and their shape is very similar, only the total thickness of the eastern fold is about half that of the western fold. Also the width of the Lägern fold is roughly half the size of the Reculet fold.

This relation is not incidental but could be demonstrated as well by other folds and even by comparing general sections of the eastern and western Jura.

Unfortunately we cannot measure the radius r of neither the Lägern nor the Reculet fold with any accuracy, nor do we know their size before the thrustplanes were formed. Consequently we are not capable of checking the equations 1 to 5.

III. 1. Until now we have assumed a sedimentary series of equal thickness. Often however a normal series thins out towards the margin of the basin (fig. 8). In

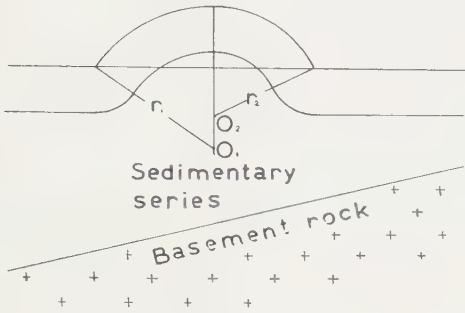


Fig. 8. Asymmetric fold due to thinning out of sedimentary series.

such case in the left half of the fold, the radius r_1 , will be dependent on the average thickness t_1 , and will be larger than r_2 , dependent on t_2 , as $t_1 > t_2$.

The maximum dip in the left limb will be greater than that in the right limb, the fold will be asymmetric.

III. 2. The increase of the load of the uplift for every unit of shortening is unvariable, e.g. although the increasing load will try to prevent the further development in the way of the simple arc, there is no discontinuity in the loading effect. Still, the ever increasing load on a restricted surface will tend to disturb the simple arc by spreading the load over a greater surface. Instead of an ever rising fold with the advantages of minimum deformation, due to minimum dip, there will be a tendency to broaden the fold avoiding the extra load, but necessitating steeper dips in a broader zone than necessary in the first case (fig. 9). Thus we see that a deviation of the simple arc by steepening the dips in one or both flanks is the result of the loading effect, and that even a small thinning out of a part of the formation will be able to call forth a marked asymmetry.

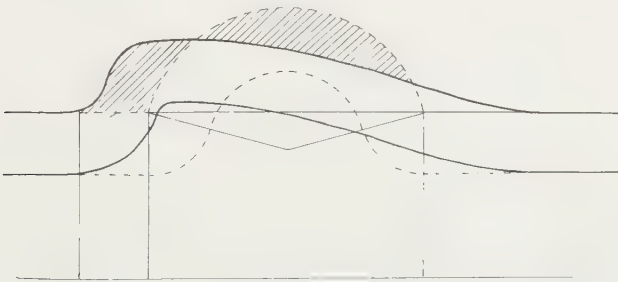


Fig. 9. Asymmetric fold due to equal loading effect.

III. 3. In order to check these theoretical conclusions we examined several well known folds of which we will cite a few here.

The first shall be the Hauensteintunnel section (BUXTORF, 1916).

The tunnel happened to cut the overthrust structure in such a way, that it disclosed the unconformable surface of the Tertiary on the Jurassic. This fortunate fact enables us to reconstruct the original position with some accuracy (fig. 10a). Apparently the thinning of the strata towards the North determined the position of the fold, and its asymmetry, the north

flank being the steep flank (fig. 10*b*). Progressive folding is shown in fig. 10*c*, the final situation in fig. 10*d*.

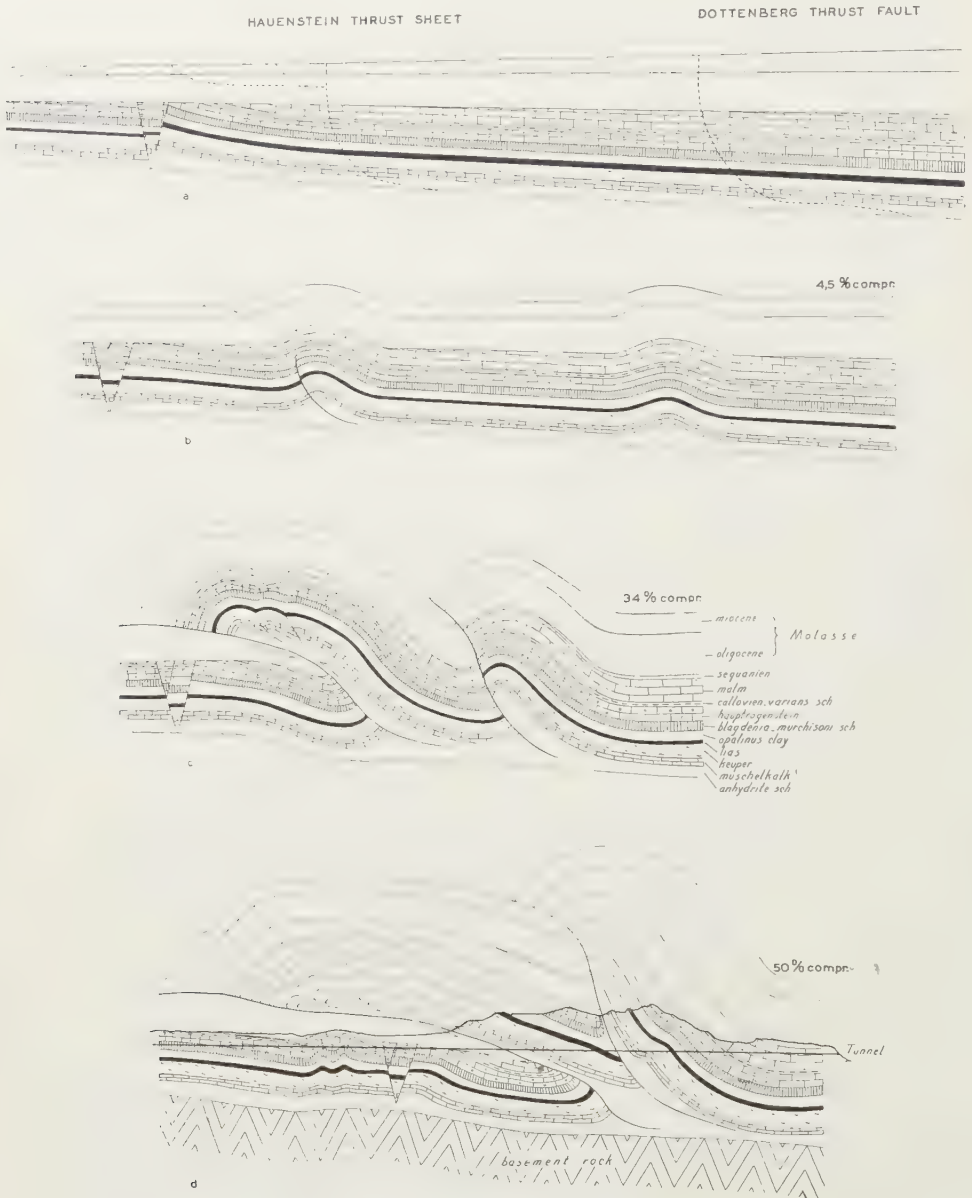


Fig. 10. Hauensteintunnel structure, its development and final stage (after BUXTORF).

The development of the fold is founded on the assumption that an asymmetric fold has been, in this example also, the forerunner of an overthrust, and illustrates our thesis of the cause of asymmetry.

In the Réculer and Läger folds a similar thinning may perhaps be

assumed but cannot be proven, as neither possesses any subsurface structure disclosed by artificial means.

The anticline of Sarrebrück (PRUVOST 1934) (Fig. 11, plate 1) gives us the same result. We find here a steep S.E. flank, partly overthrusted, due to the thinning out of the lower part of Stephanien against the overlying Holz conglomerate. The steep flank has been explored to a great extent by the mining authorities and the conclusion that the decrease in thickness and disappearance of the Laudrefang member is due to an inter-Stephanien erosion and not to later tectonical causes, seems to be conclusive.

These few examples will suffice us to understand that the primary structure of the sedimentary basin may be in a large way the determining factor of its future structural formation.

III. 4. With a view to the possibility of such close connection between the primary stratigraphic sequence of a sedimentary basin and its future tectonical structure, the Helvetian thrustsheets offered a fruitful research problem.

Analogous to the three major Alpine thrustsheet units viz.: the East-Alpine sheets characterized by thick triassic sediments, the Penninic by their Bündnerschiefer, and the Helvetian by their jurassic and cretaceous limestones, we find here the upper, middle and lower Helvetian sheets, each with their own sedimentary character. The comparison cannot be carried beyond this superficial analogy. Whereas the major units each comprise a complete stratigraphical series, from basement rock up to the Tertiary, the Helvetian sheets are mostly incomplete. Our study restricts itself to the region South and West of the Walen See (Linthtal, Glarner Alps).

The upper Helvetian sheets (Säntis, Räderten, Drusberg) comprise only the Cretaceous, from the Valenginien marls upwards, and the Tertiary. The lower Helvetian sheets show a complete series from Permian upwards, including the Tertiary, in their frontal parts, but are nearly exclusively build up by the Verrucano in their backward parts.

The Axen sheet, called the Middle Helvetian sheet, is characterized by Lias, Dogger and Malm, its frontal part being complete from Liassic upwards to the Tertiary. Roughly speaking we can characterize the three units in this way:

Lower Helvetian sheets	——	Permian
Middle " "	——	Jurassic
Upper " "	——	Cretaceous

Since the excellent work of ALBERT and ARNOLD HEIM we know that the position of the thrustsheet units in their original basin was, from North to South as follows:

N → Autochtoneous Aarmassif with its sedimentary cover and par-autochtoneous sheets → Glarner sheet, Mürtschen sheet (Lower Helvetian)

→ Axen sheet (middle Helvetian) → Säntis, Räderten, Drusberg sheet (upper Helvetian) → S.

Figure 12, plate 1, represents the reconstruction of this Helvetian basin, along these lines, as accurately as possible. The accurate sections of OBERHOLZER (1933), of which we choose section 12 as the best disclosed one, formed the base of this reconstruction. The observed thicknesses have been rigoureously maintained even when OBERHOLZER supposed an attenuation, because it seems highly improbable that a hard formation as the Malm limestone will show the same attenuation as a soft Valenginien marl. Even in the thinnest part of the Glarner or of the Mürtschen sheet nearly the whole series is complete.

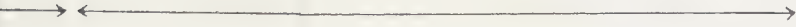
In studying the sedimentary conditions of the Helvetian basin we must realize that it represents only the Northern shelf of the Alpine basin. The Permian Verrucano and sernifite of the Glarner and Mürtschen sheets occurs in the same facies in the Southern Bergamasc Alps, in both localities thinning out and disappearing quickly Westwards. The Triassic sediments of the Helvetian shelf extend in the same facies Southwards in the Penninic sheets and acquire great thickness as limestones and marls in the southern Alps. The Liassic of the Helvetian basin is the shelf extension of the great filling up of the geosynclinal basin then situated in the Penninic centre of the Alpine basin. The Malm limestone extending a little further Northwards than the Liassic, probably continues below the Helvetian sheets even as the Liassic and the Dogger. In the Cretaceous period, however, this S—N movement of the subsidence has been arrested; the major subsidence is now found in the southern part of the shelf. In Tertiary times the whole basin was covered by Flysch sediments, the Pratigäu flysch of the Penninic sheets being very similar to the Wild flysch of the Helvetian basin.

By putting together the pieces of the different Helvetian sheets at their appropriate place the section of the original shelf was completed, but not everywhere with the same exactitude, due to the missing parts carried away by erosion.

The frontal parts of the sheets are best disclosed, their backparts often being doubtful, for instance the length of the Axen sheet is completely unknown as its backpart has been eroded away; we have drawn it at its minimum length. At the same time the future position of the thrustplane below every sheet has been drawn into the indisturbed sedimentary sequence. This could be done with great accuracy in the frontal parts and could often be followed rather far back with the help of the adjoining sections.

Studying this basin we notice first of all that the Lower, Middle and Upper Helvetian sheets are not only situated behind one another but also above one another. The Cretaceous of the U. Helv. sheets was situated above the Permian of the L. Helv. sheets and above the Jurassic of the

POSITION OF F



Säntis sheet

Drusberg sheet

and overthrust
 due to thinning of Seewerkalk?
 thinning of Valanginien and
 Kalk-Drusberg sch

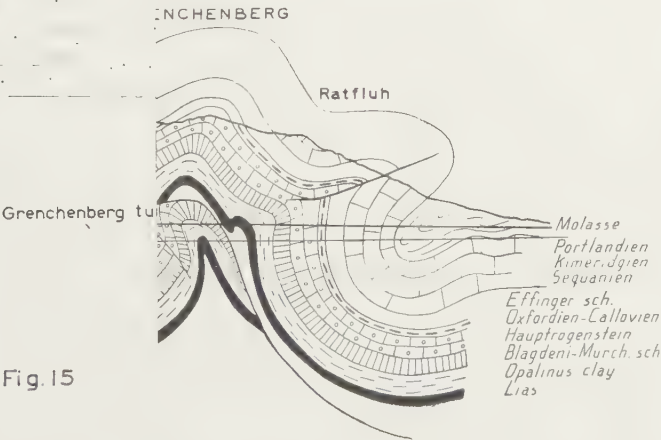
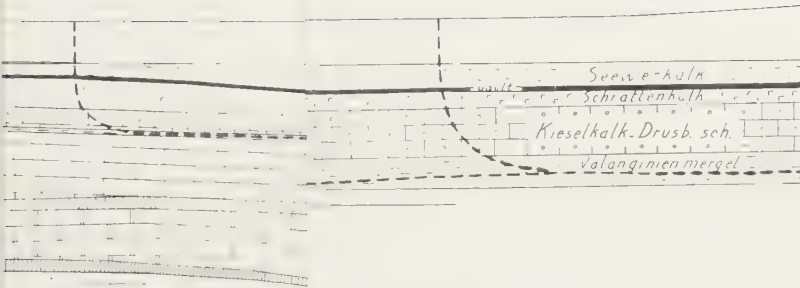


Fig.15

from its back part was that of the Mürtschen sheet, now reaching nearly as far North as the Upper Helv. sheets and still extending from root to front over the central granite mass.

This analysis shows that also in this case the tectonical structure is dependent wholly on the primary sedimentary sequence of the basin.

Lateral changes in the sedimentary sequence of the same basin must then also be followed by tectonical changes. Eastwards from the section which we chose (no. 12 of OBERHOLZER) the importance of the Lias-Dogger members decreases, consequently the Axen sheet disappears and the Upper Helv. sheets take over its function and become considerably broader in the Säntis Mountains. The disappearance of the Permian sediments Westwards mark the disappearance of the Mürtschen sheet and strong reduction of the Glarner sheet, the Axen sheet gaining in importance together with the growing mass of Liassic limestones.

The dependency of the tectonical units of the original sedimentary sequence is so clearly demonstrated in the instance of the Glarner Alps that I am confident that also elsewhere this line of research will throw unexpected light on the tectonical development of the origin of simple folds and thrustsheets.

III. 5. The development of a thrustfault out of an asymmetric anticline and eventually to a thrustsheet is a mechanical problem.

ALBERT HEIM largely guided by the structural features of the Säntis Mts in Northern Switzerland assumed that the thrustfaults were due to the extreme attenuation of the middle limb of a recumbent fold, BUXTORF (1916), familiar with the Jura Mts supposed on the contrary that a reverse fault gradually develops into a thrustfaulted anticline. He founded his opposition to HEIM's theory mainly on the fact that nowhere in the Jura Mts and neither in the Helvetian thrustsheets a single clear instance of a recumbent middle limb is known. The thrustplanes of the Helvetian thrustsheets follow over long distances the bottom of a single stratigraphical horizon, occasionally cutting obliquely through a part of the sedimentary series, but everywhere the lowest stratigraphical member of the upper sheet reposes directly on the stratigraphical highest member of the underlying tectonical unit. Sometimes the thrustplane is marked by a mylonite as the Lochsteinlimestone, but as often as not even a mylonite is absent.

The reasoning of BUXTORF would be sound, if we did not see in many instances, even in the Jura Mts, how an asymmetric anticline in lateral direction develops into an overthrust one. It is difficult to understand how a primary reverse fault could ever develop in an unbroken anticline.

The logical conclusion of these facts is that the original structure was an asymmetric anticline, but the thrustplane coming into existence long before the fold has reached the recumbent state.

The necessity of overthrusting in a relatively early stage of folding is easily understood when we continue to apply the laws of concentricity and retention of volume.

In fig. 5 and the calculation of r , where r is the maximum thickness of pure concentricity, we have shown that only the upper half of the sedimentary series can be folded strictly concentrically. As soon as an extra steepening of one flank, due to the tendency of more equal loading of the uplift, happens, the radius of the curve at that place is decreased considerably e.g. the centre O_1 (fig. 13) is replaced there by the centre O_2 . The lowest purely concentrically folded layer we call the lower concentricity boundary, which in the latter case is the horizon running through O_2 .

When we compare two layers, l_1 and l_2 , l_1 situated above O_2 and l_2 below this point, both of the same thickness, it is obvious that the volume of l_1 has not changed during folding, but that of l_2 , as drawn in fig. 13

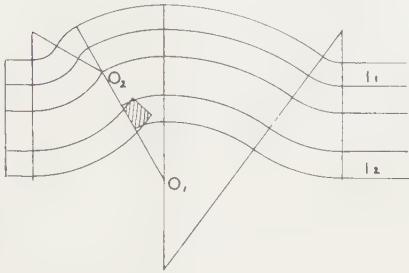


Fig. 13. Conventional way of section construction, disregarding lack of space in centre of anticline.

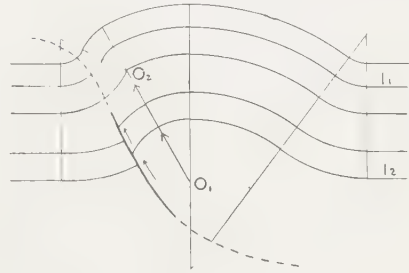


Fig. 14. The origin of an overthrust due to lack of space in centre of anticline.

has diminished by a considerable amount. This amount, hachured in fig. 13, can easily be calculated and increases downwards.

The construction method of fig. 13 is obviously wrong, although it is the usual way of construction (compare BUSK, *Earthflexures*, Cambridge 1929).

What really happens is this, that in course of the steepening of the dip in the left flank the centre O_1 rises to the position of O_2 , and every layer it passes in its way upwards breaks through as it can no longer be folded and retain its volume at the same time. Thus the reverse fault originates just above centre O_1 and follows the upward motion of the centre (fig. 14). The initial thrustfault may be nearly vertical. The strata above, and right of, the fault continue their folding movement, those left and below the fault are successively stopped in their folding as soon as they are ruptured. Finally the whole steep flank is broken by the fault along the broken line of fig. 14. The initial shape of the thrustsheet is disclosed in every well developed front of thrustsheet, and always it cuts nearly perpendicular to the stratification through the sedimentary sequence, until it has found its gliding horizon. (Compare the Grenchenberg fold, fig. 15, plate 1).

We notice that the original position of the lower concentricity boundary and that of the gliding horizon determine the shape of the fold. When we deduced in II. 3 the size of the fold from the total thickness, we assumed

measurements and calculations are tabulated, reference horizon being the base of the Sequanien.

The same calculation was executed for the neighbouring section of the Birscluse, the reference horizon being the top of the Hauptrogenstein some 150 m lower than the base of the Sequanien. The result is listed in table II.

TABLE II

	Les Raimeux	Vellerat	Combined
$a-b$ in m	840	580	1420
y in m^2	848000	560000	1408000
t Hauptrogenstein in m	1010	965	992
t base of seq. in m	1180	1115	1142

The four independent values of t compare very well, the extremes differing less than 6 % from the average.

It would be preferable to check the equation on a fold where we know by artificial or natural disclosures the actual depth of the basement, however, no such fold is known to me where both surface structure and basement rock are well enough disclosed, we will always have to compare neighbouring sections, the one checking the other.

IV. 3. In the same way we can apply the theory to different sections of the same anticline, showing varying shortening. This has been done by analysing a structure explored to great extent by drilling ¹⁾. Fig. 16 shows three sections, *A*, *B* and *C*, *A* and *B* being only some 600 m apart, *C* some 15 km further on the plunge of the same anticline.

The shape of the reference horizon, p , in sections *A* and *B*, is specially well known. As can be seen on fig. 16 the top and bottom of this layer have a totally different shape in the zone of the overthrust, still the lengths differ very little, less than 1 % of the total length, proving to a certain extent the concentricity of the folding.

In table III the results of the analysis have been listed.

In all these sections the position of the syncline was a matter of conjecture. In section *A*, the bottom of the syncline was drawn as high as possible, resulting in a minimum value of both y and t . In section *B*, the depth of syncline has been drawn more liberally, whilst in section *C*, the depth was drawn at its probable depth according to that section itself.

Assuming the value of $t = 1050$ m of section *C* to be the true folding

¹⁾ The author offers his thanks to the board of Directors of the Bat. Petr. Co. for the use he was allowed to make of their geological files.

TABLE III

	Section A ref. hor. p	Section B ref. hor. p	Section C ref. hor. p
a	6250—6300 m	6450—6400 m	4500 m
b	4250 m	4200 m	3900 m
$a-b$	2000—2050 m	2200—2250 m	600 m
Y	1 633.500 m ²	2.014.000 m ²	1.280.000 m ²
t_q			2100 m
t_p	816 m	915 m	1050 m

depth, we can correct the measured values of uplift of sections A and B by introducing this folding depth.

$$Y' = Y + n(a-b) \quad . \quad . \quad . \quad . \quad . \quad . \quad (7)$$

where n is the increase of folding depth, equal to $1050-816 = 234$ m for section A , and $1050-915 = 135$ m for section B .

We find:

$$Y' \text{ section } A = 2.101.500 \text{ m}^2$$

$$Y' \text{ section } B = 2.311.000 \text{ m}^2.$$

The value of the shortening, $a-b$, is hardly effected by increasing the folding depth, both a and b being lengthened by roughly the same amount.

In sections A and B the anticline is strongly overthrust, the amount of overthrust being 1400 m in section A and 1550 m in section B , whereas in section C the thrusting movement has only just begun and can probably be disregarded.

Comparing the shortening in the three sections we see that the difference in amount of shortening is exactly equal to the respective amounts of overthrusts. (Table IV).

TABLE IV

Shortening section A	$600 + 1400 = 2000$ m	measured 2000 — 2050 m
Shortening section B	$600 + 1550 = 2150$ m	measured 2200 — 2250 m

From this feature we may conclude that section C represents an earlier stade of compression than the sections A and B .

A continued compression of section C , would then necessarily result in the shape of fold represented by sections A and B . When, m , is the increase of shortening then the resulting uplift will be

$$Y' = Y + t m \quad . \quad . \quad . \quad . \quad . \quad . \quad (8)$$

However, before we can compare the sections we must calculate the

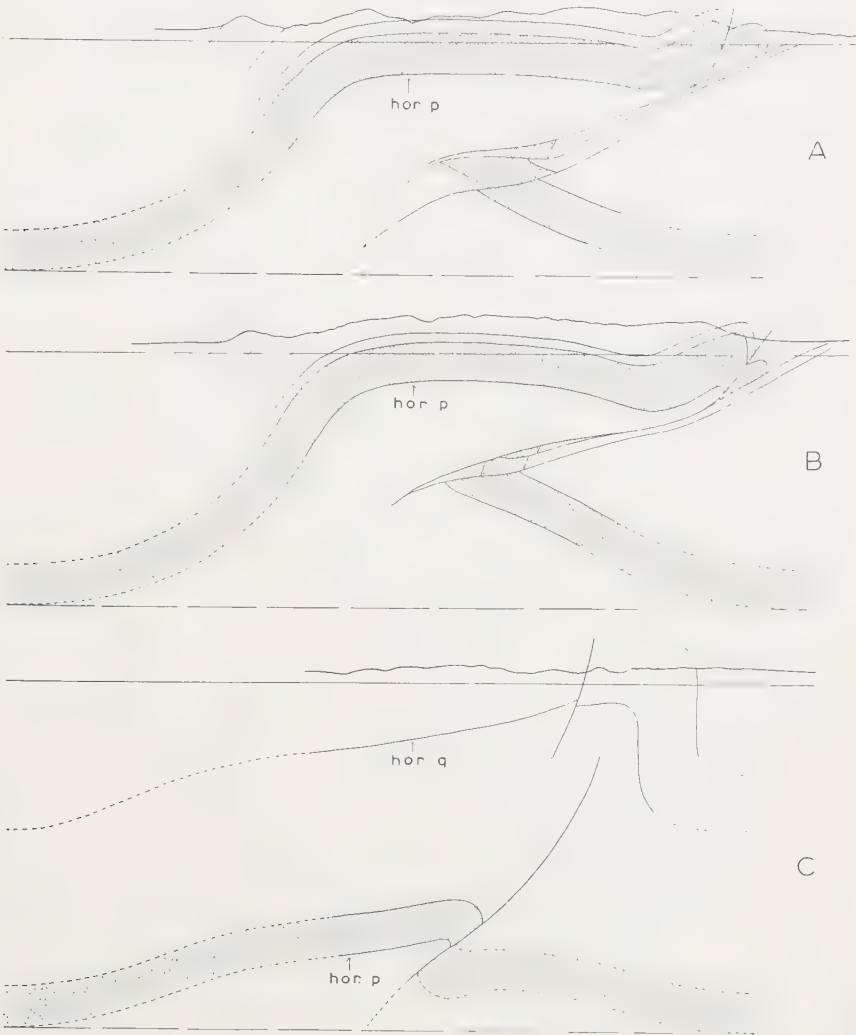


Fig. 16. Cross sections through a well explored anticline, based on drilling results.

uplift, Y_p , of the reference horizon p in section C by multiplying the folding depth $t_p = 1050$ m by the shortening $a-b = 600$, we find

$$Y_p \text{ in section C} = 630.000 \text{ m}^2.$$

Introducing this value of Y in eq. (8), and the values of 1400 m and 1550 m of m , for sections A and B respectively, we find:

$$Y' \text{ section A} = 2.100.000$$

$$Y' \text{ section B} = 2.257.500.$$

In table V the final comparison has been tabulated.

TABLE V

	Section A	Section B	Difference
Y' according to eq (7).	2101500 m ²	2100000 m ²	1500 m ² 0.07%
Y' according to eq. (8)	2311000 m ²	2257500 m ²	53500 m ² 2%

The very close agreement we notice in tables IV en V is a warrant of the validity of the theory.

We can conclude that without doubt the whole anticline has everywhere the same folding depth.

The practical value of this conclusion is manifold viz.:

1st Intermediate sections, which are badly disclosed, can be partly reconstructed by interpolating the values of Y and $a-b$; 2nd the folding depth itself may be of considerable interest; 3rd the prognose of the tectonical structure of the subsurface is much less a matter of conjecture because the length a and the shortening are known beforehand.

We must bear in mind, however, that the lower part of a fold is not necessarily folded concentrically. Already from the earliest start of the fold a part of the formation situated below the concentricity boundary must adopt itself to the available space, and this may be done by a compression fold comparable to fig. 3, or by faulting.

BIBLIOGRAPHY.

- CHAMBERLIN, R. T.: The Appalachian folds of Central Pennsylvania. Journ. Geol. Vol. 18, 228—251 (1910).
- BUXTORF: Prognosen und Befunde beim Hauensteinbasis und Grenckenbergtunnels und die Bedeutung der letzteren für die Geologie des Juragebirges. Verh. Naturf. Ges. Basel, Vol. 27 (1916).
- ALBERT HEIM: Geologie der Schweiz (1922).
- OBERHOLZER, J.: Geologie der Glarneralpen. Beitr. Geol. Karte d. Schw. N.F. 28. Bern (1933).
- PRUVOST: Bassin Houiller de la Sarre et de la Lorraine, III. Descrip. géologique. Lille (1934).
- DE SITTER, L. U.: Plastic deformation. Leidsche Geol. Med. IX, 10 (1937).
- DE SITTER, L. U. and PH. H. KUENEN: Experimental investigation into the mechanism of folding. idem, Dl. X, 217—240 (1938).

Botany. — *Some remarks on the mechanism of spiral growth of the sporangiophore of Phycomyces and a suggestion for its further explanation.* By A. N. J. HEYN. (Communicated by Prof. G. VAN ITERSON.)

(Communicated at the meeting of April 29, 1939.)

The spiral growth of the spore bearing cell of *Phycomyces*, as first described by BURGEFF, 1915, and more especially studied by OORT, 1931, has become a phenomenon of more general interest later on in relation to the study of the mechanism of cell elongation.

During elongation this unicellular sporangiophore rotates round its long axis. OORT and ROELOFSEN, 1932, were the first to endeavour to give an explanation of the phenomenon. Referring to the old hypothesis of DIPPEL, 1868, and VAN ITERSON, 1927, on the relation between protoplasmic streaming and the orientation of new particles in the cell wall, these authors investigated whether a connection existed between the phenomenon of rotation and the direction of protoplasmic streaming in the spore bearing cell of this fungus. (*A. Theory of protoplasmic streaming*).

They were unsuccessful, however, in correlating protoplasmic streaming and spiral growth, no oblique direction of streaming being observed in the zone of elongation. These observations were confirmed later on by POP, 1938, who even described protoplasmic streaming as taking place always in a direction parallel with the long axis of the organ in the elongating zone. POP, however, adheres to the theory of protoplasmic streaming as the direction of streaming observed may in some undefined way result in *oblique* orientation of cell wall molecules on account of the asymmetry of the chitin molecules.

A study of the double refraction of the cell wall, by OORT and ROELOFSEN, revealed, that the wall consists of three different layers. The middle or main layer of the wall has positive birefringence, the long axis of the index ellipsoid forming a small angle with the long axis of the wall. Of the thin layer outside the main layer, the long axis of the index ellipsoid is almost perpendicular to that of the middle layer. The birefringences of these two layers compensate each other at a distance of about 2 mm from the sporogonium (the zone of elongation also laying within these 2 mm). Below these zones the birefringence of the middle layer preponderates, whereas above it the birefringence of the outer layer predominates ¹⁾.

¹⁾ The conclusion of OORT and ROELOFSEN that in the older sporangiophore the middle layer is even completely absent in the zone of elongation does not of necessity follow from the optical data, as these data can be sufficiently explained by a *less complete crystalline structure* of the middle layer in the growth zone (as it follows from the X-ray observations to be referred to in the following).

With regards to the third layer lying inside the main layer it is sufficient to mention here that this layer is very thin and has irregular structure.

The authors supposed the birefringence of the different cell wall layers to be due to some orientation of chitin molecules or micelles in the wall, but were unable to make any definite conclusion on the orientation of these molecules on the basis of the data on double refraction, as nothing was known at that time on the relation between molecular structure and double refraction of chitin (Comp. the later investigations of DIEHL and VAN ITERSON, 1936, and DIEHL, 1936).

In 1935 a direct investigation of the molecular structure of the wall of the sporebearing cell of *Phycomyces* by means of X-ray diffraction patterns was carried out by the author of this note in order to obtain further data on the relation between the mechanism of cell elongation and the molecular structure of the cell wall. It was possible to determine the place of the chitin molecules in the cell wall and the dimensions and structure of the crystallographic cell of chitin. At the same time VAN ITERSON, MEYER and LOTMAR described the fibre diagram, obtained from the same cell wall.

The chitin molecules which form the frame of this cell wall can be conceived as consisting of ordinary cellulose chains (built up of linked glucose residue rings) with short proteid side-chains being placed alternately on each side (one side-chain corresponding to one glucose residue ring, together forming one glucosamine residue). (Comp. fig. 1).

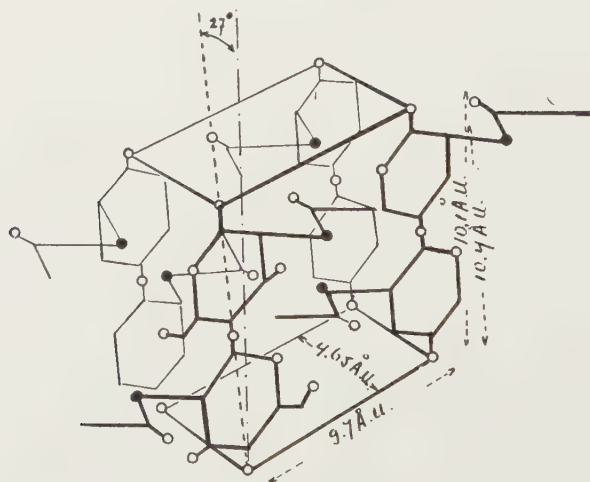


Fig. 1. The position of molecules in the unit cell of chitin. The carbon atoms are omitted. ○ Oxygen atoms. ● Nitrogen atoms. The *b* axis (10.45 Å.u.) forms an angle of $13\frac{1}{2}$ or 27 degrees with the vertical. The cellulose chains of chitin lie along the *b* axis, the protein sidechains along the *a* axis. The *c* axis agrees with the side distance of protein chains (4.6 Å.u.).

The chitin molecules proved to be situated as follows in the hollow cylinder of the cell wall of the older areas. (Comp. fig. 2 and 3). The

axes of the proteid side chains lie exactly in radial direction, being perpendicular to the surface of the wall and perpendicular above each

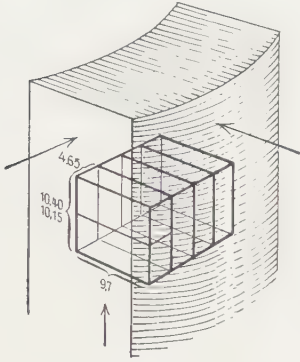


Fig. 2. Orientation of space lattice of chitin in the wall of sporangiophores of *Phycomyces*.



Fig. 3. Diagrammatic representation of the position of molecules in the wall of sporangiophores of *Phycomyces*.

other, in vertical planes of spacing of 4.65 Å. (corresponding to the identity period of proteids), and in horizontal planes of spacing of 10.15 Å. (corresponding to the fibre period of cellulose).

It can be deduced from this structure that the cellulose main chain of the chitin molecule must have oblique position, forming an angle of $13\frac{1}{2}$ or 27 degrees with the long axis of the organ. Originally an angle of $13\frac{1}{2}^\circ$ was calculated by accepting every *second* proteid side chain of *neighbouring molecules* as laying above each other in vertical direction. This is illustrated by fig. 4b. There is perhaps as much reason, for accepting *all* successive proteid side chains as laying above each other in the *same* vertical plane, as illustrated by fig. 4c. In the latter case the angle calculated of the long axis of the chitin molecules with the vertical is 27° (arc $\tan 4.65$). With regard to the other directions the cellulose main chain (10,15) must be placed in such a way in the wall that the planes of the glucose anhydride rings and of the glucosamine residues are perpendicular to the surface of the cell wall. (Comp. fig. 3).

This conclusion of the position of the chitin molecules in the cell wall is in good accordance with the results on double refraction obtained by OORT and ROELOFSEN, if it is assumed that the long axis of the index ellipsoid is parallel with the length direction of the chitin molecules, and that the X-ray diffraction pattern is mainly due to the thick main layer of the cell wall. Accepting this for granted it may be concluded in its turn that the orientation of chitin molecules in the thin outer layer of the same wall is perpendicular to the orientation of the molecules in the main layer. The outer layer therefore can be described as having "tube" structure, as it consists of long chitin chains or micelles encircling the organ, these

chains being almost perpendicular to the long axis of the organ; — in the same way the main layer can be described as having "fibre" structure.

Returning to the explanations of spiral growth the hypothesis was originally suggested on the basis of the X-ray observations that a causal relation exists between the oblique position of the molecules in the main layer of the older cell wall and the rotation of the organ round its axis; a sliding of chitin molecules along the oblique planes of greatest weakness in the crystallites (the planes of the glucosamine residues) being supposed (B. "*Structural theory*"). The maximum angle of spiralling possible would than be 27 ($13\frac{1}{2}$) degrees.

CASTLE detected the important fact that temperature influences the rate of rotation much more than the rate of elongation, so that the steepness of the average inclination of the spiral (angle with the long axis) is greater at higher temperatures. Temperatures of 27 or 28 degrees C. abolish rotational growth altogether, or rarely produce rotation in opposite direction, elongation continuing.

From these experimental data objections can be derived to a structural theory as given above, as temperature must be expected to affect rotation and elongation in the same way if mere sliding along oblique crystalplanes of constant slope of $13\frac{1}{2}$ or 27 degrees takes place in spiral growth. Such objections would have no more ground, however, if it is accepted that the rotational component and the angle of spiralling is not only dependent on the angle between the chitin molecules and the long axis of the organ but also on the *number* of chitin molecules involved, the angle of spiralling becoming gradually smaller than the angle of the planes of greatest weakness, if the number of chitin micelles in vertical direction decreases.

A decrease of the number of these micelles in the elongating zone under the influence of temperature can be quite well expected as temperature can be presumed much more to affect the process of formation of new cell wall particles than the process of elongation. (The temperature coefficient of plastic stretching in cell walls was found to be 1.2 in a special case).

The absence of rotation of the sporebearing cell before formation of the spore mass, as described by CASTLE can be also interpreted in a similar way by assuming that at *that period of rapid elongation chitin molecules are not yet present* in vertical direction in the elongating zone, the *primary* wall in which the molecules have transverse orientation being present only here (as supposed by OORT and ROELOFSEN also for the full grown sporangioophore, comp. footnote ¹)).

Although none of the experimental data of CASTLE are therefore in definite contradiction to the structural theory it may be of interest to point out here a modification of this theory by which the theory of protoplasmic streaming is combined with the structural theory, (but in an other way as was suggested by POP). This theory can be summarized as follows.

In the main cell wall layer of the zone of elongation, the chitin molecules are *originally deposited in the direction of the long axis, parallel with the*

direction of protoplasmic streaming, conforming to the theory of DIPPEL—VAN ITERSON. At that moment the molecules have not yet attained complete crystalline configuration, as can be seen from the X-ray diagram. But very soon they arrange themselves in the denser crystal lattice. *The transition into the denser crystal lattice must be accompanied by the inclining of the molecules into an oblique position of finally $13\frac{1}{2}$ or 27 degrees with the long axis of the organ; — otherwise the observed orientation of the proteid side-chains in the crystal lattice would not be realized.* This is illustrated by fig. 4a—c.

The inclining of the chitin molecules is caused by forces of crystallization (secondary valence forces); presumably especially the attraction between

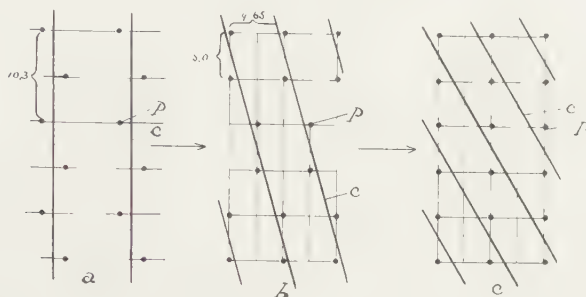


Fig. 4. Grid of chitin. *C*, axis of chains of cellulose compound of chitin molecule. *P*, axis of side chains of the protein compound (vertical to the plane of the paper and the surface of the cell wall).

a. Presumed primary position of chitin molecules in the zone of elongation, shortly after being deposited, the long axis of the molecules parallel with the long axis of the organ.

b. Later position of chitin molecules in crystal lattice, the molecules forming an angle of $13\frac{1}{2}^\circ$ with the length direction of the organ.

c. The same, the molecules forming an angle of about 27° with the length direction of the organ, all proteid chains laying above each other in the same planes.

CO and NH groupings in the crystal playing a part. This inclining of molecules in the cylindric cell wall must go hand in hand with a rotation of the unicellular organ if all or most molecules incline to the same side; the forces therefore causing spiral growth must be identical to forces of crystallization (C. "Crystallization theory").

The thin outer layer of the wall will offer some resistance to this process of rotation, as its molecules have transverse orientation, but being much thinner than the main wall it will be carried along in the rotation. Perhaps the faint striping (folding) on the outside of this layer is due to passive rotation. (The middle layer has *active* rotation). The combination of the rotating forces and the extending forces of elongation will result in the spiral growth observed.

It may be of interest to compare this crystallization theory with some later experimental data and considerations of CASTLE (1934—'37). Endeavouring to explain the spiral growth of *Phycomyces* CASTLE suggested

that the origin of spiral growth is due to the interaction between turgor and elastic forces in the membrane. He based this suggestion on observations on a special very illustrative model, consisting of a set of parallel vertical dowels fixed at their base. A narrow compression ring pushed over the dowels causes them to thrust in slightly against a spool at their top. Spiral twisting occurs if the ring is pushed down and the dowels obtain a complex curvature with an inflexion point. This model concurs in so far with nature that the elongating zone of the organ, tapering towards the top, also shows a similar kind of sigmoid curve of its cell wall. Furthermore CASTLE found that in cells of different types of curvature of the cell wall in the elongating zone the angle of spiralling also tends to be different.

By these experiments a *causal relation between curvature of the cell wall and rotation* is made very plausible indeed, but it would be too far-fetched to presume from this analogy that spiral growth can be *explained* by the twisting of elastic elements of the cell wall, resolving *bending stresses imposed on them by the turgor pressure*. (D. "*Theory of turgor pressure*"); a comparison of the compressing ring of the model and the turgor pressure being hardly possible.

The illustrative model of CASTLE would be much more applicable, however, were it used to explain the relations demanded by the crystallization theory. It is obvious that the *compressing ring of CASTLE's model can be directly compared with the forces of crystallization*, causing rotation in the way described above.

Under the influence of crystallization forces a twisting of elastic elements occurs just as in the model of CASTLE, namely a transition of (elastic) chitin molecules or micelles from the vertical into the oblique position; a shaping of the cell wall in the elongating region, as described by CASTLE and as illustrated by his model will be the result.

CASTLE recently suggested a new theory of spiral growth; he emphasized the fact that under uniform internal pressure the tensile stress in the cell wall of a cylindric cell is greater in the length direction than in the transverse direction. Oblique tension forces in the cell wall, which according to him would be the result, would cause a deposition of new cell wall particles in oblique direction, which would in some way cause spiral growth (E. "*Theory of cell wall stress*"). When accepting this theory it must be explained why not all cylindric cells have spiral growth.

From the 5 theories on spiral growth existing at present and described above the structural and crystallization theories appear to be the most probable to the author of this note and anyhow they are not in disaccordance with any of the experimental facts available at present. Further researches will be necessary to substantiate these theories.

Taking one of these theories for granted, *the spiral growth of Phycomyces can be considered as a very illustrative example of the role of the structure of the cell wall and of the forces of crystallization in the process of cell elongation.*

REFERENCES.

- CASTLE, E. S., *Science*, **80**, 362 (1934).
- *J. Cell. and Comp. Physiol.*, **7**, 445 (1936a).
- *J. gen. Phys.*, **19**, 797 (1936b).
- *J. Cell. and Comp. Physiol.*, **8**, 493 (1936c).
- *Proc. Nat. Acad. Sci.*, **22**, 336 (1936d).
- *J. Cell. and Comp. Physiol.*, **9**, 477 (1937a).
- *J. Cell. and Comp. Physiol.*, **10**, 113 (1937b).
- DIEHL, J. W., *Chem. Weekbl.*, **33**, 36 (1936).
- und G. VAN ITERSON, *Koll. Zs.*, **73**, 142 (1936).
- DIPPEL, L., *Abh. Naturf. Ges. Halle*, **10**, 55 (1868).
- GONELL, H. W., *Z. phys. Chem.*, **152**, 18 (1926).
- HEYN, A. N. J., *Protoplasma*, **25**, 372 (1935).
- *Proc. Kon. Akad. v. Wetensch., Amsterdam*, **37**, 132 (1936a).
- *Nature*, **137**, 277 (1936b).
- ITERSON, G. VAN, *Chem. Weekbl.*, **24**, 166 (1927).
- *Chem. Weekbl.*, **30**, 1 (1933).
- *Proc. 6th Int. bot. Congr.*, **II**, 291 (1936).
- *Protoplasma*, **27**, 190 (1937).
- ITERSON, G. VAN, K. H. MEYER and W. LOTMAR, *Rec. trav. chim.*, **55**, 61 (1936).
- MEYER, K. H. and G. W. PANKOW, *Helv. chim. Acta*, **18**, 589 (1935).
- OORT, A. J. P., *Proc. Kon. Akad. van Wetensch., Amsterdam*, **34**, 564 (1931).
- and P. A. ROELOFSEN, *Proc. Kon. Akad. van Wetensch., Amsterdam*, **35**, 898 (1932).
- POP, L. J., *Proc. Kon. Ned. Akad. v. Wetensch., Amsterdam*, **41**, 661 (1938).
- PRESTON, R. D., *Proc. Leeds Phil. Soc.* **III**, part. V, 327 (1936).
- SINGER, R., *Ztschr. physik. Chem. A*, **150**, 257 (1933).

Plantkunde. — *Proeven over het uitloopen van de knollen en het ver-
vroegen van den bloei bij Freesia hybriden (with summary).* Door
ANNIE M. HARTSEMA en IDA LUYTEN. (Mededeeling N^o. 59 van
het Laboratorium voor Plantenphysiologisch Onderzoek.) (Aange-
boden door Prof. A. H. BLAAUW).

(Communicated at the meeting of April 29, 1939.)

Sedert eenige jaren worden behalve de witte, uit zaad gekweekte Freesia's (*Freesia refracta alba*) ook Freesia's met gekleurde bloemen voor de snijbloemencultuur gebruikt. Deze gekleurde Freesia's, waarvan de door de firma C. G. van Tubergen gewonnen variëteiten *Daffodil* en *Buttercup* zeer bekend zijn, worden vrijwel uitsluitend uit knollen voortgekweekt. Tot voor eenigen tijd was het zaad hiervan n.l. zeer kostbaar; nu men in de laatste jaren er in geslaagd is ook hier te lande zaad te winnen, mag verwacht worden, dat de prijs geen beletsel voor deze wijze van cultuur behoeft te zijn. Een nadeel blijft echter, dat uit zaad gekweekte planten kleurafwijkingen geven. Hoogstens 60 % van de zaden geeft n.l. planten met gekleurde bloemen.

Bij de cultuur uit knollen kan men gewoonlijk midden Juni de nieuwe knollen oogsten: in September-October worden deze dan weer geplant. De Rijkstuinbouwconsulent te Aalsmeer maakte ons er opmerkzaam op, dat een gedeelte van deze knollen na het planten niet uitloopt, ja soms geeft een geheele partij geen blad. Bij onderzoek blijkt dan, dat de oude knol geen spruit gegeven heeft, maar dat zich in plaats daarvan op den ouden knol een nieuwe knol gevormd heeft. Nu is het opvallend, dat dit „slaper“-verschijnsel zich nooit voordoet bij knollen, die uit Zuid-Frankrijk worden aangevoerd. Het leek ons daarom waarschijnlijk, dat wij de oorzaak van dit verschijnsel moesten zoeken in een onjuiste temperatuurbehandeling gedurende de maanden dat de knollen droog bewaard worden. Naast het onderzoek naar deze temperatuur, werden ook nog enkele trekproeven opgezet. De resultaten van deze voorloopige trekproeven vindt men in het tweede gedeelte van deze publicatie beschreven. Tevens werd materiaal gefixeerd om den tijd van bloemaanleg vast te kunnen leggen. Dit laatste materiaal wacht nog op bewerking.

Invloed van de temperatuur gedurende de bewaarperiode.

Op 25 Juni 1935 ontvingen wij van een kweker te Aalsmeer een partijtje van de gele variëteit *Daffodil* (*Freesia refracta alba* x *Freesia Chapmani*). Wij zochten de grootste knollen uit (gewicht per 12 stuks 75.5 gram) en brachten 48 stuks naar ieder van de volgende temperaturen: 9°—13°—17°—20°—23°—25½°—28°, terwijl de luchtvochtigheid steeds op ongeveer 70 % werd gehouden.

10 Weken later, n.l. op 4 September, werden de knollen geplant (12 per kistje van $22\frac{1}{2} \times 20 \times 18$ cm). Als grondmengsel werd gebruikt $\frac{3}{5}$ bladgrond, $\frac{1}{5}$ verteerde koemest en $\frac{1}{5}$ scherp zand, na het planten werd de grond in de kistjes bedekt met een laagje scherp zand om beschimmelen tegen te gaan. Het grondmengsel was goed vochtig gemaakt en er werd, althans in het begin, niet meer gegoten. De kistjes werden gedurende 1 week bij 15° C. en daarna bij $10-11^{\circ}$ C. gezet.

3 Weken na het planten, op 25 September, waren de te voren bij $20^{\circ}-23^{\circ}-25\frac{1}{2}^{\circ}$ en 28° C. bewaarde knollen zoover uitgelopen, dat de kistjes naar het licht moesten worden overgebracht: ze werden in een kas van 11 à 12° C. geplaatst. De spruitlengte varieerde nogal sterk, was gemiddeld het langst bij 23° ; het aantal uitgelopen knollen was 37 bij 20° , 44 bij 23° , 42 bij $25\frac{1}{2}^{\circ}$ en 43 bij 28° .

Op 27 September gingen ook de kistjes van de bij 17° bewaarde knollen naar het licht, hoewel hier nog slechts enkele spruiten te voorschijn gekomen waren. Van de bij 13° bewaarde knollen werden de kistjes op 4 October overgebracht; de bij 9° bewaarde knollen waren zelfs op 16 Januari 1936 nog niet opgekomen; ze vertoonden alle het beeld van de z.g. „slapers”.

De proeven bleven in kas $11^{\circ}-12^{\circ}$ staan, totdat de eerste bloeiwijzen

TABEL 1. 1935/1936.

Voorbehandeling	Datum over- brengen n. kas $11^{\circ}-12^{\circ}$	Aantal spruiten	Gem. spruit lengte in cm.	Datum over- brengen n. kas 17°	Datum 1e bloem open	Aantal opge- komen	Aantal bloeiend
n = 48							
10 wk. 9°	—	—	—	—	—	0	0
10 wk. 13°	4 Oct.	—	—	3 Jan.	14 Jan.	31	3
10 wk. 17°	27 Sept.	—	—	3 Jan.	15 Jan.	45	4
10 wk. 20°	25 Sept.	37	5.3	3 Jan.	16 Jan.	48	2
10 wk. 23°	25 Sept.	44	7.4	27 Dec.	10 Jan.	48	7
10 wk. $25\frac{1}{2}^{\circ}$	25 Sept.	42	6.0	3 Jan.	12 Jan.	48	8
10 wk. 28°	25 Sept.	43	3.5	27 Dec.	9 Jan.	48	8
n = 24							
6 wk. $25\frac{1}{2}^{\circ}$	27 Sept.	18	5.8	14 Dec.	1 Jan.	22	12
+ 4 wk. 9°							
4 wk. $25\frac{1}{2}^{\circ}$	7 Oct.	15	7.6	3 Jan.	13 Jan.	13	2
+ 6 wk. 9°							

zichtbaar werden: daarna werden de kistjes overgebracht naar kas 17°, waar de eerste bloem opening op 16 Januari 1936.

In tabel 1 vindt men een overzicht van de resultaten der hier genoemde temperatuurbehandelingen. Het aantal bloeiende planten was zeer gering. Wij vermoedden dat wij dit voor een groot gedeelte aan één of meer cultuurfouten moesten toeschrijven. Door het planten in kistjes is de kans op uitdrogen n.l. vrij groot. Het volgende jaar werd dit ondervangen door de kistjes in natten turfmoel in te graven. Verder wees een kweker ons op mogelijk kalkgebrek. Een ander jaar werd dus kalk toegevoegd. Ook de geringe grootte van de knollen zou nog een oorzaak van het slechte bloeiresultaat kunnen zijn. In volgende jaren vonden wij hiervoor echter in onze verdere proeven geen enkele aanwijzing.

Uit de beide laatste groepen van tabel 1 (dit zijn twee toegevoegde proeven, ieder bestaande uit 24 stuks) blijkt dat 66k de bewaartemperatuur invloed heeft op den bloei. De knollen van deze groepen werden gedurende 6 resp. 4 weken bij 25½° bewaard en daarna 4 weken resp. 6 weken bij 9° (tot den plantdatum, 4 September). Wij zien dat 12 van de 22 opgekomen planten bloieden, d.i. dus ruim 50 % na de behandeling 6 wk. 25½° + 4 wk. 9°. Ook het opengaan der bloemen had eerder plaats, n.l. reeds op 1 Januari. Hierin ligt een aanwijzing voor vroegen bloei: in plaats van de warme zomerbehandeling voort te zetten tot begin September, kan men deze eerder afbreken: door bewaren bij 9° gedurende de laatste weken krijgt men snelleren en beteren bloei dan na voortgezette behandeling van 25½°. Breekt men echter de behandeling van 25½° eerder af (4 weken), dan vermindert daardoor het uitloopen der knollen (13 van de 24) en de bloei (2 van de 13). Bezien we nog eens het opkomen van de proeven die gedurende 10 weken dezelfde bewaartemperatuur hadden, dan blijkt dat de proeven met 10 wk. 17° en 10 wk. 13°, die bij het overbrengen naar de kas maar enkele spruiten hadden, later toch nog uitgelopen zijn; n.l. 45 en 31 knollen zijn opgekomen. Bij 17° zien we dus reeds eenigen invloed van de nadeelige bewaartemperatuur optreden. Bij 13° treedt deze sterker voor den dag, terwijl zooals we reeds boven vermeldden 9° alle knollen tot slapers gemaakt heeft. Bij 28°, 25½°, 23° en 20° zijn *alle* knollen uitgelopen; bij de 3 eerstgenoemde temperaturen kwam echter het grootste aantal tot bloei (tabel 1).

Het volgende jaar werden deze proeven herhaald, deels met materiaal dat geoogst werd van de hier beschreven proeven, deels met knollen, die op 18 Juni 1936 rechtstreeks van den kweker ontvangen werden. Deze wogen 92 gram per 12 stuks, terwijl die van den eigen oogst slechts 58.5 gram per 12 stuks waren. Om ook ditmaal begin September te kunnen planten, werden de temperatuurbehandelingen gedurende 11 weken toegepast. Al deze proeven werden op 3 September geplant bij 9°, met uitzondering van de laatste groep, die wij ter vergelijking pas op 1 October wilden planten. Zoodra de spruiten flink zichtbaar waren, werden de kistjes overgebracht naar het licht in kas 9°. In verband met andere proeven

was dit jaar n.l. geen kas van 11 à 12° beschikbaar. Het verblijf bij deze lagere temperatuur is de oorzaak geworden van de totale mislukking van den bloei. Toch willen wij deze proeven hierbij vermelden, omdat de invloed van de temperatuur gedurende de bewaarperiode op het uitloopen der knollen hier wel duidelijk blijkt (zie tabel 2).

TABEL 2. 1936/37.

Voorbehandeling	Datum overbrengen naar kas 9°	Aantal uitgelopen knollen	Totaal aantal geplant
11 wk. 23°	6 October	42	48
11 wk. 28°	12 October	48	48
8 wk. 25½° + 3 wk. 17°	6 October	47	48
6 wk. 25½° + 5 wk. 17°	6 October	42	48
11 wk. 23°	11 November	24	48
11 wk. 25½°	26 October	29	48
6 wk. 25½° + 5 wk. 17°	26 October	24	48
7 wk. 25½° + 4 wk. 9°	6 November	14	36
11 wk. 25½° + 4 wk. 9°	7 November	36	48

De eerste 4 proeven zijn uitgevoerd met de zelf-geoogste knollen, ze zijn alle goed uitgelopen, maar minder snel dan het vorige jaar, tengevolge van de lagere temperatuur. De laatste 5 proeven zijn uitgevoerd met de gekochte knollen, die gekweekt waren in een warenhuis. Na het rooien werden ze direct aan ons toegezonden. Het is opvallend dat deze knollen zooveel minder goed uitliepen dan de zelf-geoogste. De laatste groep, die na 11 weken 25½° nog 4 weken droog bleef liggen bij 9°, is nog de beste, hoewel hier ook nog 25 % der knollen slapers werden.

Op 15 Juni 1937 werden de knollen van al deze proeven gerooid en uitgezocht voor nieuwe proeven. Het gewicht was nu 76 gram per 12 stuks. De knollen werden weer gedurende 11 weken behandeld en op 2 September geplant. Evenals in 1935 werden de kistjes eerst 1 week bij $\pm 15^\circ \text{C}$. in 't donker geplaatst, daarna iets hoger dan in 1936, n.l. in 12 à 13° (donker), totdat ze overgebracht moesten worden naar kas 13°. Met het zichtbaar worden der bloeiwijzen werden de kistjes tenslotte overgebracht naar kas 17°.

In tabel 3 vindt men de verschillende behandelingen en de resultaten daarvan.

Daar uitsluitend behandelingen waren gekozen, waarbij alle knollen uit zouden loopen, werd het aantal dat uitliep niet apart vermeld. Alleen bij de kort-durende warmtebehandeling, 6 weken 25½° gevolgd door 5 weken

TABEL 3. 1937/38.

Voorbehandeling	Aantal geplant	Datum overbrengen naar kas 17°	Datum 1e bloem open	Aantal bloeiende planten	Aantal niet-bloeiende planten
11 wk. 23°	48	13 Dec.	25 Dec.	11	37
11 wk. 25½°	48	13 Dec.	25 Dec.	11	37
11 wk. 21°	48	28 Dec.	31 Dec.	9	39
8 wk. 25½°	36	13 Dec.	24 Dec.	10	26
+ 3 wk. 17°					
6 wk. 25½°	36	28 Dec.	31 Dec.	8	27
+ 5 wk. 15°					
15 wk. 25½°	48	28 Jan.	—	0	48

17°, was 1 knol niet uitgelopen. Verder werd 1 groep gedurende 15 weken met 25½° behandeld in verband met het planten op 29 September. Wel liepen deze knollen alle uit, maar er kwam geen enkele bloem te voorschijn.

Ook van de andere groepen was de bloei zeer matig, hoogstens 28 %. Wij zullen zien dat het bloeipcentage bij de voor vroegen bloei behandelde groepen beter is, hoewel ook daarbij nooit 100 % bereikt wordt. De oorzaak van dit slechte bloeien moet wel gezocht worden in de culturomstandigheden, bijv. in het feit dat wij onze proeven moesten uitplanten in kistjes en niet in den vollen grond, zooals in de praktijk gebruikelijk is. Verder is het licht in de door ons gebruikte kas niet gunstig, de kas is aan de noordzijde van het laboratorium gebouwd en heeft een dubbelwandig glazen dak. Om de lage temperatuur te kunnen handhaven, is n.l. gebruik van een aan de zuidzijde gelegen kas niet mogelijk.

Dat niettegenstaande deze slechte culturomstandigheden de voor vroegen bloei behandelde groepen zooveel beter bloeiden, zooals wij ook op blz. 440 reeds opmerkten, kan tweërlei oorzaak hebben. In de eerste plaats kan dit aan de daarbij gebruikte temperatuurcombinatie liggen. In de tweede plaats is het mogelijk dat de lichtintensiteit en de daglengte, die in de wintermaanden sterk afnemen, tijdens den korteren ontwikkelingstijd van de vroeg-bloeiende groepen nog juist voldoende zijn, maar bij de later-bloeiende te gering worden.

Wij hopen door voortgezette proefnemingen hierover nadere gegevens te verkrijgen.

Voorloopige proeven over het vervroegen van den bloei.

In tabel 1 vonden wij reeds aanwijzingen voor het verkrijgen van vroegeren bloei, n.l. door de knollen in plaats van 10 weken slechts 6 weken bij 25½° te bewaren en daarna naar 9° over te brengen. De eerste bloemen



Fig. 1. *Freesia hybrida* var. *Daffodil*. 15 Juni 1937 ontvangen; 7 wk. 25½° + 4 wk. 9°; 2 Sept. geplant.
Begin van den bloei 14 Dec.; foto 20 Dec. 1937.

gingen dan op 1 Januari open. In het volgende jaar mislukte de bloei tengevolge van de te lage kasttemperatuur.

In 1937 werden, zooals reeds vermeld is op blz. 441, alle proeven na het planten eerst 1 week bij $\pm 15^\circ$ geplaatst en daarna bij 13° . De knollen wogen bij het rooien op 15 Juni 76 gram per 12 stuks; ze werden op 2 September geplant. Tabel 4 geeft de waargenomen resultaten.

TABEL 4. 1937/38.

Voorbehandeling	Aantal geplant	Datum overbrengen naar kas 17°	Datum 1e bloem open	Aantal bloeiend	Aantal niet-bloeiend
5 wk. $25\frac{1}{2}^\circ$ + 6 wk. 13°	36	30 Nov.	14 Dec.	20	16 (3)
7 wk. $25\frac{1}{2}^\circ$ + 4 wk. 9°	36	30 Nov.	14 Dec.	23	13 (2)
7 wk. $25\frac{1}{2}^\circ$ + 4 wk. 13°	36	30 Nov.	9 Dec.	26	10
9 wk. $25\frac{1}{2}^\circ$ + 2 wk. 9°	36	30 Nov.	16 Dec.	20	16
9 wk. $25\frac{1}{2}^\circ$ + 2 wk. 13°	36	30 Nov.	18 Dec.	29	7 (1)

De bloei begon ditmaal reeds op 9 December, n.l. bij de groep die gedurende de bewaarperiode na 7 weken $25\frac{1}{2}^\circ$ overgebracht was naar 13° . Uit de tabel blijkt wel, dat het voor den vroegen bloei heel belangrijk is, dat de warmte-behandeling niet te kort en ook niet te lang duurt, daar zoowel na 5 weken $25\frac{1}{2}^\circ$ als na 9 weken $25\frac{1}{2}^\circ$, beide gevolgd door 13° , de bloei later begon. Wel waren in 't laatste geval meer planten tot bloei gekomen. Werd 7 weken $25\frac{1}{2}^\circ$ gevolgd door 9° , dan was het vervroegend effect niet zoo duidelijk. Fig. 1 geeft een beeld van deze groep op 20 December; de bloei begon echter reeds op 14 December. Bij de beoordeeling van de bloeipercentsages moet men in aanmerking nemen, dat enkele planten ziek bleken te zijn (zie de getallen tusschen haakjes in de laatste kolom).

Het bloeipercentsage was in 1937/38 veel beter, d.w.z. 55—82 %, wat bij de genoemde ongunstige culturomstandigheden bevredigend kan worden genoemd.

Het aantal bloemen was in den regel 3 tot 6 per stengel; 7 en 8 bloemen kwamen zeer zelden aan een bloeiwijze voor.

In 1938 werden echter ook proeven genomen met de variëteit *Buttercup* (*Freesia refracta alba* x *Freesia Chapmani*). De knollen, die wij op 17 Juni ontvingen, waren zwaarder dan die van *Daffodil*, n.l. 140 gram per 12 stuks.

Het blijkt dat bij de behandeling voor den vroegen bloei verschillende

knollen slapers werden (tabel 5). Daarom is het noodig dat wij ook met deze variëteit proeven nemen over den invloed van de temperatuur op het uitloopen der knollen, zooals wij in 1935—1937 met de variëteit *Daffodil* deden. Het kan dan blijken, of deze *Buttercup*-knollen na de 10 weken temperatuurbehandelingen 20° , 23° , $25\frac{1}{2}^{\circ}$, 28° , alle kunnen opkomen (vergel. tabel 1) of dat in elk geval een gedeelte slapend blijft (tabel 2, 2de gedeelte). Zooals tabel 5 laat zien, is het aantal temperatuurcombinaties uitgebreid, door behalve bij $25\frac{1}{2}^{\circ}$ ook bij 23° te bewaren en daarna niet alleen bij 9° maar ook bij 11° en 13° te plaatsen.

TABEL 5. 1938.

Voorbehandeling	Aantal	Datum over- brengen naar kas 17°	Aantal uit- ge- loopen	Datum 1e bloem open	Aantal bloeiend	Aantal niet- bloeiend
7 wk. $25\frac{1}{2}^{\circ}$ + 4 wk. 9°	36	16 Nov.	4	1 Dec.	3	1
7 wk. $25\frac{1}{2}^{\circ}$ + 4 wk. 13°	36	16 Nov.	13	30 Nov.	12	1
7 wk. 23° + 4 wk. 11°	36	—	0	—	—	—
9 wk. $25\frac{1}{2}^{\circ}$ + 2 wk. 9°	36	22 Nov.	31	7 Dec.	30	1
9 wk. $25\frac{1}{2}^{\circ}$ + 2 wk. 13°	36	22 Nov.	26	8 Dec.	26	0
9 wk. 23° + 2 wk. 11°	36	22 Nov.	9	12 Dec.	9	0

Deze variëteit reageert zeer sterk op kleine temperatuursveranderingen, wat zoowel uit het uitloopen der knollen blijkt, als uit de bloeipercentsages. Zoo blijkt 7 weken warmte te kort te zijn: bij 7 weken $25\frac{1}{2}^{\circ}$ gevolgd door 13° komen er slechts 13 knollen tot ontwikkeling, waarvan 12 bloeien. 9 Weken $25\frac{1}{2}^{\circ}$ is veel beter, maar zelfs 9 weken 23° is nog onvoldoende. Uit het aantal bloeiende planten blijkt, dat de variëteit *Buttercup* veel gemakkelijker tot bloei te brengen is dan de variëteit *Daffodil*. Op één na kwamen alle uitgelopen planten ook tot bloei (vergelijk bijv. tabel 5 met tabel 4). Het aantal bloemen per stengel is bij deze variëteit ook veel beter, n.l. meestal 7—9. Bovendien ontwikkelden zich hier steeds een of meer bloeiende zijstengels. Ook ditmaal was 7 weken $25\frac{1}{2}^{\circ}$ gevolgd door 4 weken 13° de eerst bloeiende groep. Fig. 2 geeft een beeld van de bloeiende groep 9 weken $25\frac{1}{2}^{\circ}$ + 2 weken 9° op 12 December, d.i. 5 dagen nadat de eerste bloem opengegaan is. Men ziet op deze foto duidelijk het groote aantal bloemen per stengel, maximaal 11.

Vatten wij de resultaten van onze proeven met *Freesia hybriden* samen, dan konden wij dus

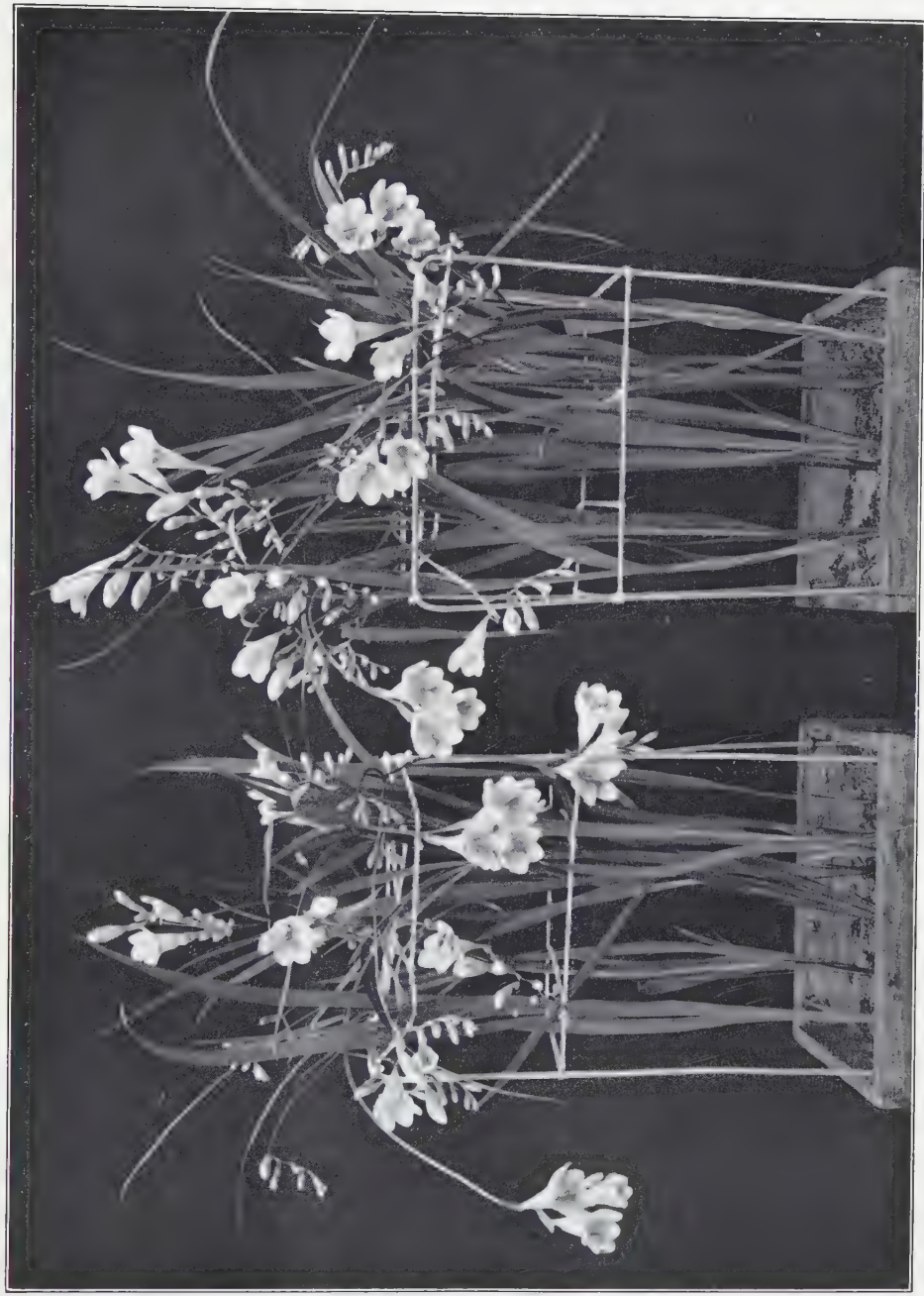


Fig. 2. *Freesia hybrida* var. *Buttercup*. 17 Juni 1938 ontvangen; 9 wk. $25\frac{1}{2}^{\circ}$ + 2 wk. 9° ; 2 Sept. geplant.
Begin van den bloei 7 Dec.; foto 12 Dec. 1938.

1e. het slapen blijven van de knollen tegengaan door warmtebehandeling gedurende de zomermaanden en wel

voor de var. *Daffodil* met $25\frac{1}{2}^{\circ}$ gedurende 6—11 weken

voor de var. *Buttercup* met $25\frac{1}{2}^{\circ}$ gedurende *minstens* 9 weken.

2e. het vroeg in bloei komen van de knollen bevorderen door een speciale temperatuurbehandeling gedurende de zomermaanden en wel

voor de var. *Daffodil* met 7 weken $25\frac{1}{2}^{\circ}$ gevolgd door 4 weken 13°

voor de var. *Buttercup* met 9 weken $25\frac{1}{2}^{\circ}$ gevolgd door 2 weken 9° .

In de literatuur vonden wij een artikel van HOSAKA (Effects of temperature treatment on the flowering of the bulbous plants. 2nd Report on Freesia forcing; Journ. of the Horticult. Association of Japan, Vol. 9 N^o. 2, 1938) waarin proeven worden beschreven met knollen van *Freesia refracta alba*. Voor zoover wij uit het Japansche résumé (dat voor ons vertaald werd) begrijpen kunnen, vond HOSAKA een gunstigen invloed van 60 dagen $13\frac{1}{2}^{\circ}$ C. bij in het najaar geplante knollen. Het is echter niet duidelijk of deze temperatuur direct na het rooien dan wel na een bewaarperiode bij hogere temperatuur wordt toegepast.

Verder zijn in „De Bloemisterij” verschillende artikeltjes verschenen over de cultuur van Freesia-hybriden, waarin men warm-bewaren der knollen gedurende de zomermaanden aanbeveelt, zonder daarbij temperaturen of duur van de behandeling te noemen. Van de cultuuraanwijzingen, die verder vermeld worden, hebben wij gaarne gebruik gemaakt.

Wageningen, April 1939.

SUMMARY.

Results of the temperature-treatment in summer on the sprouting of the tubers and the early flowering of Freesia hybrids.

We ascertained that the phenomenon of non-sprouting of coloured Freesia hybrids, so-called “sleepers”, can be influenced by temperature-treatments during the summer-months, i.e. the time after lifting and before replanting.

Table 1 (7th column) shows that only after the treatments of 10 weeks 28° , $25\frac{1}{2}^{\circ}$, 23° , and 20° all tubers (48) sprouted; after 10 weeks 9° not a single leaf appeared.

It is evident now that for the variety *Daffodil* 9—11 weeks $25\frac{1}{2}^{\circ}$ (for the variety *Buttercup* at least 9 weeks $25\frac{1}{2}^{\circ}$) after lifting are sufficient to guarantee the sprouting of the tubers.

Early flowering of the variety *Daffodil* was obtained by removing the tubers after seven weeks from $25\frac{1}{2}^{\circ}$ C. to 13° . With the variety *Buttercup* earliest flowering occurred after a treatment of 9 weeks $25\frac{1}{2}^{\circ}$ C. followed by 2 weeks 9° C. In these treatments the percentage of flowering plants was much higher than in all experiments described above (cf. tables 4 and 5). The researches will be continued.

Anatomy. — *Rindenoberfläche, resp. Rindengewicht und Gehirngewicht.*
Von R. BRUMMELKAMP. (Communicated by Prof. C. U. ARIËNS
KAPPERS).

(Communicated at the meeting of April 29, 1939.)

Die vergleichende Untersuchung nahe verwandter Tierarten, die in Körpergröße und Gehirngewicht stark divergieren, wie z.B. Katze und Tiger, lehrt uns, dass, je mehr das Gehirngewicht zunimmt, je mehr die Gehirnoberfläche ¹⁾ sich faltet. Ein näheres Eingehen auf diese Tatsache führt uns zu folgenden Schlüssen: Bei gleichförmigen Körpern nimmt die Oberfläche mit der $\frac{2}{3}$ Potenz des Körpervolumens, bezw. -Gewichtes zu; nimmt die Oberfläche mehr zu, wie es der $\frac{2}{3}$ Potenz des Volumens entspricht, so muss eine Zunahme der Oberflächenfaltung hiervon die Folge sein. Aus der tatsächlichen Zunahme der Oberflächenfaltung schliessen wir also, dass die Oberflächenzunahme die $\frac{2}{3}$ Potenz des Volumens übersteigt. Wäre diese Potenz gleich eins ($1 > \frac{2}{3}$), so würde dies heissen, dass die Oberfläche proportional dem Volumen zunimmt. Dies ist aber nicht ohne weiteres ersichtlich und bedarf einer näheren Untersuchung.

Zur Entscheidung dieser Frage kann ich teils Daten aus dem Schrifttum, teils aus eigenen Untersuchungen anführen. Bei Benutzung der im Schrifttum festgelegten Daten ist es wichtig, nur solche zu verwenden, welche mit der gleichen Methode, von ein und demselben Autor gesammelt sind, an Material, das auf ein und dieselbe Weise vorbehandelt ist. Diese Einschränkung vorausgesetzt, wenden wir uns zuerst den Literaturdaten zu.

In erster Linie möchte ich hier die wertvollen Untersuchungen von ARIËNS KAPPERS nennen. Dieser Autor bestimmte bei einer Anzahl von Gehirnen verschiedener Arten das *Gewicht* der grauen Masse des Neokortex. Für uns von Wichtigkeit sind die Ergebnisse bei einigen Affen und Menschen.

Ich führe hiervon folgende Daten an:

¹⁾ Zur Bestimmung der Rindenoberfläche hat man verschiedene Methoden erdacht, welche teils nur noch historischen Wert haben (BAILLARGER, CALORI), teils noch nähere Betrachtung verdienen (WAGNER, JENSEN, HENNEBERG, BRODMANN, TRAMER, LÉBOUCQ, u.a.). Die Methoden lassen sich in drei Gruppen verteilen: Bei der ersten Gruppe wird die Gehirnoberfläche zwecks Messung mit verschiedenen geeigneten Stoffen belegt, so z.B. mit *Goldblattpapier* (WAGNER), *Stanniol* (JENSEN), oder *Seidenpapier* (BRODMANN, HENNEBERG). Bei der zweiten Gruppe sucht man die Gehirnoberfläche mittels eines *chemischen Niederschlages* und nachfolgender Titrierung (LÉBOUCQ) zu bestimmen. Bei der dritten Gruppe endlich wird die Oberfläche auf *kurvimetrischem Wege* (TRAMER, DAVISON, BRUMMELKAMP) bestimmt. BOK hat die TRAMERSchen Methode einer wesentlichen Modifikation unterworfen.

	Gehirngewicht	Rindengewicht
<i>Semnopithecus cephalophus</i> :	54.1 g;	26.6 g
<i>Hylobatus syndactylus</i> :	87.0 g;	50.5 g
<i>Simia satyrus</i> :	245.2 g;	136.7 g
<i>Mensch (klein)</i> :	909.75 g;	453 g
<i>Mensch (gross)</i> :	1248.25 g;	650.25 g

In der angeführten Reihe verhalten sich also

die Gehirngewichte dieser Arten:

	<i>Semnopithecus</i> <i>cephalophus</i>	<i>Hylobatus</i> <i>syndactylus</i>	<i>Simia</i> <i>satyrus</i>	<i>Mensch</i> (klein)	<i>Mensch</i> (gross)
wie {	54.1	: 87	: 245.2	: 909.75	: 1248.25
d.i. }	1	: 1.61	: 4.53	: 16.82	: 23.07

die entsprechenden Rindengewichte:

wie {	26.6	: 50.5	: 136.7	: 453	: 650.25
d.i. }	1	: 1.90	: 5.14	: 17.03	: 24.44

Diese Vergleichung lehrt uns, dass die Rindengewichte sich fast in derselben Weise verhalten wie die Gehirngewichte; ebenfalls leuchtet ein, dass das relative Rindengewicht der schwereren Gehirne ein wenig zunimmt. Diese Zunahme ist aber nur sehr gering und ist vielleicht dem Umstande zuzuschreiben, dass die mittlere Rindendicke mit der Schwere der Gehirne etwas zunimmt (ERNST DE VRIES). Aus der nahezu gleichen (mittleren) Dicke der Rinde dieser Gehirne folgt, dass ebenfalls die Rindenoberfläche sich dem Gehirngewichte proportional verhält.

Von Wichtigkeit sind auch noch die Untersuchungen LEBOUQs. Dieser fand folgende Daten:

	Mann	Weib	Trogl. niger	<i>Simia satyrus</i>
Gehirngewicht	1462 g	1335 g	390 g	370 g
Rindenoberfläche	1924 qcm	1780 qcm	623.5 qcm	616 qcm
Das Verhältnis der Ge-	1462	: 1335	: 390	: 370
hirngewichte ist: {	3.95	: 3.61	: 1.05	: 1
Das Verhältnis der Rin-	1924	: 1780	: 623.5	: 616
denoberfläche ist: }	3.12	: 2.89	: 1.01	: 1

KRAUS, DAVISON und WEIL, resp. DAVISON und KRAUS fanden folgende Daten:

	Mensch (erwachsen) ¹⁾	Mensch (Neonatus)	Affe ¹⁾
Gehirngewicht:	1490 g	445 g	66.25 g
Rindenoberfläche:	2895.4 qcm	995.46 qcm	141.8 qcm
Das Verhältnis der Ge-	1490	: 445	: 66.25
hirngewichte ist: d.i. }	22.49	: 6.72	: 1
Das Verhältnis der Rin-	2895.4	: 995.46	: 141.8
denoberfläche ist: d.i. }	20.42	: 7.02	: 1

¹⁾ Mittelwert aus 2 Exemplare.

BRODMANN fand bei einigen Affen Folgendes:

	Cercopithecus	Gibbon	Cynocephalus	Schimpanse
Gehirngewicht:	106 g	118 g	158 g	295 g
Rindenoberfläche:	14641 qmm	16301 qmm	21321 qmm	39572 qmm
Das Verhältnis der	{ 106	: 118	: 158	: 295
Gehirngewichte ist: d.i. }	1	: 1.11	: 1.49	: 2.78
Das Verhältnis der	{ 14641	: 16301	: 21321	: 39572
Gehirnoberfläche ist: d.i. }	1	: 1.11	: 1.46	: 2.70

Aus den Literaturdaten von ARIËNS KAPPERS, LEBOUQC, KRAUS, DAVISON, WEIL, c.s. geht also hervor, dass bei verwandten Arten (höheren Affen und Menschen) bzw. innerhalb einer Art (Menschen) die Gehirnoberflächen nahezu den Gehirngewichten proportional sind. Soweit ich sehen kann, haben die Autoren diese Konsequenz noch nicht aus ihren Daten gezogen.

Wegen der Wichtigkeit der Frage, ob tatsächlich die aufgehobene Proportionalität zwischen Oberfläche und Gewicht eine allgemeine Eigenschaft ist, welche für das Gehirn verwandter Arten überhaupt gilt, oder aber nur auf die höheren Affen und den Menschen beschränkt ist, habe ich auch einige niedere Tierarten in meine nachprüfende Untersuchung bezogen.

Für die diesbezügliche Untersuchung standen mir in erster Linie die vollständigen Serienschritte der Gehirne des „Nederlandsch Centraal Instituut voor Hersenonderzoek“ Amsterdam, Leiter: Prof. Dr. C. U. ARIËNS KAPPERS, zur Verfügung. Untersucht wurden die Gehirne von *Talpa europaea*, *Erinaceus europaeus*, *Mus musculus*, *Mus norvegicus*, *Sciurus vulgaris*, *Cavia cobaya*, *Lepus cuniculus*, *Tragulus javanicus*, *Sus scrofa*, *Leontopithecus rosalia*, *Cebus fatuellis*, *Nemestrinus nemestrinus* und Mensch.

Die von mir angewandte Methode rührt von TRAMER her. Dieser Autor kam auf den Gedanken, die Oberfläche des Gehirns auf eine flache Ebene zu projizieren. Er benutzte dazu vollständige Reihen von Serienschritten. Der Umfang jedes Schnittes wurde einzeln mittels eines Kurvimeters ausgemessen. Die verschiedenen Längen, welche er in dieser Weise erhielt, wurden danach nebeneinander senkrecht auf eine Grundlinie gezeichnet, in Entfernungen, die den gegenseitigen Entfernungen der ausgemessenen Schnitten der Serie proportional waren. Danach wurden die Endpunkte dieser senkrechten Linien durch eine vielfach gebrochene Linie miteinander verbunden. In dieser Weise erhielt er eine Ebene, die annähernd mit der wirklichen Gehirnoberfläche in bestimmter Weise proportional war.

Es braucht kaum gesagt zu werden, dass auch diese Methode mit Fehlern behaftet ist. Erstens nenne ich die allgemein bekannte Tatsache, dass nicht alle Schnitte in genau derselben Weise von den fixierenden und färbenden Flüssigkeiten beeinflusst werden. Zweitens, dass beim Nachzeichnen und Ausmessen mittels des Kurvimeters kleine Fehler gemacht werden. Drittens, dass die Kuppe einer Rindenwindung eine geringe Dehnung, das Tal eine Ineinanderdrängung

erfährt, wobei unsicher bleibt, ob diese beiden Erscheinungen einander die Wage halten. Schliesslich sei noch ein systematischer Fehler erwähnt. Wie gesagt, wurden die verschiedenen Längen der gemessenen Umfänge nebeneinander, in Entfernungen die den gegenseitigen Entfernungen der ausgemessenen Schnitte entsprechen, senkrecht auf eine Grundlinie errichtet. Durch dieses Verfahren werden nicht die wirklichen gekrümmten Abstände zwischen den nachgezeichneten Zirkumferenzen verwendet, sondern ihre Projektionen auf der sagittalen Hauptachse. Der Fehler welcher hierdurch gemacht wird, wird aber bei gleichförmigen Körpern, wie den Gehirnen verwandter Arten, annähernd einen relativ gleichen Wert haben. Weil wir nun nicht auf absolute Zahlen hinauszielen, sondern uns mit Verhältnissen begnügen, dürfen wir erwarten, dass dieser systematische Fehler nicht allzu störend auf die erhaltenen Zahlen einwirken wird. Dass diese Vermutung zu Recht besteht, geht aus einer Vergleichung unserer Zahlen mit denen LEBOUQUES, KRAUS' c.s. und BRODMANN'S hervor. Erwähnenswert ist dass es BOK gelungen ist, durch eine Modifikation der TRAMER'Schen Methode diesen systematischen Fehler zu beseitigen. Auf den *Verhältnisszahlen* hat jedoch diese Beseitigung keinen bedeutenden Einfluss; für das Studium der wirklichen Oberfläche ist dagegen die BOK'sche Modifikation unentbehrlich.

In der nachstehenden Tabelle I sind die, in der von mir angewandten Weise, erhaltenen Zahlen gesammelt.

TABELLE I.

	Namen	Gehirngewicht (in gr.)	Rindenoberfläche (in qcm.)
<i>Insectivora</i>	1. <i>Talpa europaea</i>	0.936	0.75
	2. <i>Erinaceus europaeus</i>	3.15	2.367
<i>Rodentia</i>	3. <i>Mus musculus</i>	0.36	0.534
	4. <i>Mus norvegicus</i>	1.59	2.385
	5. <i>Sciurus vulgaris</i>	6.10	4.649
	6. <i>Cavia cobaya</i>	4.73	3.468
	7. <i>Lepus cuniculus</i>	11.20	8.44
<i>Ungulata</i>	8. <i>Tragulus javanicus</i>	15.85	15.577
	9. <i>Sus scrofa</i>	104.00	100.809
<i>Primaten</i>	10. <i>Leontopithecus rosalia</i>	12.80	13.355
	11. <i>Cebus fatuellis</i>	55.00	55.037
	12. <i>Nemestrinus nemestrinus</i>	70.00	69.794
	13. <i>Homo sapiens</i>	1400.00	717.436

Vergleichen wir an Hand dieser Tabelle die nahe verwandten Arten untereinander, so ergeben sich folgende Verhältnisse:

Für die *Insectivoren*: *Talpa europaea* und *Erinaceus europaeus* verhalten sich die Hirngewichte wie:

$$0.936 : 3.15 = 1 : 3.365$$

die Rindenoberfläche wie: $0.75 : 2.367 = 1 : 3.156$

Für die *Rodentier*:

	Mus musculus	Mus nor- vegicus	Sciur. vulg.	Cavia cob.	Lepus cuniculus
die Gehirngewichte wie:	0.36	1.59	6.10	4.73	11.20
d.i. wie:	1	4.41	16.94	13.14	31.11
die Rindenoberfl. wie:	0.534	2.385	4.649	3.468	8.44
d.i. wie:	1	4.47	8.70	6.49	15.80

Für die *Ungulaten*: *Tragulus javanicus* und *Sus scrofa* verhalten

sich die Gehirngewichte wie: 15.85 : 104.00 = 1 : 6.562
 die Rindenoberfl. wie: 15.577 : 100.809 = 1 : 6.472

Für die *Primates*:

	Leontopith. rosalia	Cebus fat.	Nemestrinus nemestrinus	Mensch
die Gehirngewichte wie:	1280	55.00	70.00	1400.00
d.i. wie:	1	4.30	5.47	109.37
die Rindenoberfl. wie:	13.355	55.037	69.794	717.436
d.i. wie:	1	4.12	5.23	53.72

Zwei Tatsachen gehen aus diesen Vergleichen eindeutig hervor. Die *eine* ist, dass bei nahe verwandten Arten, wie den angeführten *Insectivoren* (*Talpa*, *Erinaceus*), *Rodentien* (*Mus musculus*, *Mus norvegicus* einerseits, *Cavia cobaya* und *Lepus cuniculus* anderseits) und *Affen* (*Leontopithecus rosalia*, *Cebus fatuellis*, *Nemestrinus nemestrinus*), innerhalb jeder Gruppe, das Gewichtsverhältnis der Gehirne dem Oberflächenverhältnis gleichgesetzt werden kann, dass also für diese Arten gilt: $E \propto R$ (worin E das Gehirngewicht, R die Rindenoberfläche ist), d.h. pro Einheit Gehirngewicht, ist die Rindenoberfläche konstant. Die *zweite* Tatsache ist, dass bei verwandten, jedoch einander *ferner* stehenden Arten wie Maus und Kaninchen oder niedere Affe und Mensch, innerhalb jeder Gruppe, das Gehirngewicht um das Doppelte zunimmt, im Vergleich zur Rindenoberfläche, dass also für diese Arten gilt: $E \propto 2 \cdot R$, d.h. pro Einheit Gehirngewicht ist die Rindenoberfläche bei den niederen Tieren derselben Ordnung um das Doppelte vermehrt.

In Anlehnung an ARIËNS KAPPERS habe ich nun in zweiter Linie für einige Gehirne das (Trocken-)gewicht der Rinde bestimmt. Nachdem die Gehirne in Serienschnitten von 1 mm dick geschnitten waren, wurde mit einem feinen Starmesser die Rinde genau an der Grenze zwischen weisser und grauer Substanz abgeschnitten, in Alcohol abs. aufbewahrt bis völlige Entwässerung, an der Luft getrocknet und dann das Trockengewicht bestimmt. Diese Bestimmungen wurden ausgeführt an einem Gehirn einer normalen erwachsenen Frau; eines Mikrozephalens; eines erwachsenen Schimpansen und eines *Macacus rhesus*.

Gefunden wurde:

TABELLE II.

Namen	Gehirngewicht	Rindentrocken- gewicht
Normale erw. Frau	1160 gr.	32.5302 gr.
Mikrozephale	452 gr.	12.8436 gr.
Schimpanse	340 gr.	10.9200 gr.
Macacus rhesus	50 gr.	2.8266 gr.

Vergleichen wir an der Hand dieser Tabelle (II) die Gehirngewichte und Rindentrockengewichte, so ergeben sich folgende Verhältnisse:

	Macacus rhesus	Schimpanse	Mikrozephale	Normale Frau
die Gehirngewichte				
verhalten sich wie:	50	: 340	: 452	: 1160
d.i. wie:	1	: 6.80	: 9.04	: 23.2
die Rindentrocken-				
gewichte wie:	2.8266	: 10.9200	: 12.8436	: 32.5302
d.i. wie:	2	: 7.73	: 9.08	: 23.02

Aus diesen Vergleichen geht hervor, *erstens* dass bei einander nahe stehenden Arten, wie Schimpanse, Mikrozephale und Mensch das Rindentrockengewicht pro Einheit Gehirngewicht nahezu konstant ist; *zweitens* dass bei niederen Affen wie Macacus rhesus das Rindentrockengewicht pro Einheit Gehirngewicht um das Doppelte vermehrt ist; ein Ergebnis also, das sich vollkommen deckt mit der Schlussfolgerung auf Seite 450, wenn man statt Rindentrockengewicht, Rindenoberfläche setzt.

Die *erste* Tatsache, dass bei nahe verwandten Arten eine Proportionalität zwischen Rindenoberfläche c.q. Rindentrockengewicht und Gehirngewicht existiert, ist an sich nicht befremdend. Die Rinde ist ein Oberflächenorgan, dessen Zellen ihre langen Fasern in die Tiefe senden, und dort die weisse Substanz bilden. Das Gewicht des Grosshirns wird, abgesehen von Riechhirn, hauptsächlich durch die Massen von Rinde und weisser Substanz bestimmt. Die Masse und damit das Gewicht des Grosshirns, steht also in fester Beziehung zur Menge der Rindenzellen, welche, wie bekannt, die Ausdehnung, c.q. das Volumen und auch das Gewicht der Rinde und der weissen Substanz bestimmen. Solange man bei seinen Vergleichen innerhalb einer Gruppe von nahe verwandten Arten bleibt, die nach einem einheitlichen Plan aufgebaut sind, halten die Oberflächenausdehnung, resp. das Gewicht der Rinde und das Gehirngewicht einander offenbar die Wage, d.h. dann gilt die Formel $E \propto R$. Die *zweite* Tatsache, dass zwischen einander fernerstehenden, doch derselben Ordnung angehörenden Arten, wie z.B. Maus und Kaninchen, oder niedere Affe und Mensch, die Formel $E \propto 2 \cdot R$ gilt, weist darauf hin, dass bei den höheren Repräsen-

tanten dieser Gruppen die Anzahl der Fasern sich vermehrt hat, und damit auch das Gesamtgewicht des Gehirns vermehrt ist, ohne dass es zu einer übereinstimmenden Oberflächen- resp. Gewichtsvermehrung der Rinde kam. Durch diesen Umstand wird die relative Rindenmasse bei den niederen Repräsentanten um zweimal grösser als bei den höheren Repräsentanten derselben Ordnung. Umgekehrt heisst dies, dass bei den höheren Repräsentanten je Einheit zweimal mehr Fasern vorhanden sind. Vielleicht hängt diese Faservermehrung mit einer Steigerung der Assoziationsmöglichkeiten zusammen, einen Gedanken, auf den schon VON ECONOMO hingewiesen hat. Dass diese Faservermehrung gerade eine Verdoppelung ist, lässt sich im Sinne HEIDENHAINs aus generellen Protomerenspaltungen begreifen.

LITERATURVERZEICHNIS.

1. ARIËNS KAPPERS, Proc. Kon. Akad. v. Wetensch., Amsterdam, **28**, 844—855 (1925).
2. BOK, Nederl. Tijdschr. v. Geneeskunde (1939).
3. BRODMANN, Verhandlung der Gesellschaft deutscher Naturforscher und Aertze in Wien (1913).
4. BRUMMELKAMP, Normale en abnormale hersengroei in verband met de cephalisatie-leer. Uitg. N.V. N. H. Uitg. Mij, Amsterdam (1937).
5. ———, Proc. Kon. Ned. Akad. v. Wetensch., Amsterdam, **41**, N^o. 10 (1938).
6. DAVISON and KRAUS, Arch. of Neurol. and Psych. (1929).
7. KRAUS, DAVISON and WEIL, Arch. of Neurol. and Psych. (1928).
8. VON ECONOMO, Zellaufbau der Grosshirnrinde des Menschen. Julius Springer. Berlin (1927).
9. LÉBOUCQ, Comptes rendus de l'Association des Anat. Prague, 2—4 Avril 1928.
10. ———, Le rapport entre le poids et la surface de l'hémisphère cérébral chez l'homme et les singes. Bruxelles (1928).
11. TRAMER, Arbeiten aus dem Hirn-Anatomischen Institut in Zürich (1916).
12. ERNST DE VRIES, Anat. Anz., Bd. **39** (1910).